Aerodynamic Forces and Heat Transfer of Sphere and Sharp Cone in Hypersonic Flow

A project present to
The Faculty of the Department of Aerospace Engineering
San Jose State University

in partial fulfillment of the requirements for the degree
Master of Science in Aerospace Engineering

By

Josue Lopez

May 2014

approved by

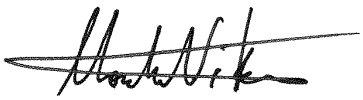

Dr. Nikos Mourtos
Faculty Advisor

San José State
UNIVERSITY

ABSTRACT

Aerodynamic Forces and Heat Transfer of A Sphere and Sharp Cone In Hypersonic Flow

By

Josue Lopez

Computational Fluid Dynamics (CFD) has become a very useful tool when it comes to simulating a flow over a blunt body at any Mach number. Some programs do not yield very good results at hypersonic velocities, due to the high temperatures and the reactions of the flow involving the high temperature chemistry. The CFD software in this analysis is STAR CCM+, which is capable of simulating hypersonic flow and account for chemistry at high velocities. The scope of this project is to calculate lift, drag and heat transfer using Newtonian and modified Newtonian to compare to Computational Fluid Dynamics simulations. The comparison will be from a range of Mach numbers from Mach 5 to Mach 15 in intervals of 5. The geometries analyzed will be a sphere and cone of various semi-apex angles. As the semi-apex angle varies, the shock detachment distance also varies affecting the heat transferred to the nose of vehicle. The goal is to compare the accuracy in between analytical and CFD simulation results to observe which method yields better results when comparing to experimental data.

Table of Contents

List of Figures

List of Tables

Nomenclature

θ - Angle at which a surface is inclined with respect to the free stream in Newtonian Theory.

α - Angle of attack

ε - Semi-apex angle of a circular sharp cone

β - Wave angle for exact oblique shock theory in Eq. 8

ϕ - Angle between a normal to the surface and free stream in Newtonian Theory and Meridian angle when looking at a cone, from the base or the sharp end, at an angle of attack

Introduction

Hypersonic flight has been a major topic in the field of Aerospace Engineering ever since flight has been an interest to man. It all started in the early 1900s with the Wright brothers, by designing and building the first aircraft that was able to sustain flight. Throughout the years, there has been substantial research to improve flight conditions, and flight capabilities in the hypersonic regime. Hypersonic flight is labeled as the regime when the flow (or a vehicle) travels five times the speed of sound or faster (Mach ≥ 5) although nothing out of the ordinary occurs at Mach 5, as it is the case at Mach 1 with the sonic boom. In hypersonic velocity regime, there are certain physical flow phenomena that are very important as the Mach number increases to higher values. At times some of the phenomena may become an important aspect at Mach 3 and sometimes at around Mach 7. Hypersonic velocities are not very common in aircraft; they are mostly seen in re-entry vehicles when they enter the atmosphere. For example, the Apollo lunar capsule reached a velocity greater than Mach 36 as it re-entered the atmosphere. Recently hypersonic flight has been considered for aircraft, and some prototypes have been tested by the United States Air Force, such as the X-51A Waverider.

As Mach number increases so does the temperature, and some of the phenomena that takes place is the dissociation of certain elements in the flow. Temperatures surrounding the vehicle can reach +3,000 K, which was the case for the Apollo lunar capsule when it re-entered the atmosphere [5]. Temperatures are a major concern for re-entry vehicles; the temperatures need to be controlled to be able to keep the vehicle safe as well as the crew. Heat transfer considerations need to be addressed very seriously

when dealing with hypersonic velocity, which is why the geometrical shape of a hypersonic vehicle is important, as well as for drag consideration in aircraft.

The scope of this paper is to analyze various geometrical shapes (vehicles) using Newtonian and Modified Newtonian theories to obtain lift/drag coefficients and heat transfer data at various Mach numbers. The cone shape will also be analyzed at an angle of attach to compare to the accuracy of computational fluid dynamic simulations in a hypersonic flow regime.

Literature Review

The reasoning behind this project is based on the interest for hypersonic velocity flight. It is a topic that has been highly researched since the early 1900's and there has been much speculation about it in the 21st century; which has caught the attention of many. Although technology is very advanced, there are no aircrafts that can travel at hypersonic speed or even at supersonics speeds on a regular basis. If commercial aircraft could travel at hypersonic speeds nothing would be the same; general population would travel from one side of the planet to the other without much difficulty. Many engineering applications rely on the computer to carry on many of the complicated and tedious array of calculations needed to decipher certain problems. Although the computer is a very helpful and powerful tool, sometimes it is not very accurate on certain applications due to its complexity. If it's too complicated for a computer to carry on the calculations, it is definitely impossible, or near impossible, to do it by hand. In the branch of Aerospace Engineering, when trying to model a flow, computational fluid dynamics simulation programs are used. The programs are chosen depending on the regime that it's being analyzed and the accuracy of the results vary. The simulations do not yield very accurate results in aerodynamic, nor heat transfer data for hypersonic regimes, due to the complexity of the physics involved with the flow. It is very difficult to account for all major disciplines simultaneously, when analyzing hypersonic vehicles in terms of their aerodynamics. The simulations are not always good, but for certain flow regimes the simulations are very accurate, which is why computational fluid dynamics simulation programs are used.

Typically during the conceptual design process of a hypersonic entry vehicle, various methods are employed to improve the speed of the computational simulations. One of the methods tends to be panel methods in conjunction with Newtonian flow theory to obtain some aerodynamic characteristic at hypersonic velocities. Using alternative methods comes at the expense of a small reduction in reliability of the method and the limited amount of vehicle shapes that can be analyzed using these alternative methods. The geometrical shapes used in panel methods are generally chosen among shapes that provide the necessary aerodynamics performance, such as lift and drag for certain mission requirements. Computational fluid dynamics has more substantial requirements to analyze a given vehicle [2].

Given that computational fluid dynamics simulations do not yield very accurate results for hypersonic flow, due to the complicated physical phenomena involved, research has been done on comparing the accuracy of computational fluid dynamics programs with experimental data gathered from a hypersonic shock tunnel for a given blunt body prototype vehicle. The objective of the research is to validate the codes of computational fluid dynamic programs by comparing the results to experimental data and Newtonian theory. The subject used is a 60^{o} blunt cone prototype at $\alpha = 0^{o}$. The methodology for the validation of the CFD code was to calculate aerodynamic forces and convective heat transfer rates using Newtonian and Modified Newtonian theories. The same data was collected from a wind tunnel using the prototype, and finally the same data was obtained using a CDF simulator. The experiment took place in a hypersonic shock tunnel HST2 with a flow of Mach 5.75. The equipment used was an accelerometer-based three-component balance system to obtain the coefficient of drag, and platinum thin-film

gauges attached to the surface of the prototype to obtain the convective heat transfer to the body. The computational based program used for the simulations was an Axi-Symmetric Navier-Stokes simulator.

The results generated from all three methods were very satisfactory in accordance to the objective of the research. The theoretical, Newtonian and modified Newtonian theories, calculations of the coefficient of drag differed from the experimental value by 6%, while the computational value over predicted the coefficient by 9% from the experimental data. For the convective heat transfer rate, the measured value was 11% higher than the theoretical value, and the computational value was 2% lower at the stagnation point. The results obtained from the study were satisfactory to validate the code used in the computational program to simulate hypersonic flow and generate reasonable values. Although the computational simulator over predicted the drag coefficient, it was within a reasonable margin in which the safety factor for any design will account for the error. For the convective heat transfer rate the computational value was only 2% lower than the experimental value, being a really good result since heat transfer is very important at hypersonic velocities [2].

Theory

Hypersonic flight has become of great interest today, and new vehicle concept designs are being developed to travel at high Mach numbers. Hypersonic aerodynamics is very important due to certain physical phenomena that do not occur at lower supersonic speeds. The flow field in hypersonic flight is dominated by the phenomena, which involves high temperature flow dynamics. Unlike subsonic and supersonic flows, hypersonic flow is nonlinear and the hypersonic aspect of a flow may become important at Mach 3. Moreover, as Mach numbers increases the phenomena becomes more critical.

Newtonian theory was investigated at the end of the seventeenth century, before thermodynamics, kinetic theory and viscous stresses were developed, which is why some of the analyses and results may be in error in comparison to today's knowledge in the subject. At the time Sir Isaac Newton did not have an intuition of the shock wave or the shock layer, and he did not realize the flow velocity necessary for compressibility to dominate the flow field. Sir Isaac Newton's approach was from a set of basic laws and a theoretical model of a physical problem leading to a solution for the problem. Therefore, Newtonian theory is often used to estimate the pressure distribution over a surface of a body in hypersonic flow.

Newtonian Theory

The oldest and most commonly used method in the realm of hypersonic flow is Newtonian theory. The well known Newtonian sine-squared law is used in local surface inclination methods. Considering a surface inclined at angle θ to the free stream, the flow comprises of an infinite number of particles that impact the surface and then travel

tangentially to the surface. At the moment of impact, particles lose their normal component but are able to keep the tangential component. The rate of change of the normal component of momentum is equal to the force applied on the surface by the impact. This is shown in Fig. 1, where the free stream velocity normal to the surface is $V_\infty \sin\theta$.

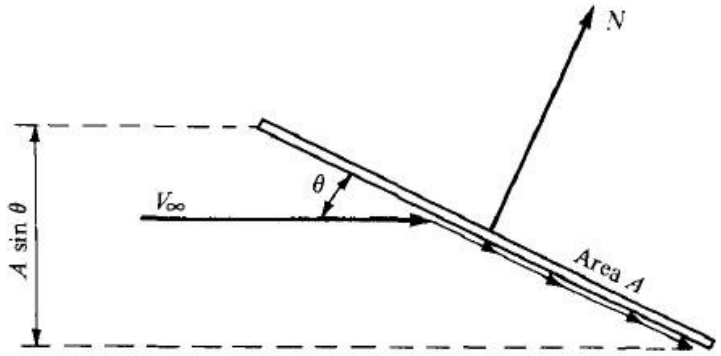

Figure 1: Representation of Newtonian impact theory

If the area of the surface is A, the mass flow component on the surface is ρ_∞ Asinθ V_∞. Therefore, the rate of change of momentum is

(mass flow) * (change in normal component of velocity)

$(\rho_\infty V_\infty A\sin\theta) * (V_\infty \sin\theta) = \rho_\infty$ [illegible] $A\sin^2\theta$

Which then yields Newton's second law, the force normal to the surface:

$N = \rho_\infty$ [illegible] $A\sin^2\theta$ Eq. (1)

The force acts as the rate of change of momentum, and the force per unit area can be characterized as:

[illegible] $= \rho_\infty$ [illegible] $\sin^2\theta$ Eq. (2)

Considering the normal force per unit area in terms on aerodynamics, Newton's model adopts a stream of particles moving parallel towards the surface, with a rectilinear motion with no random motion. It is known that moving gas is composed of random motion of the particles, as well as guided motion. Also, the static free stream pressure p_∞ is measured from random motion particles only. Therefore, the guided motion particles in the model are the result of the normal force per unit area (N/A). Accounting for the pressure of random motion and guided motion particles, the force per unit area can be denoted as the pressure difference above p_∞, explicitly $p - p_\infty$. Consequently, equation 2 can be written as:

$$p - p_\infty = \rho_\infty V_\infty^2 \sin^2\theta \qquad \text{Eq. (3)}$$

Equation 3 can also be ascribed in terms of the pressure coefficient $C_p = (p - p_\infty) /$ as:

Which can also be expressed as:

$$C_p = 2\sin^2\theta \qquad \text{Eq. (4)}$$

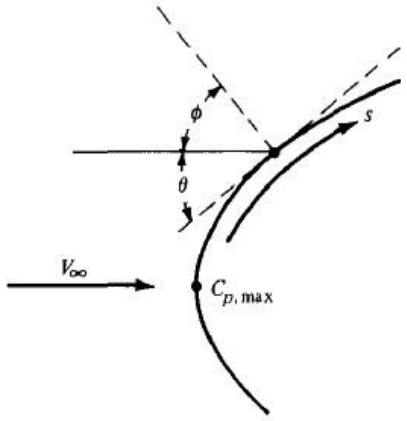

Figure 2: Angle distinction for Newtonian theory

Newton's sine-squared law states that the pressure coefficient is proportional to the sine square of the angle between a tangent to the surface and to the free stream. Newtonian theory can also be expressed in terms of the angle between a normal to the surface and free stream, and the angle is represented by ϕ as shown in Figure 2. In terms of ϕ, Equation 4 becomes:

$$C_p = 2\cos^2\phi \quad \text{Eq. (5)}$$

The physical meaning for the theory can be derived from hypersonic oblique shock relations for C_p with free stream conditions.

$$C_p = \frac{!}{\text{Y!!}}[\quad ! - \quad \frac{!}{!}\ ] \quad \text{Eq. (6)}$$

Equation 7 is given after taking the limit as the Mach number increases to infinity:

$$C_p = \frac{!}{\text{Y!!}}[\quad !\ ] \quad \text{Eq. (7)}$$

Considering that the heat capacity ratio (Υ) goes to 1 as the Mach number goes to infinity, Equation 8 is derived from taking both limits as $M_\infty \to \infty$ and $\to 1$ yields:

$$C_p = 2\sin^2\beta \quad \text{Eq. (8)}$$

Equation 8 results from the exact oblique shock theory, and for the moment β is the wave angle, not the deflection angle. Considering the density relation for exact oblique shock, Equation 9:

$$\frac{!_!}{!} = \frac{\text{Y!! }!_!{}^!!"\#^!!}{(\quad)} \quad \text{Eq. (9)}$$

Equation 10 was derived as the limit of M_∞ goes to infinity:

$$\frac{\rho_2}{\rho_1} = \frac{(\gamma+1)M_1^2}{(\gamma-1)M_1^2+2} \qquad \text{Eq. (10)}$$

In addition to $M_\infty \to \infty$, also $\to 1$, resulting in equation 11:

$$\frac{\rho_2}{\rho_1} \to \infty \qquad \text{Eq. (11)}$$

As shown in Equation 11, the density behind the shock is very large, and the shock wave follows the shape along the body surface. This is good for $M_\infty \to \infty$ and small deflection angles.

$$\frac{\rho_2}{\rho_1} = \frac{\tan\theta}{\tan(\beta-\theta)} \qquad \text{Eq. (12)}$$

Considering that $\to 1$, $M_\infty \to \infty$, and θ and β are small then $\beta = \theta$ and the shock wave rests on the body, and the results becomes Equation 4:

$$C_p = 2\sin^2\theta \quad \text{Eq. (4)}$$

The Newtonian model of fluid flow accounts for the particles that impact the frontal area of the body only, since the particles cannot turn around and impact the back area of the body. Therefore, the back area of the body does not have any impact pressure, and the pressure on this area can be assumed to be ambient, $p = p_\infty$. Consequently, the pressure coefficient on the back area is zero.

Modified Newtonian Theory

The maximum pressure, as well as maximum pressure coefficient (C_p), occurs at the stagnation point. Whereas in a blunt body it will be at $\theta = \pi/2$ and $\phi = 0$, with a $C_p = 2$. Maximum pressure coefficient occurs as $M_\infty \to \infty$, at a normal shock wave at hypersonic speeds. The flow across a normal shock can be described by:

$$p_\infty + \rho_\infty \; !^{!} = p_2 + \rho_2 \; !^{!} \qquad \text{Eq. (13)}$$

Across a normal shock wave the flow velocity decreases such that the flow behind the shock wave is subsonic. At hypersonic speed it can be assume that $(\rho_\infty \; !^{`}) >> (\rho_2 \; !^{`})$, resulting in a limiting circumstance as $M_\infty \rightarrow \infty$, where:

$$p_2 - p_\infty = \rho_\infty \; !^{!}$$

or

$$C_p = \frac{!! \;\; ! \; !!}{-} = 2 \qquad \text{Eq. (14)}$$

The maximum pressure coefficient occurs for an infinite Mach value, for a large but finite Mach number the coefficient of pressure is less than 2. The maximum C_p occurs at the stagnation point, and can be denoted as $C_{p,max}$ as in Figure 2. For a given M_∞, $C_{p,max}$ can be calculated using normal shock wave theory using:

$$C_{p,max} = \frac{!}{} \left(\frac{^{!,!}}{} - 1 \right) \qquad \text{Eq. (15)}$$

Downstream of the stagnation point the C_p can be presumed to follow the sine-squared theory by Newtonian theory, classified as:

$$C_p = C_{p,max} \sin^2 \theta \qquad \text{Eq. (16)}$$

In terms of blunt bodies, Modified Newtonian theory, Equation 16, is more accurate than Newtonian theory, Equation 4.

Impact Theory Modified

As previously mentioned, Newtonian Theory assumes the Mach value to be very high and the value of specific heat ratio to be unity, which yield Eq. 4. This equation only accounts for the angle of attack, and when dealing with circular geometries with varying semi-apex angles Eq. (4) may not be adequate for the analysis. Therefore, several modifications have been done to Eq. (4) in order to incorporate the semi-apex angle and the meridian angle along the circular shape, to define the pressure coefficient at any given point in the shape as a function of angle of attack and semi-apex angle. In Eq. (4) the value of θ is the local angle of attack to the free stream, and for a cone the value of $\sin\theta$ is given by:

$$\sin\theta = \sin\varepsilon * \cos\alpha + \cos\varepsilon * \sin\alpha * \cos\phi \qquad \text{Eq. (17)}$$

Where, ε is the semi-apex angle in a circular cone, α is the angle of attack with respect to the free stream flow, and ϕ is the meridian angle measured from the windward. Given that more angles are introduced into the equation, the angle referred to as the angle of attack is changed from θ to α, as it is typically know as. This expression was derived using shock layer theory in an approach to derive an approximation for the pressure coefficient involving the semi-apex angle, angle of attack and meridian angle. The approximations were by Laval, Cheng and Guiraud, and the full derivation can be found in ref. [7].

Heat Transfer

Aerodynamic heating is a key element in hypersonic flow. As the velocity climbs into the hypersonic regime, heat flux increases to the cubed of the velocity. The shock wave formed due to hypersonic velocities reaches very high temperatures by the flow

impact where the air elements dissociate. The temperature in the shock wave can reach beyond 9000 K, to the point of ionization of Oxygen (O_2) and Nitrogen (N_2) at very high Mach values. The shock layer thickness formed gives some cooling time/distance before reaching the surface of the body. Typically, the temperature that reaches the body is significantly smaller than the shock wave temperature; since the usual method of aerodynamic heating from shock layer to the surface is by means of thermal conduction. Therefore, a greater shock layer thickness can be achieved by having a blunted body, which in return yields a smaller heat flux. However, at hypersonic velocities the shock layer temperature becomes extremely hot to the point that it also emits thermal radiation, which turns out to be the dominant source of heat transfer at temperatures higher than 1000 K on the shock layer. Consequently, as the shock layer reaches ionization temperatures thermal radiation becomes a substantial portion of the heat transferred to the body surface, and convective heating is negligible.

For a slender sharp cone the oblique shock wave is very close to the body. The shock layer between the shock wave and the body is very thin. A major interaction between the inviscid flow behind the shock and viscous boundary layer on the surface occurs as a result of a thin shock layer. As a result that hypersonic vehicles usually fly at high altitudes where density is low, the boundary layer becomes thicker, which in some cases is of the same magnitude as the shock layer thickness. Thermal conduction is a physical characteristic of viscous flow in addition to friction. Where friction dissipates heat over a body, which comes in kinetic energy from the moving flow, and the flow velocity is decreased as an effect of friction. The loss of kinetic energy resurfaces as internal energy of the fluid, causing the temperature to rise. Hence, aerodynamic heating

is an important value to consider for hypersonic flight. In this paper, the heat transfer of a sphere and a sharp cone are being approximated analytically. The heat transfer rate equation used for a sphere was the following:

Eq. (18)

Where R is the radius of the sphere, V_∞ and ρ_∞ are the free stream velocity and density respectively. The static enthalpy and enthalpy at the wall are defined by h_0 and h_w respectively. For a sharp cone a similar equation was used, where the equation is a function of the semi apex angle, ε, and cord length, x:

Eq. (19)

The values for h_0 are as follows for sphere and cone respectively:

$$h_0 = h_\infty + 0.5\ V_\infty^2$$

$$h_0 = h_\infty + 0.4\ V_\infty^2$$

Where the free stream enthalpy is equivalent to the specific heat of the free stream, times the free stream temperature, $h_\infty = C_p * T_\infty$.

STAR CCM+

The STAR-CCM+ software is an engineering physics simulator within a single integrated package with multiple tools. In the acronym STAR-CCM+, the "CCM" stands for "computational continuum mechanics", where the application employs a client-server architecture to allow users to solve problems from a lightweight computer, and the heavy math algorithm, is done on a remote machine. This type of application allows for computational time to be reduced substantially.

STAR-CCM+ is an entire engineering processor used for solving problems involving

flow (of fluids or solids), heat transfer, and stress. It is composed of a suite of integrated components that is combined in order to provide a software that is able to address a wide variety of modeling needs, such as:

- 3D-CAD modeler
- CAD embedding
- Surface preparation tools
- Automatic meshing technology
- Physics modeling
- Turbulence modeling
- Post-processing
- CAE integration

STAR-CCM+ is based on object-oriented programming, which is designed to handle large models using an architecture meshes, solves and post-processes over multiple computing resources without requiring additional effort from the user.

The object-oriented programming nature of the code can be seen in the user interface. An object tree is provided for each simulation, containing object representations of all the data associated with the simulation. The objects presented on the simulation tree are located on the server, which can run as either a serial or a parallel process. A client interface connects to a server, and displays the simulation objects available on that server.

3D-CAD Modeler

3D-CAD is a feature-based parametric solid modeler within STAR-CCM+ that allows geometry to be built for CFD simulation. The geometry created with 3D-CAD is stored as 3D-CAD models, which can then be converted to geometry parts for integration with the meshing and simulation process. A major feature of 3D-CAD is design

parameters, which allows the user to modify the 3D-CAD model from outside of 3D-CAD. Another benefit is that it allows the user to solve for a particular geometry, change the size of one or more components, and quickly re-run the case.

CAD Embedding

STAR-CCM+ simulations can be set up, runned and post-processed using other CAD and PLM environments such as SolidWorks, CATIA V5, Pro/ENGINEER, and NX. CFD results are linked directly to the CAD geometry (a process called associativity). After any modification in the CAD model the simulation results can be updated by using the "update solution" button.

Surface Preparation Tools

One of STAR-CCM+'s main components is an automated process that links a powerful surface wrapper to the manufacturers unique meshing technology. The surface wrapper significantly reduces the time spent on surface cleanup and, for problems that involve large assemblies of complex geometry parts, reduces the entire meshing process to hours instead of days.

This method works by 'shrink-wrapping' a high-quality triangulated surface mesh onto any geometrical model, closing holes in the geometry and joining disconnected and overlapping surfaces, providing a single manifold surface that can be used to automatically generate a computational mesh without user intervention. STAR-CCM+ also includes a set of surface-repair tools which allows users to interactively improve the quality of imported or wrapped surfaces, offering the choice of a completely automatic repair, user control, or a combination of both.

Automatic Meshing Technology

This tool in STAR-CCM+'s single integrated process provides a fast, and automatic route from complex CAD to CFD mesh. Advanced automatic meshing technology can generate a polyhedral or predominantly hexahedral control volumes. The use of a polyhedral mesh has proven to be more accurate for fluid-flow problems than a hexahedral or tetrahedral mesh of a similar size (number of cells); meanwhile, it is considerably more difficult to create. This meshing technology offers a combination of speed, control, and accuracy. For problems involving multiple frames of reference, fluid-structure interaction and conjugate heat transfer, STAR-CCM+ can automatically create conformal meshes across multiple physical domains.

An important part of mesh generation for accurate CFD simulation is the near-wall region, or extrusion-layer mesh. STAR-CCM+ automatically produces a high-quality extrusion layer mesh on all walls in the domain. In addition, the user can control the position, size, growth-rate, and number of cell layers in the extrusion-layer mesh.

Physics Models

Some of the STAR-CCM+'s physics modeling capabilities include:

Solvers

- Segregated
- Coupled
- Finite volume solid stress

Time

- Steady state
- Implicit and explicit unsteady
- Harmonic balance

Turbulence

- RANS
- RSM
- LES/DDES
- Lamina-turbulent transition

Compressibility

- Ideal Gas
- Real Gas

Heat transfer

- Conjugate heat transfer (CHT)
- Multiband and gray thermal surface to surface radiation
- Solar radiation
- Discrete ordinates radiation (DOM) including participating media

Multiphase

- Lagrangian particle tracking
- VOF (incompressible and compressible)
- Cavitation & boiling
- Eulerian multiphase
- De-icing & De-fogging
- Melting & solidification

Moving Mesh

- Dynamic Fluid Body Interaction (DFBI or 6DOF)
- Rigid body motion
- Mesh morphing
- Multiple reference frames (MRF)

Combustion & chemical reaction

- Reaction kinetics

- Eddy break up (EBU)
- Presumed probability density function (PPDF)
- Complex chemistry
- Ignition
- NOx modeling

Distributed Resistance (Porous media)

- Anisotropic
- Orthotropic
- User defined
- Porous baffles

Turbulence Modeling

In addition to its provision for inviscid and laminar flow, STAR-CCM+ has a comprehensive range of turbulence models:

- k-epsilon (Standard, V2F, Realizable, Two-layer)
- k-omega (Standard, SST and BSL)
- Reynolds Stress (RSM – linear and quadratic)
- Spalart-Allmaras Turbulence models
- Boundary-layer transition
- Large Eddy Simulation (LES)
- Detached Eddy Simulation (DES, in the new Delayed Detached Eddy Simulation or DDES formulation)

Post-processing

STAR-CCM+ contains a suite of post-processing tools designed to enable the user to obtain maximum value and understanding resulting from the CFD simulation. This includes scalar and vector scenes, streamlines, scene animation, numerical reporting, data plotting, import and export of table data, and spectral analysis of acoustical data.

CAE Integration

Several third-party analysis packages can be coupled with STAR-CCM+ to further extend the range of possible simulations available. Co-simulation is possible using Abaqus, GT-Power, WAVE and OLGA, and file-based coupling is possible for other tools such as Radtherm, NASTRAN and ANSYS.

Modeling High Speed Flows

At high Mach numbers, extreme temperatures occur along with dissociation, or ionization, of the gas must be considered. The Mach number regimes, and the appropriate models to use, vary by gas and upstream temperature and pressure. For air however, the following general guidelines can be used:

Up to Mach 3 a calorically perfect gas assumption, namely ideal gas with constant specific heats, can be used.

From Mach 3-10 a thermally perfect gas assumption, namely ideal gas with temperature-varying specific heats, can be used.

From Mach 10-30, the dissociation needs to be modeled more accurately, so a real gas model and chemically reacting flow is used. The gas dissociation can be modeled by using finite rate chemistry models in the code, where the user will need to supply the reactions and reaction mechanisms. This will provide the correct specific heats and gamma values.

Any flow above Mach 30, involving dissociation, requires solving the Navier-Stokes equations together with the Maxwell equations, which are not inherently supported in STAR-CCM+.

Eulerian- Lagrangian Multiphase

Multiphase modeling allows solving the flow and thermal fields of two or more different materials simultaneously. Interactions between the materials can be considered with the materials being solid, liquid or gas.

The Eulerian Multiphase model (EMP) can be used for dispersed multiphase flows including bubbly, droplet and particle flows. This modeling approach is used where incompressible or compressible techniques would require excessively large meshes to resolve the free surfaces.

Lagrangian multiphase modeling tracks idealized particles or groups of particles (parcels) through the domain. These particles may be solid, fluid (droplets) or gaseous (bubbles). The interaction with the continuous phase may be either one or two way coupled, including the effects of turbulence, heat, mass and momentum transfer if so required.

Physics Models

- Three Dimensional
- Steady
    - Controls the size of the local time-steps being used in the time-marching procedure. For steady simulations, the local time-step is used by the pseudo time-step associated with the iterations. For transient simulation, the local time-step is used within a time-step.

- Gas (Air with density and dynamic viscosity of each altitude)
- Coupled Flow
    - Solves the conservation equations for mass and momentum simultaneously using a time- (pseudo-time-) marching approach. The preconditioned form of the governing equations used by the Coupled Flow model makes it suitable for solving incompressible and isothermal flows.

This formulation is robust for solving flows with dominant source terms, such as rotation. Another advantage of the coupled flow solver is that CPU time scales linearly with cell count; in other words, the convergence rate does not deteriorate, as the mesh is refined.

The coupled algorithm yields more robust and accurate solutions in compressible flow, particularly in the presence of shocks

- Real Gas
- Coupled Energy (Used to determined heat transfer)
- Turbulent
    - Accurate prediction of turbulent flow calculates quantities such as drag, and heat transfer. For most engineering analyses, the main interest is in the prediction of the mean (averaged) flow field. The effect of the fluctuations, around the average or filtered flow field, is included using a turbulence model.

- SST K-Omega model
    - Two transport equations are solved, the turbulent eddy-viscosity is defined as a function of the *turbulent kinetic energy* (k) with the turbulent dissipation rate replaced by the *specific dissipation rate* (omega) in the definition of the turbulent eddy-viscosity. The method mainly focuses in separated flows, low-Reynolds number (i.e. transitional) flows, or when the solution of the very near-wall physics is of prime importance.

- Reynolds-Averaged Navier-Stokes
    - The RANS equations are the time-averaged equations of motion for fluid flow. The RANS equations are primarily used to describe turbulent flows.

- All y+ Wall Treatment Three types of wall treatment are provided depending on the turbulence model that is chosen for the simulation:
    - The all-y+ wall treatment is a hybrid treatment that attempts to emulate the

high-y+ wall treatment for coarse meshes and the low-y+ wall treatment for fine meshes and is also formulated in order to produce reasonable answers for meshes of intermediate resolution (that is, when the wall-cell centroid falls within the buffer region of the boundary layer, where 5<y+<30).

In the case of a turbulence model using a two-layer approach, a modified all-y+ wall-treatment is applied to account for the fact that only the turbulence production is solved to the wall. The turbulence production term at the wall is determined with the all-y+ wall treatment. The turbulence dissipation rate term however becomes a function of wall-distance in the near-wall layer, which is then is blended smoothly with values computed from solving the transport equation away from the wall.

Meshing

The type of meshing used was trimmer mesh. This type of mesh is more efficient at putting cells in the desired areas. A trimmer mesh with the grid lines aligned with the flow often provides the most efficient approach to getting good results. Typical trimmer meshes contain 4-40 million cells, depending on the complexity of the geometry and flow field, and the near-wall treatment.

The type of cell used in the meshing was prism layer. This type of meshing layer yields a good resolution of the boundary layer is critical; therefore the thickness of the prism layer should be designed such that the entire boundary layer is contained within it. The use of wall functions rather than integrating to the wall can be appropriate (for SST K-Omega turbulence model) depending on factors, including:

- Desired accuracy
- Relative importance of skin friction drag
- Importance of transition

- Existence/importance of separation/reattachment on smooth boundaries
- For integrating to the wall, 20-30 prism layers are typically used, with the near-wall y+ being on the order of 1
- For wall functions, 5-8 prism layers are typically used, with the near-wall y+ being on the order of 50-150

Methodology

Determining aerodynamic forces and heat transfer data on a sphere and cone is the objective to accomplish. The sphere is the same from any angle, meaning it cannot be put at an angle of attack because it yields the same result, it is only being evaluated for the drag coefficient and heat transfer. The cone is evaluated at various semi-apex angles, and angles of attack. The cone does not yield a lift coefficient at zero angle of attack, only when the angle of attack is greater than zero.

Drag Coefficient of a Sphere

Returning to the concept of Newtonian impact theory, a body in a fluid flow only accounts for the particles that impact the frontal area of the body since the particles cannot turn around and impact the back area of the body. Therefore, the back area of the body does not have any impact pressure, and the pressure on this area can be assumed to be ambient, $p = p_\infty$. Hence, the impact area on a sphere is only the frontal area, a hemisphere. The drag is calculated by integrating over the front half of the sphere, substituting the difference of surface pressure and free stream pressure. The pressure differences are substituted using Newtonian Theory equation, listed as Eq. (4). Once the drag is obtained it can be non-dimensionalized to determine the drag coefficient. The analytical calculations can be found in Appendix 1.

Heat Transfer of a Sphere

Heat transfer was determined by obtaining the heat flux utilizing Eq. (18) for a sphere. The heat transfer varies as the Mach number increase, as well as the radius of the sphere increases. The free stream conditions used were at sea level; such as temperature, pressure and density. The temperature at the shock wave depended on the Mach and radius of the sphere, which determines the shock layer thickness. As the radius of the sphere varies, the shock layer thickness varies as well having an effect on the heat flux into the sphere. When the shock layer is greater there is more air in between the detached shock wave and the surface of the body, which could help reduce the heat flux, as there is a larger heating of the air and smaller heating of the body.

Lift and Drag Coefficients of a Sharp Cone

As already mentioned, a body in a fluid flow only accounts for the particles that impacts the frontal area and the back area does not have any impact pressure. When a sharp cone is at zero angle of attack, the whole cone has an impact pressure; hence it also has a coefficient of pressure. As the cone is at zero angle of attack the flow impact is the same everywhere. The drag coefficient for a cone at zero angle of attack can be determined using Newtonian theory by determining the drag force due to pressure over the total surface area of the cone.

When the cone is at an angle of attack the flow will impact the entire cone as well as if the angle of attack is smaller or equal to the semi apex angle of the cone. Once the angle of attack is greater than the semi apex angle, the top part of the cone will not be impacted by the fluid flow, therefore that section of the cone will have a $C_p = 0$, as is it defined in Newtonian theory. The pressure coefficient at any point in the cone can be

determined by using Eq. (4) and Eq. (17), which is a function of the semi-apex angle in a circular cone, ε, angl e of attack, α, and the meridian angle, ϕ, measured from the windward to leeward. The angle at which the flow does not impact the surface is determined by:

$$\cos^{-1}\left[\frac{\quad}{\quad}\right] \qquad \text{Eq. (20)}$$

Eq. (20) is the limit at which the pressure coefficient is integrated to determine the coefficient of normal force and lift coefficient. The complete analytical calculations to determine coefficients of lift and drag can be found in Appendix 1.

Heat Transfer of a Sharp Cone

The heat flux for a cone was determined as a function of the semi-apex angle, using Eq. (19). To determine the enthalpy it was necessary to use oblique shock theory and exact method tables from ref [4] and [5] to determine the temperature at the shock with respect to the free stream temperature. As the Mach value increases, the temperature at the shock wave also increases having an effect on the static enthalpy used to determine the heat flux. The free stream conditions used were sea level, such as the density and pressure.

STAR CCM+ Set Up

Procedure

The first step in the simulation is creating the geometry and determining a domain where the flow will be analyzed. In the cases simulated, the object being analyzed (sphere or cone) was placed inside a domain (box) where each side is specified as an inlet, outlet or symmetry. The domain was significantly larger, about 20 times the length on each

side, than the object of interest to avoid the walls to have an affect on the final results.

The second step was to set up the boundary conditions of the domain, with an inlet, outlet, symmetry plane(s), wall(s) and far field. The far field boundary is set to 'free stream' boundary condition type. Angles of attack are defined by changing the far field boundary condition flow direction, not the orientation of the body. Half-body with a symmetry plane was used to reduced simulation time.

The thirds step, proceeding from the boundary conditions, is to set up the physics and meshing initial conditions on the geometry and boundary conditions of the domain. The initial conditions for the set ups being analyzed were as follows:

- Three Dimensional
- Steady
- Gas (Air with density and dynamic viscosity of each altitude)
- Coupled Flow
- Real Gas
- Coupled Energy (Used to determined heat transfer)
- Turbulent
- SST K-Omega model
- Reynolds-Averaged Navier-Stokes
- All y+ Wall Treatment

The fourth step, once all the initial conditions have been specified, is to proceed and do the surface mesh followed by a volume mesh of the geometry and domain. The mesh will be accomplished using all the initial condition values specified in the previous step.

The fifth step is to specify the data to be collected from the simulation using the 'reports' tab on the drop tree, such as the lift (cone), drag and heat transfer coefficients.

Results

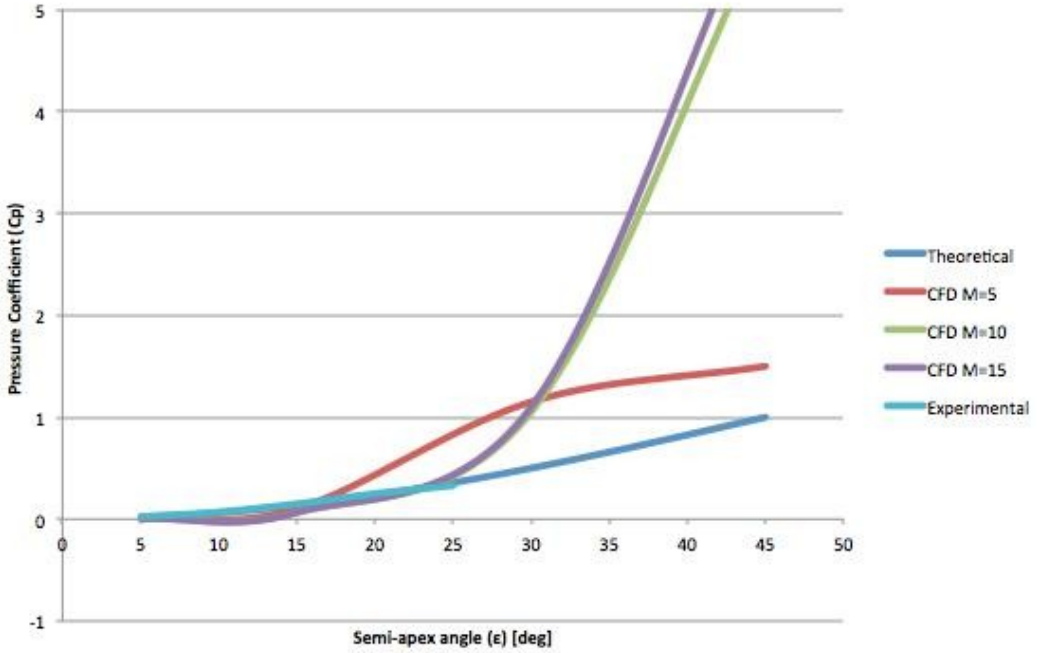

Figure 3: Pressure Coefficient distribution as a function of sharp cone Semi-apex angle (ε), comparing various methods at zero angle of attack ($\alpha = 0^o$)

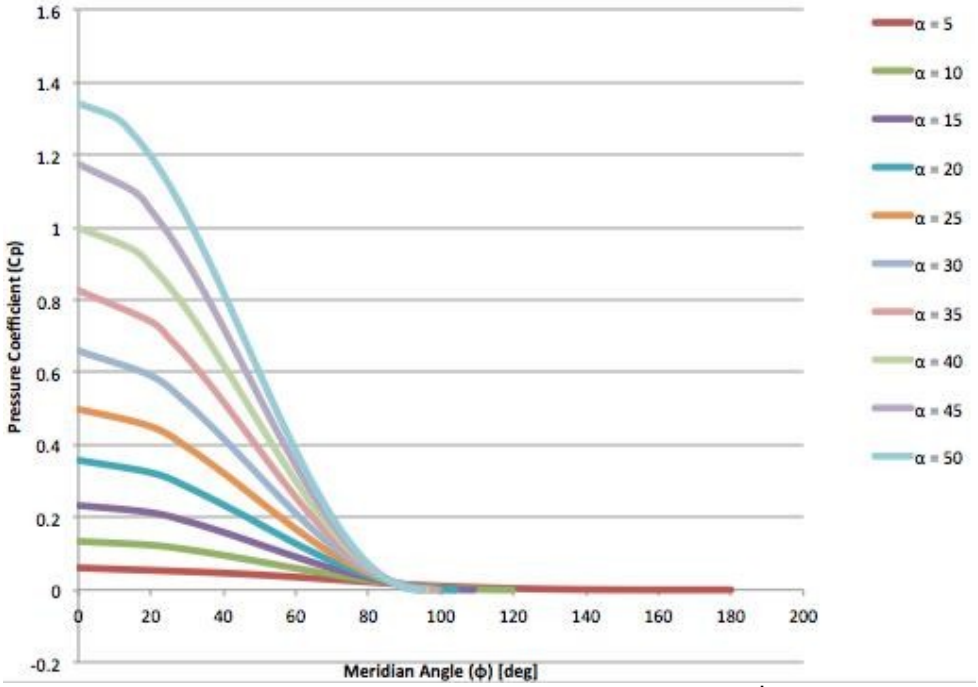

Figure 4: Pressure Coefficient distribution as a function of meridian angle (ϕ) for a five-degree semi-apex angle cone ($\varepsilon=5^o$) at various angles of attack (α)

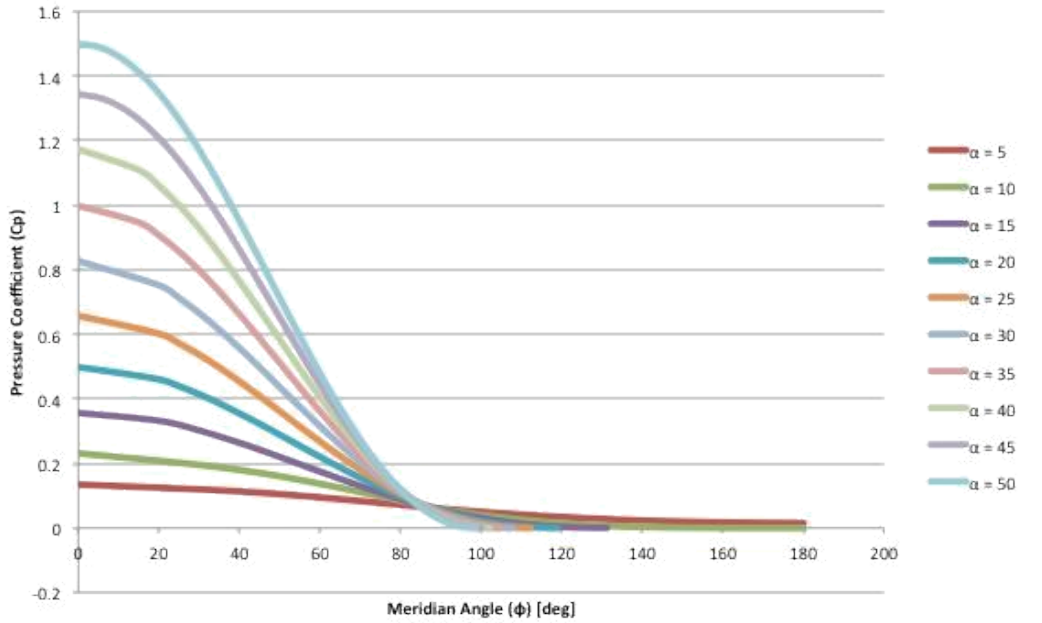

Figure 5: Pressure Coefficient distribution as a function of meridian angle (ϕ) for a ten-degree semi-apex angle cone ($\varepsilon=10^{o}$) at various angles of attack (α)

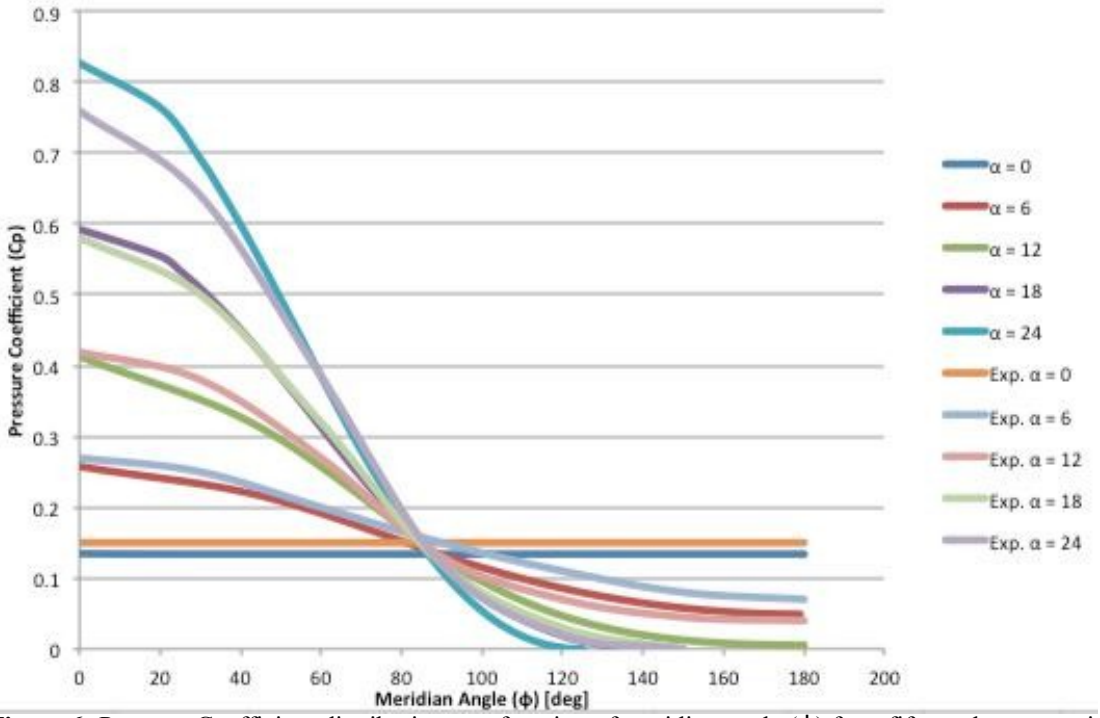

Figure 6: Pressure Coefficient distribution as a function of meridian angle (ϕ) for a fifteen-degree semi-apex angle cone ($\varepsilon=15^{o}$) at various angles of attack (α)

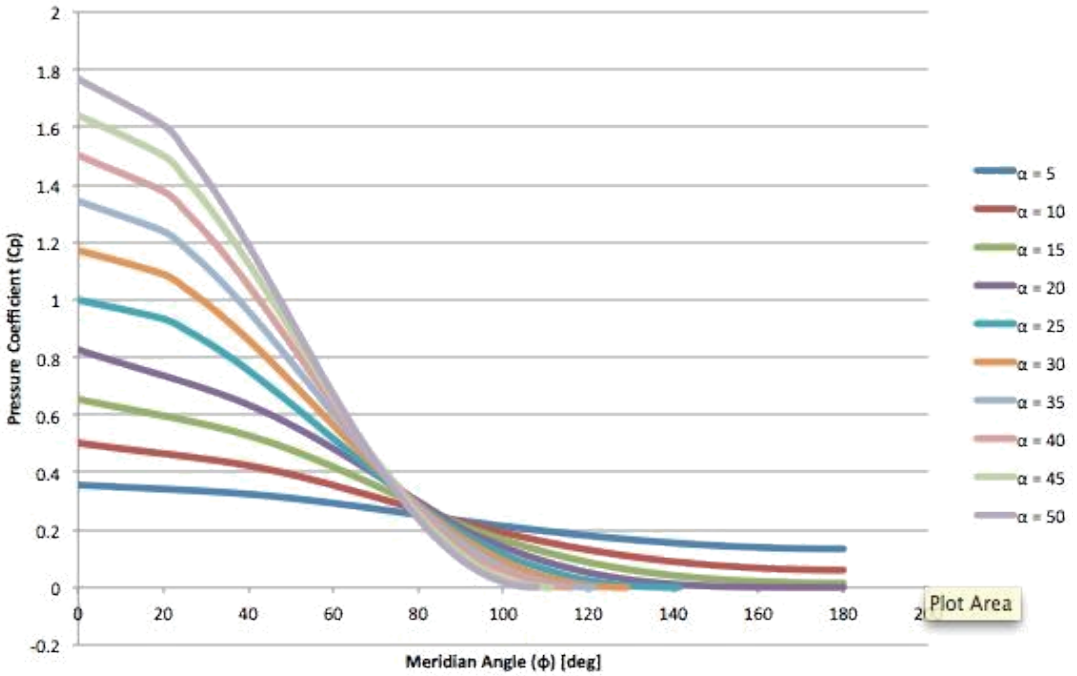

Figure 7: Pressure Coefficient distribution as a function of meridian angle (ϕ) for a twenty-degree semi - apex angle cone ($\varepsilon=20^{o}$) at various angles of attack (α)

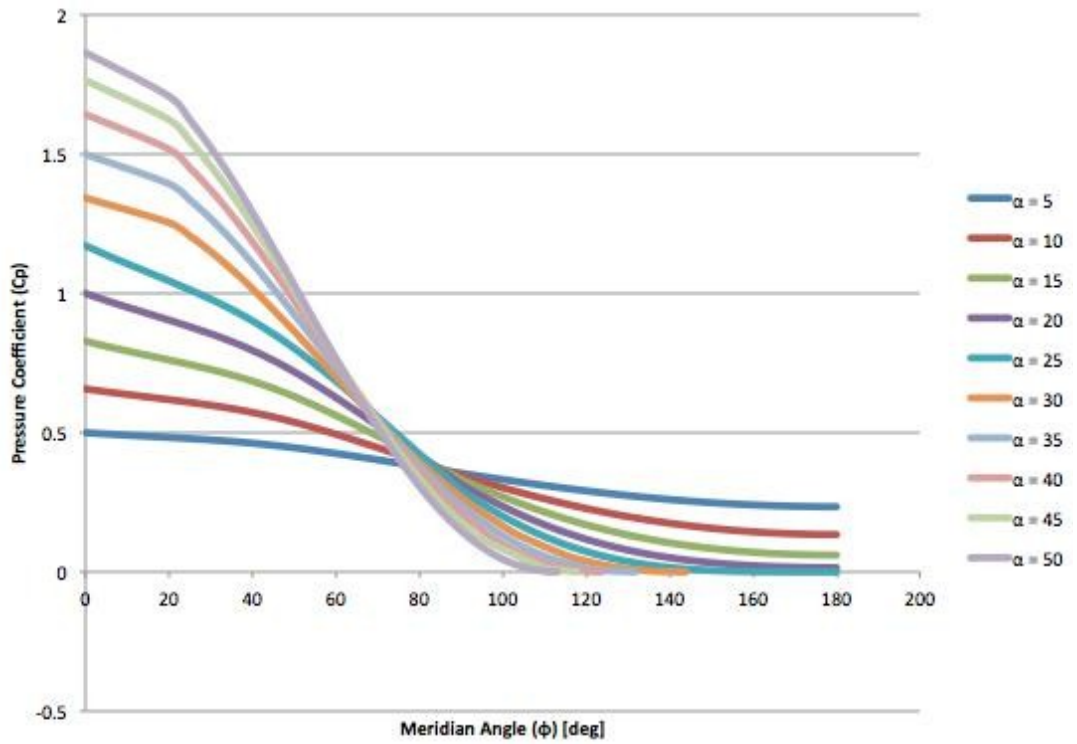

Figure 8: Pressure Coefficient distribution as a function of meridian angle (ϕ) for a twenty five-degree semi-apex angle cone ($\varepsilon=25^{o}$) at various angles of attack (α)

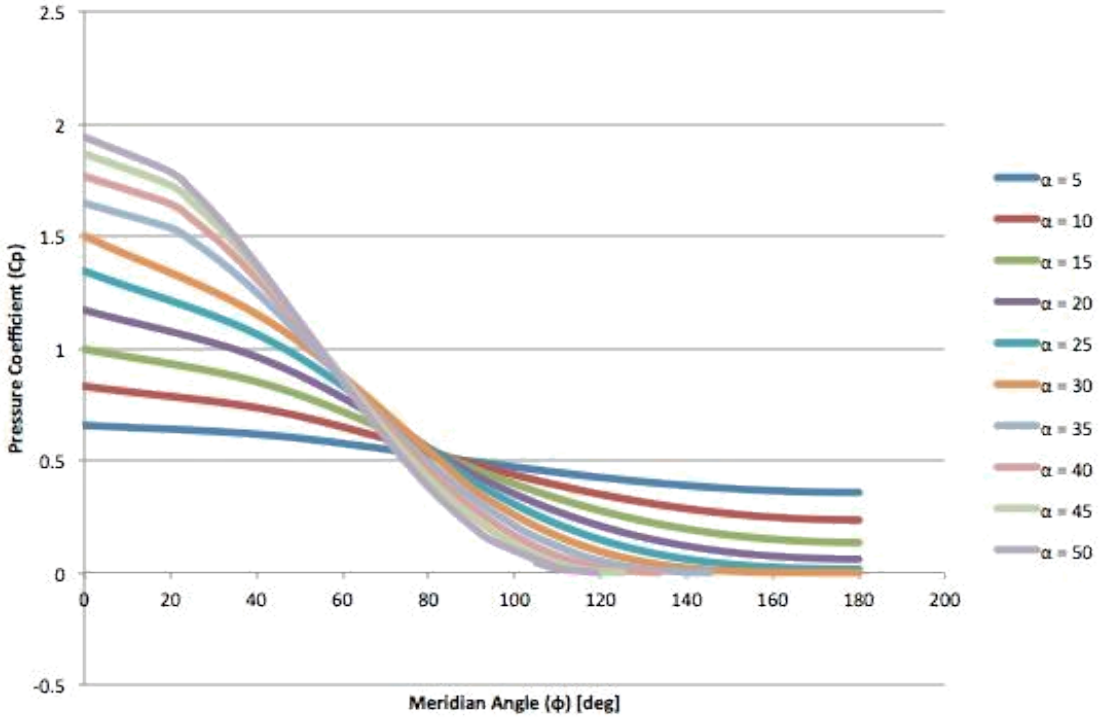

Figure 9: Pressure Coefficient distribution as a function of meridian angle (ϕ) for a thirty-degree semi-apex angle cone ($\varepsilon=30^{o}$) at various angles of attack (α)

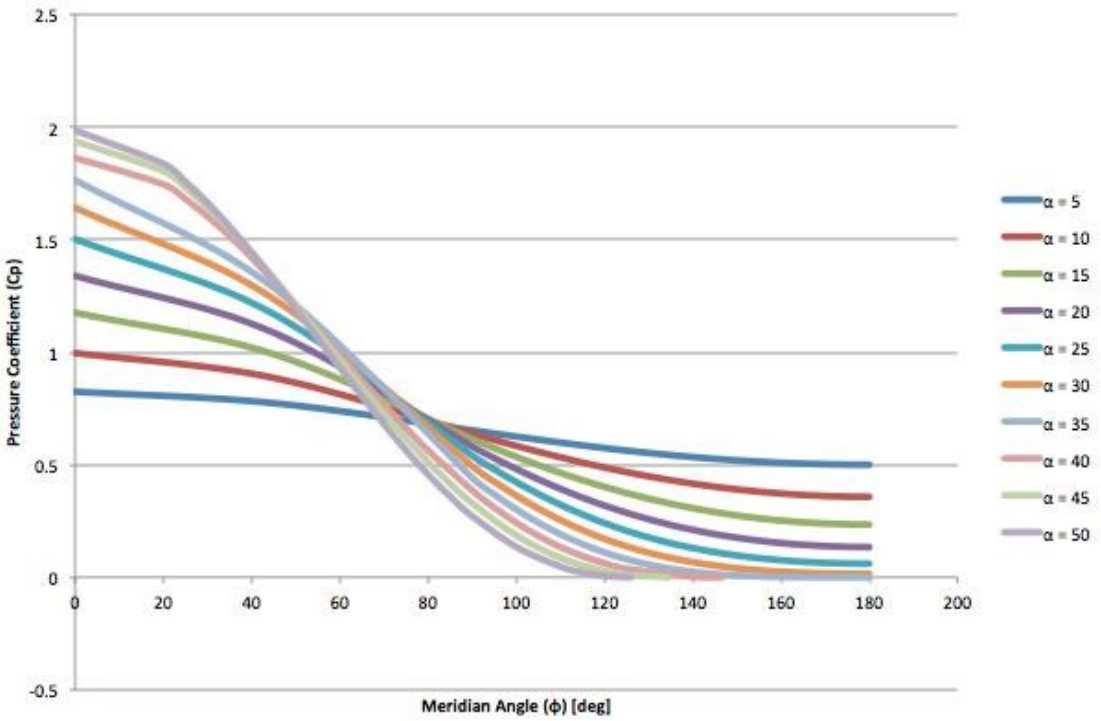

Figure 10: Pressure Coefficient distribution as a function of meridian angle (ϕ) for a thirty five-degree semi-apex angle cone ($\varepsilon=35^{o}$) at various angles of attack (α)

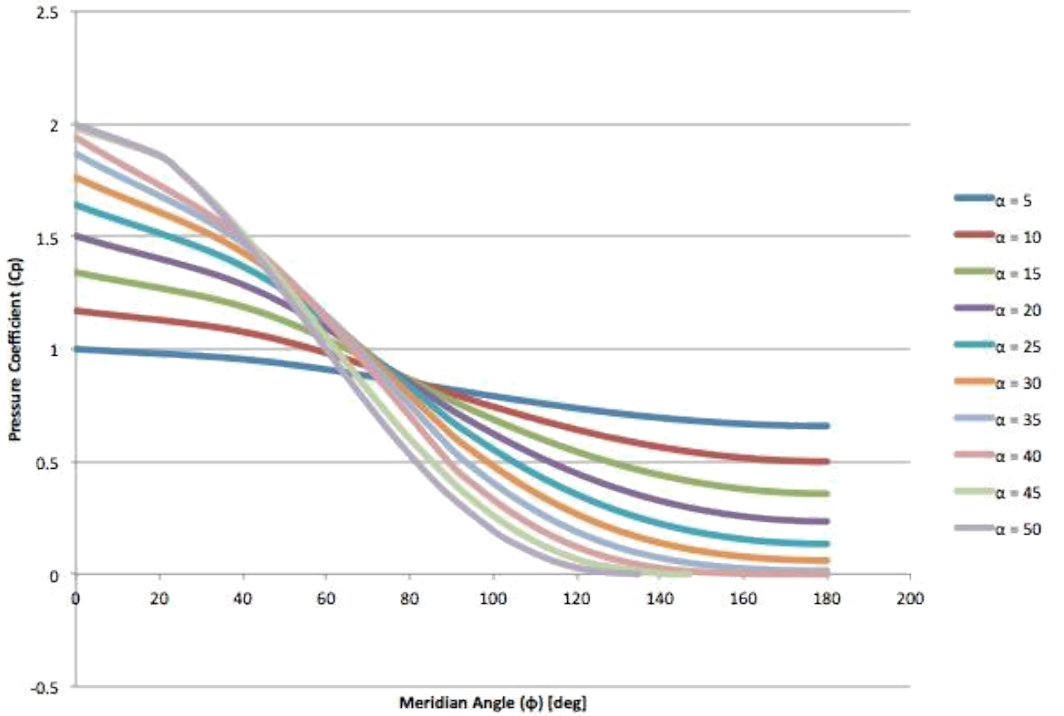

Figure 11: Pressure Coefficient distribution as a function of meridian angle (ϕ) for a forty-degree semi-apex angle cone ($\varepsilon=40^{o}$) at various angles of attack (α)

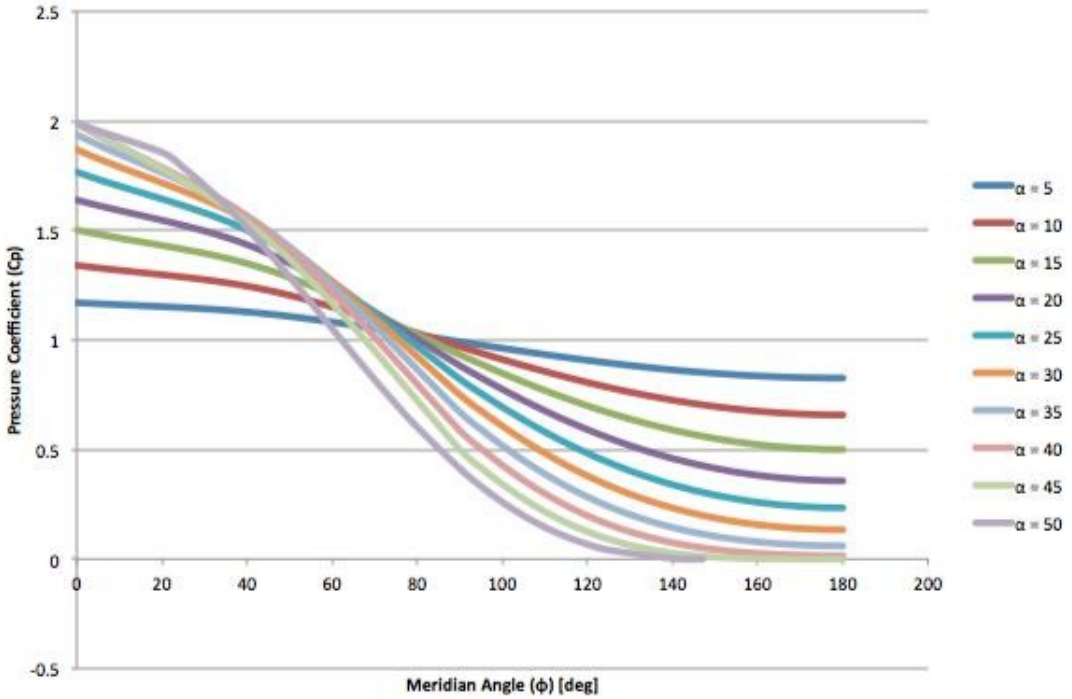

Figure 12: Pressure Coefficient distribution as a function of meridian angle (ϕ) for a forty five-degree semi-apex angle cone ($\varepsilon=45^{o}$) at various angles of attack (α)

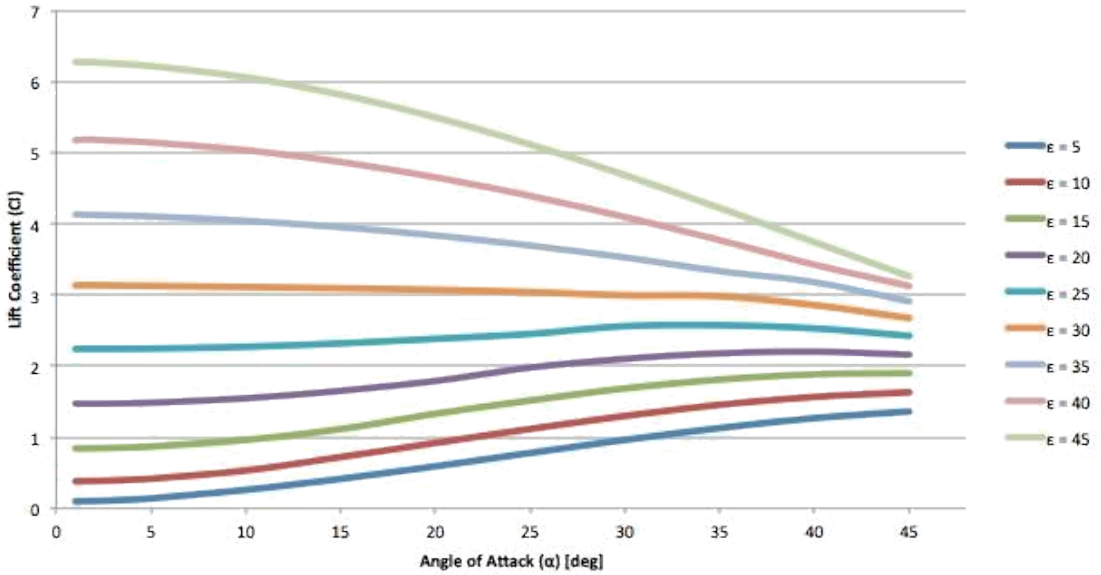

Figure 13: Lift Coefficient as a function of increasing angle of attack (α) for various semi-apex angles (ε) in a sharp cone

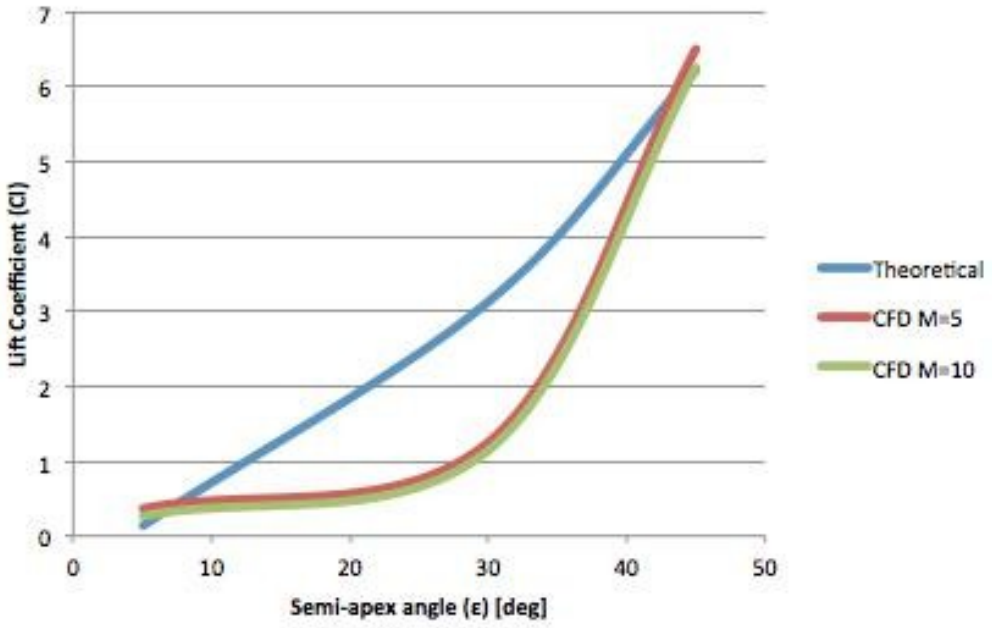

Figure 14: Lift Coefficient as a function of sharp cone semi-apex angle (ε), theoretical and CFD comparison at five-degree angle of attack ($\alpha=5^{o}$)

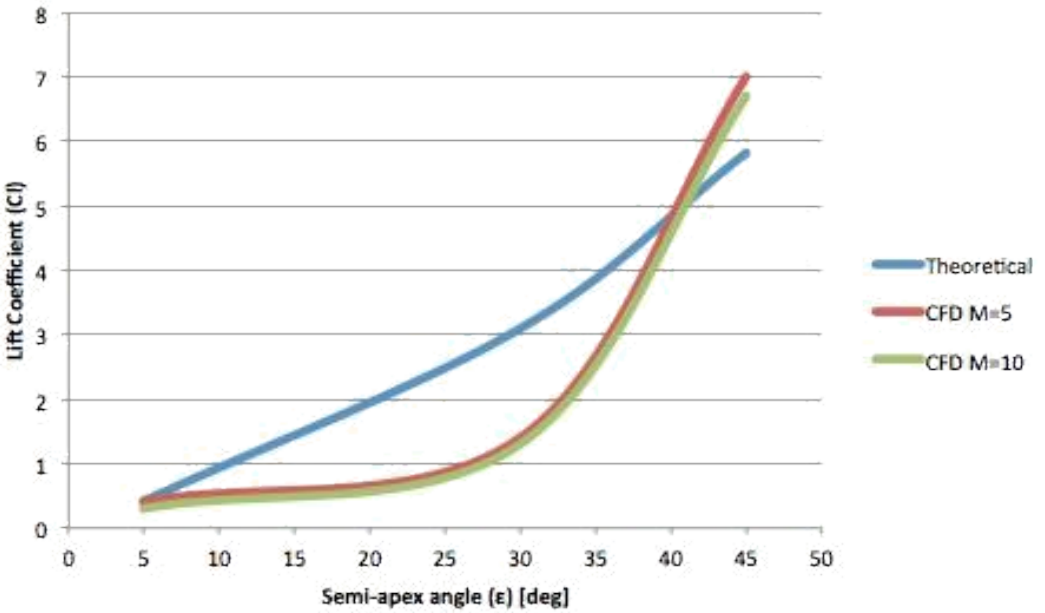

Figure 15: Lift Coefficient as a function of sharp cone semi-apex angle (ε), theoretical and CFD comparison at fifteen-degree angle of attack ($\alpha=15^{o}$)

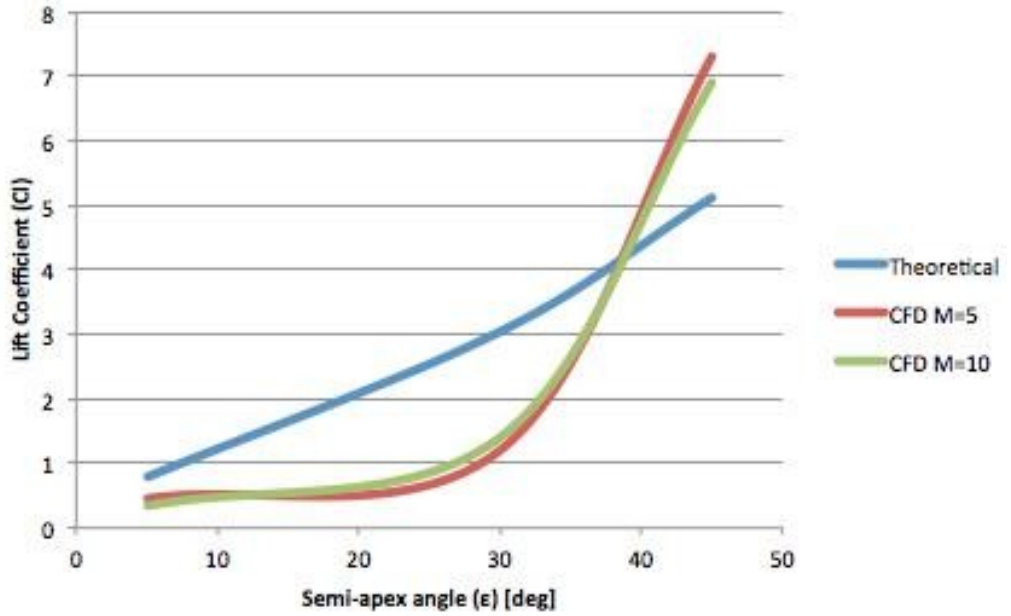

Figure 16: Lift Coefficient as a function of sharp cone semi-apex angle (ε), theoretical and CFD comparison at twenty-five-degree angle of attack ($\alpha=25^{o}$)

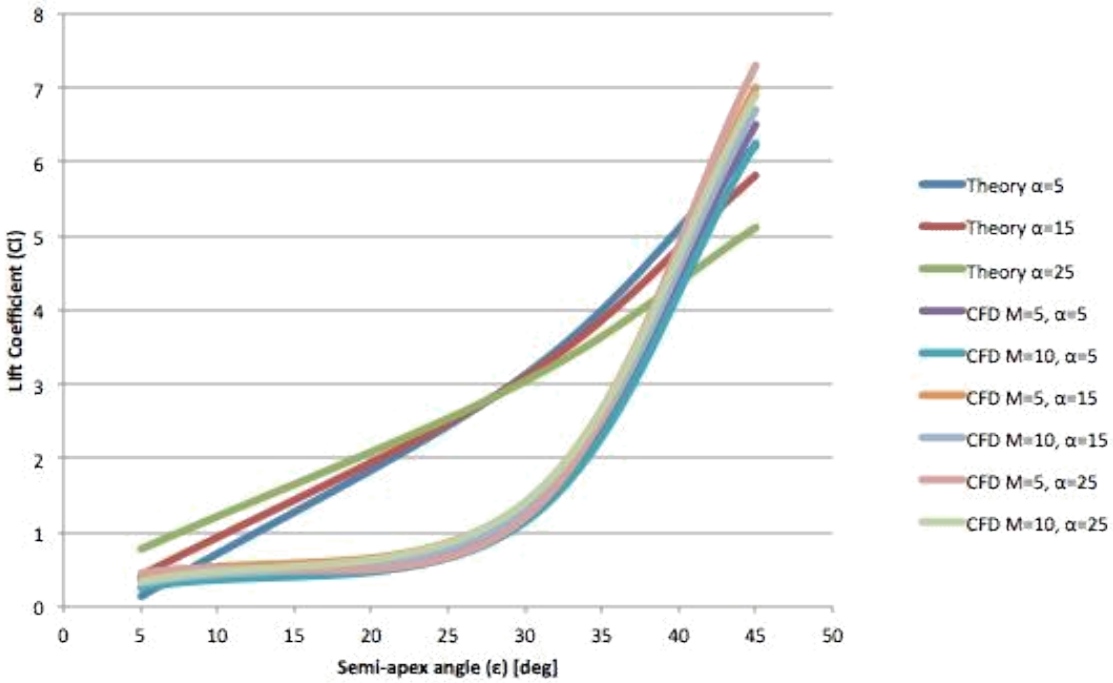

Figure 17: Lift Coefficient as a function of sharp cone semi-apex angle (ε), theoretical and CFD comparison at five, fifteen, and twenty five-degree angle of attack (α=5^{o}, 15^{o}, 25^{o})

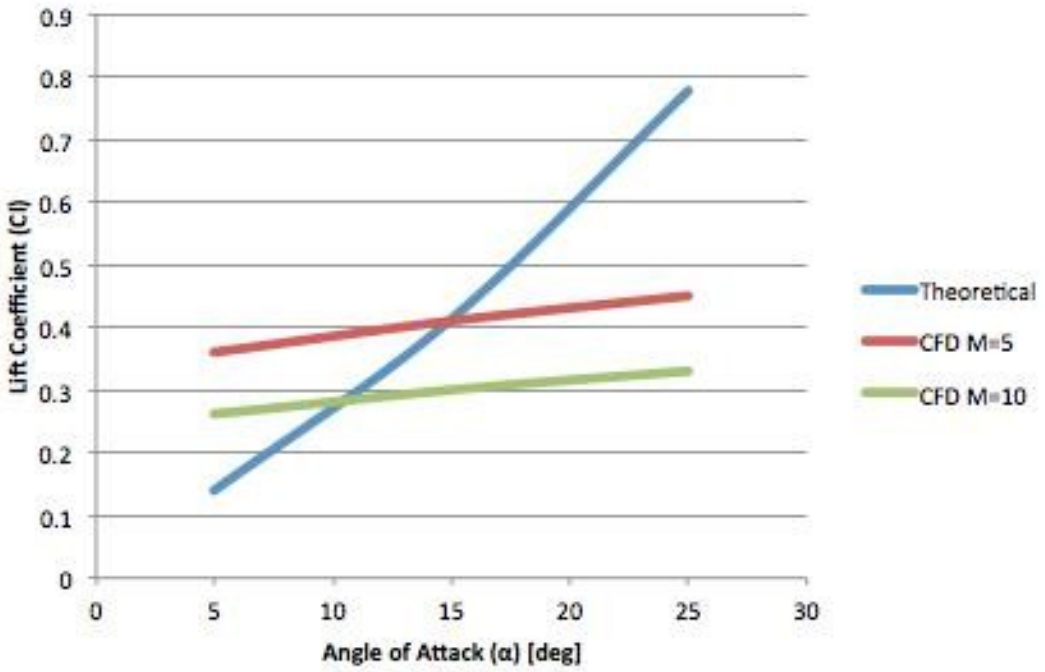

Figure 18: Lift Coefficient as a function of angle of attack (α), theoretical and CFD comparison for a five-degree sharp cone semi-apex angle (ε=5^{o})

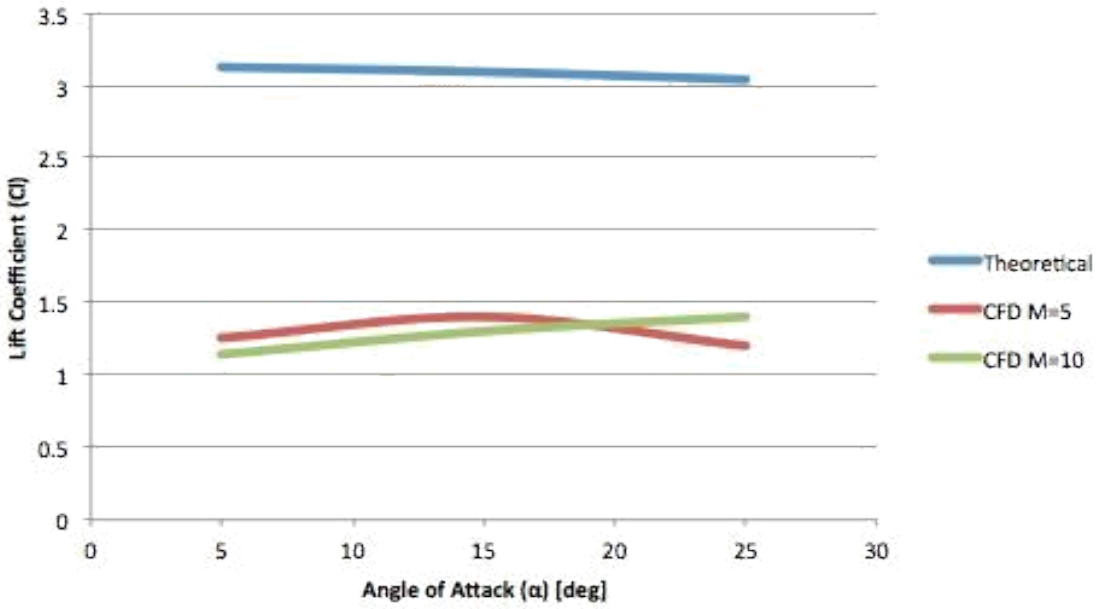

Figure 19: Lift Coefficient as a function of angle of attack (α), theoretical and CFD comparison for a thirty-degree sharp cone semi-apex angle ($\varepsilon=30^{o}$)

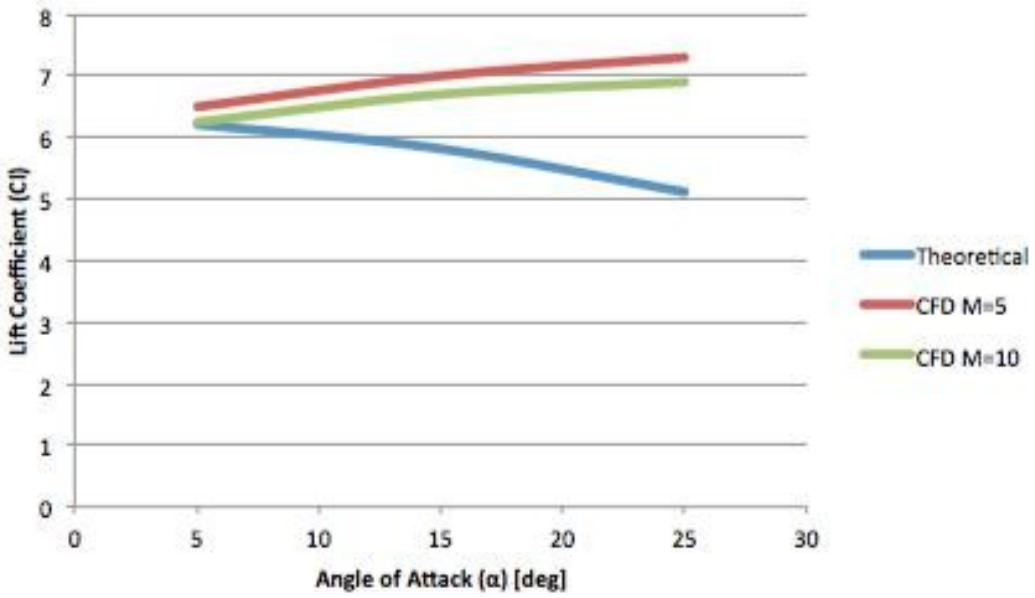

Figure 20: Lift Coefficient as a function of angle of attack (α), theoretical and CFD comparison for a forty five-degree sharp cone semi-apex angle ($\varepsilon=45^{o}$)

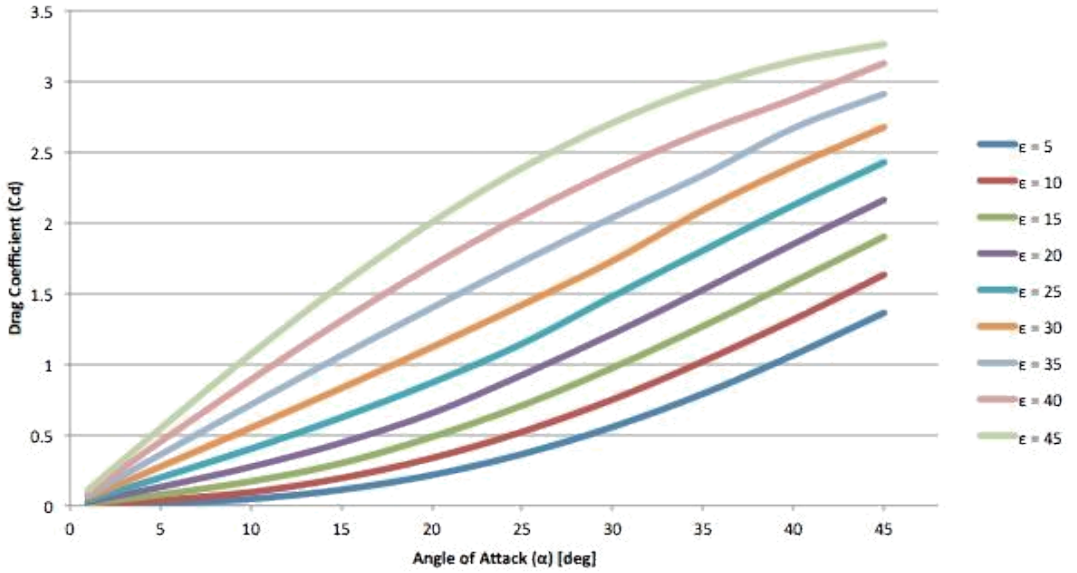

Figure 21: Drag Coefficient as a function of increasing angle of attack (α) for various semi-apex angles (ε) in a sharp cone

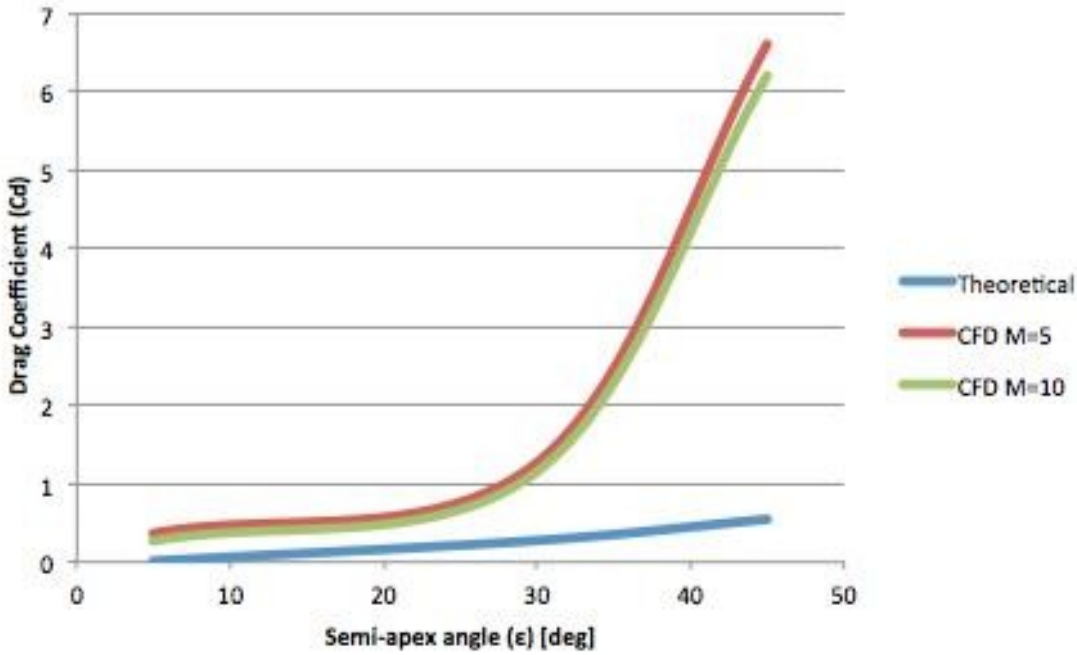

Figure 22: Drag Coefficient as a function of sharp cone semi-apex angle (ε), theoretical and CFD comparison at five-degree angle of attack ($\alpha=5^{o}$)

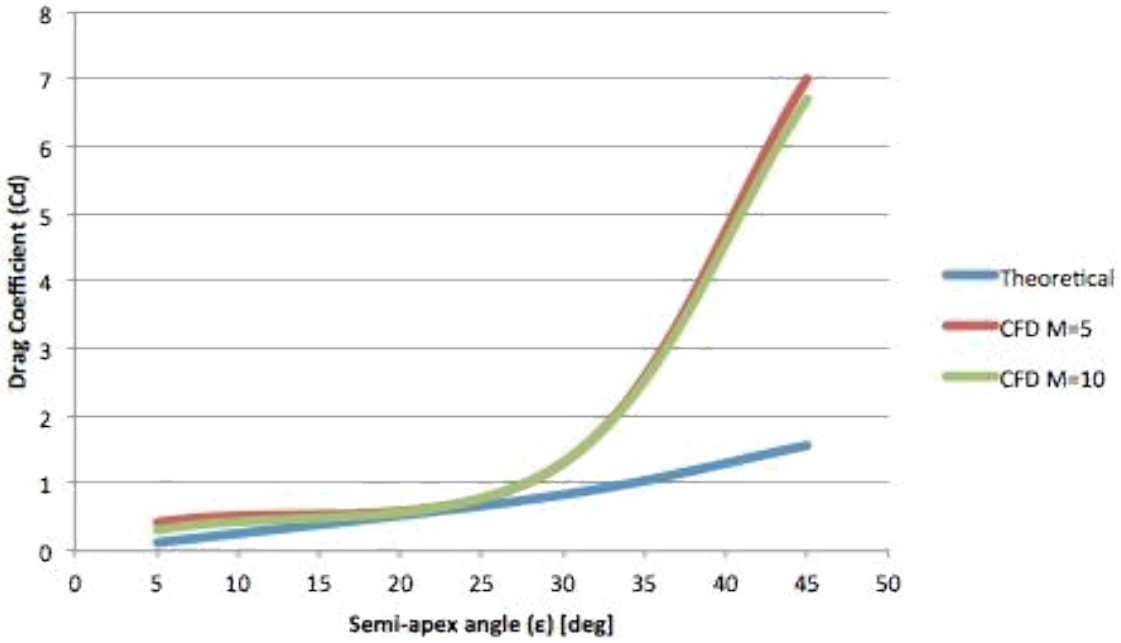

Figure 23: Lift Coefficient as a function of sharp cone semi-apex angle (ε), theoretical and CFD comparison at fifteen-degree angle of attack ($\alpha=15^{o}$)

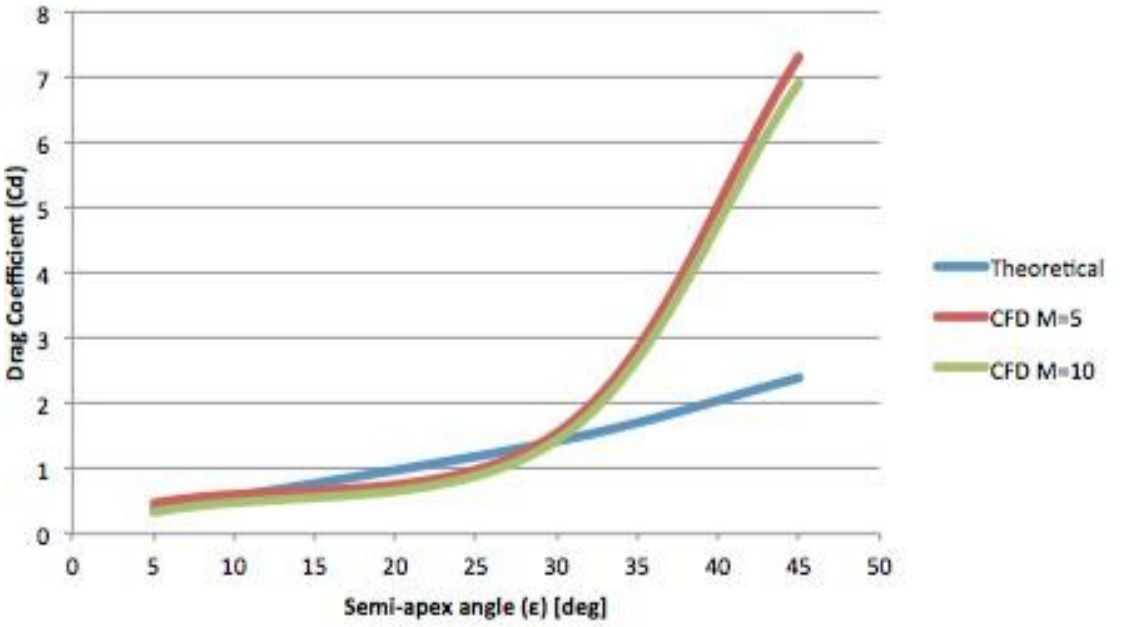

Figure 24: Lift Coefficient as a function of sharp cone semi-apex angle (ε), theoretical and CFD comparison at twenty-five-degree angle of attack ($\alpha=25^{o}$)

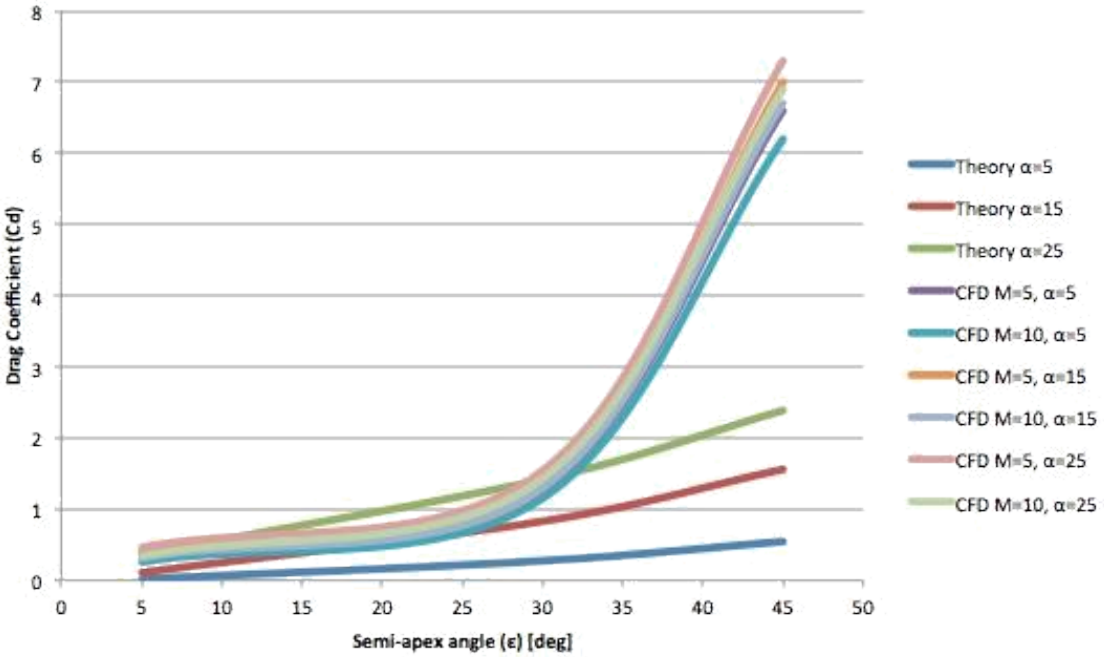

Figure 25: Drag Coefficient as a function of sharp cone semi-apex angle (ε), theoretical and CFD comparison at five, fifteen, and twenty five-degree angle of attack ($\alpha=5^o$, 15^o, 25^o)

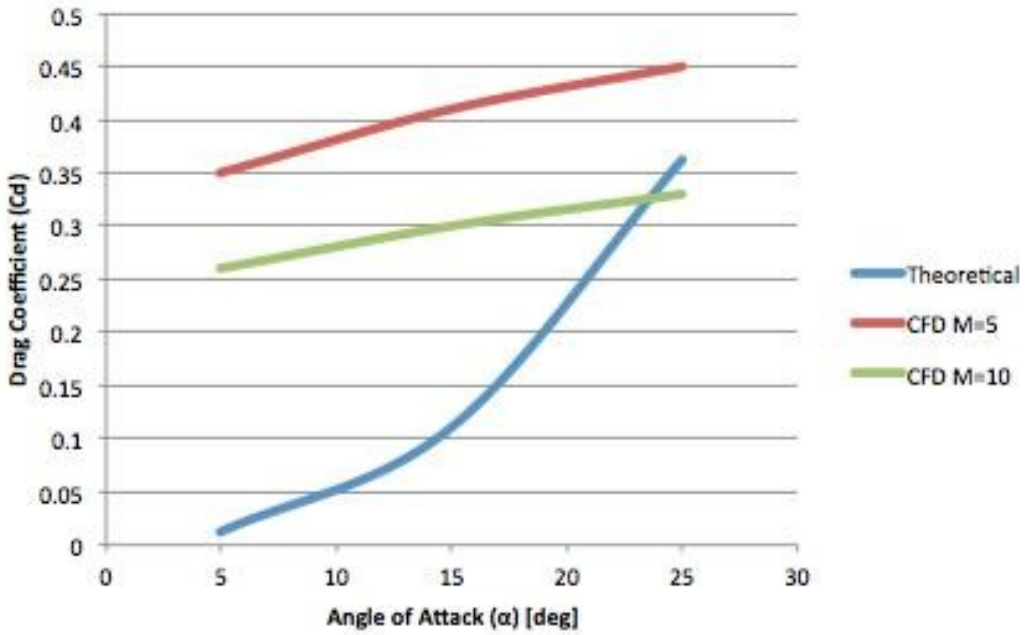

Figure 26: Drag Coefficient as a function of angle of attack (α), theoretical and CFD comparison for a five-degree sharp cone semi-apex angle ($\varepsilon=5^o$)

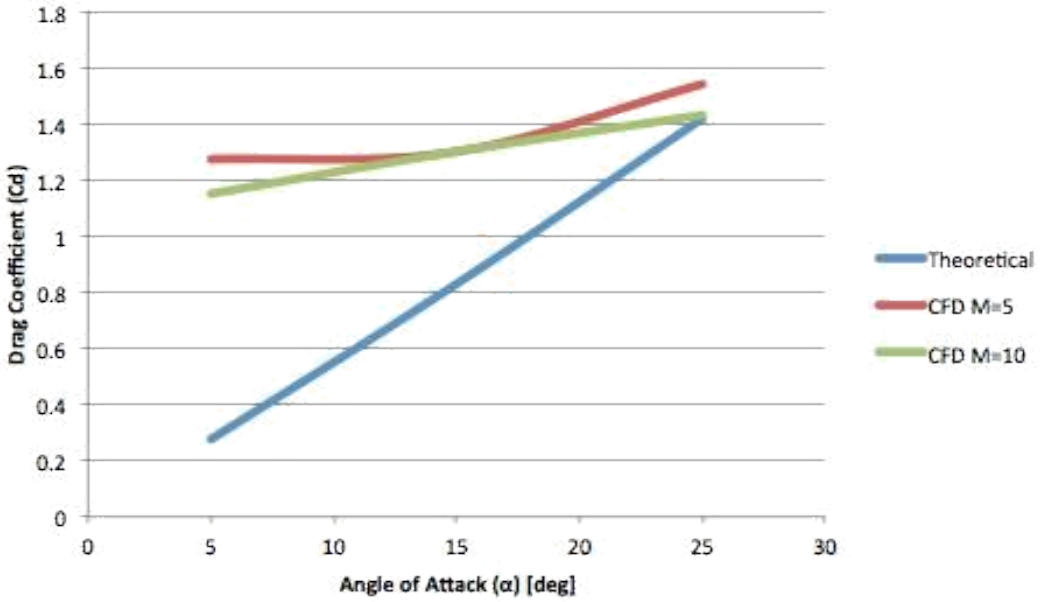

Figure 27: Drag Coefficient as a function of angle of attack (α), theoretical and CFD comparison for a thirty-degree sharp cone semi-apex angle ($\varepsilon=30^{o}$)

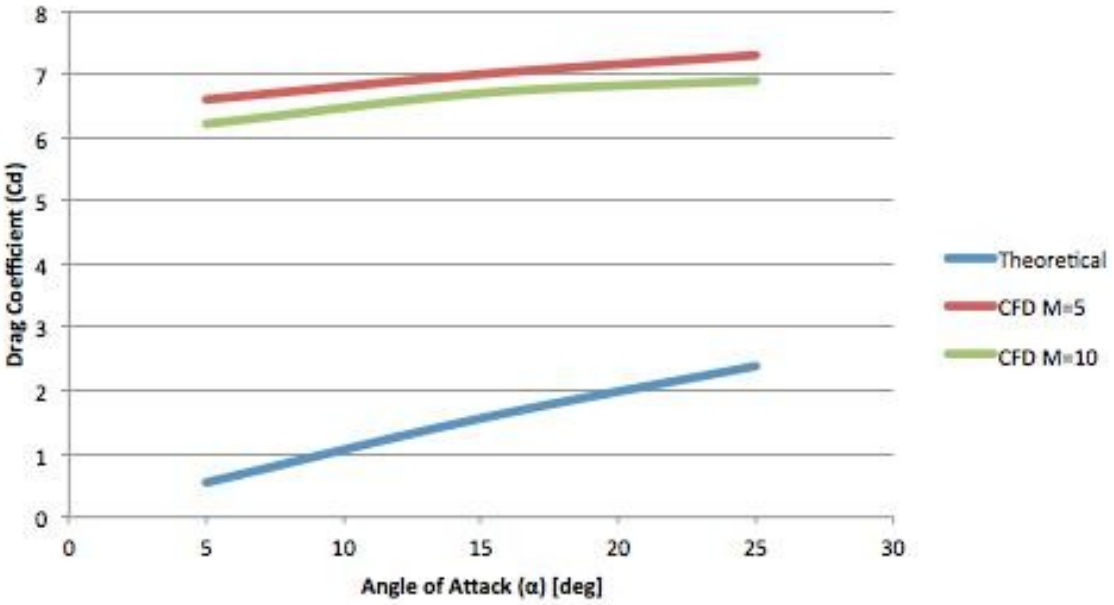

Figure 28: Drag Coefficient as a function of angle of attack (α), theoretical and CFD comparison for a forty five-degree sharp cone semi-apex angle ($\varepsilon=45^{o}$)

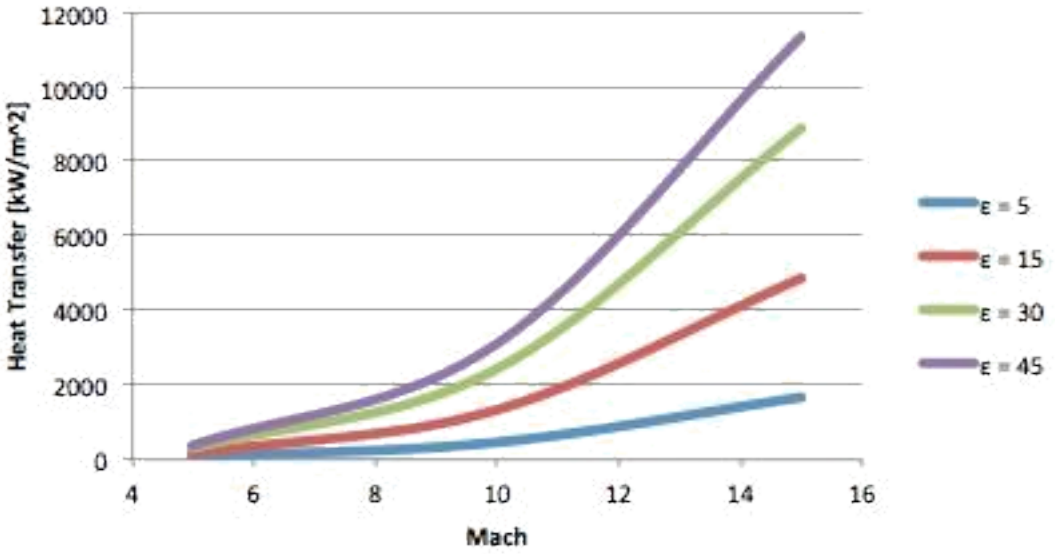

Figure 29: Theoretical Heat Transfer as a function of Mach number and semi-apex angles (ε), for a cone

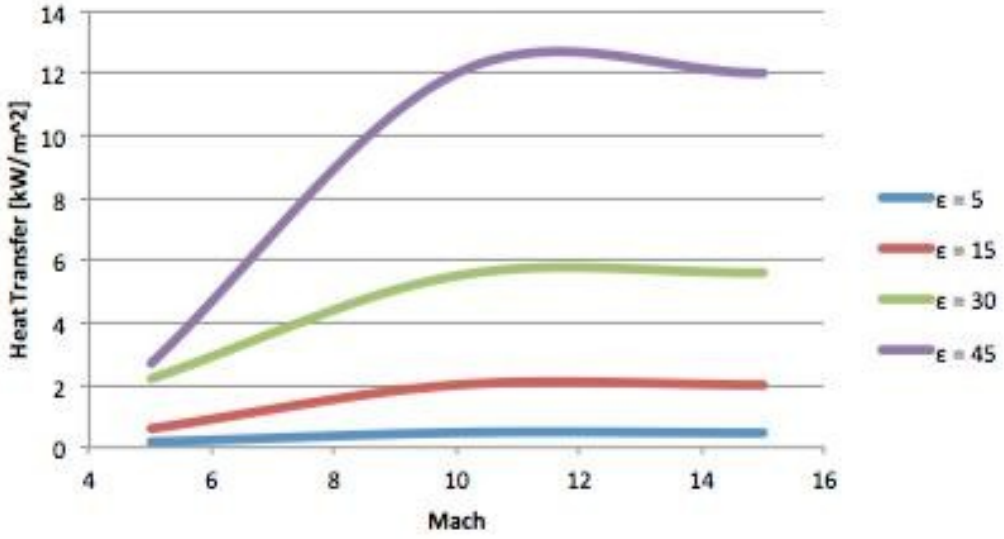

Figure 30: CFD Simulation Heat Transfer as a function of Mach number and semi-apex angles (ε), for a cone

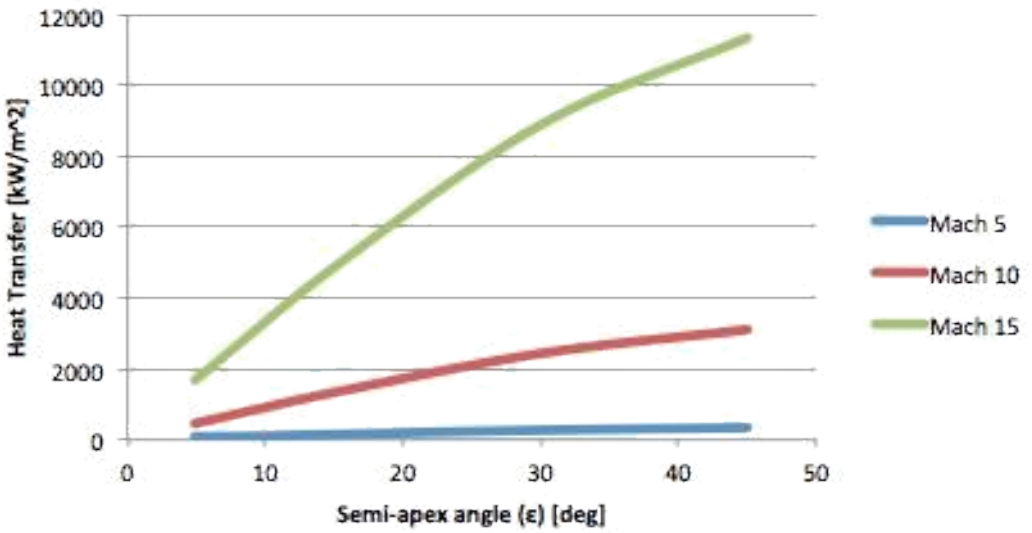

Figure 31: Theoretical Heat Transfer as a function of semi-apex angle (ε) for various Mach numbers

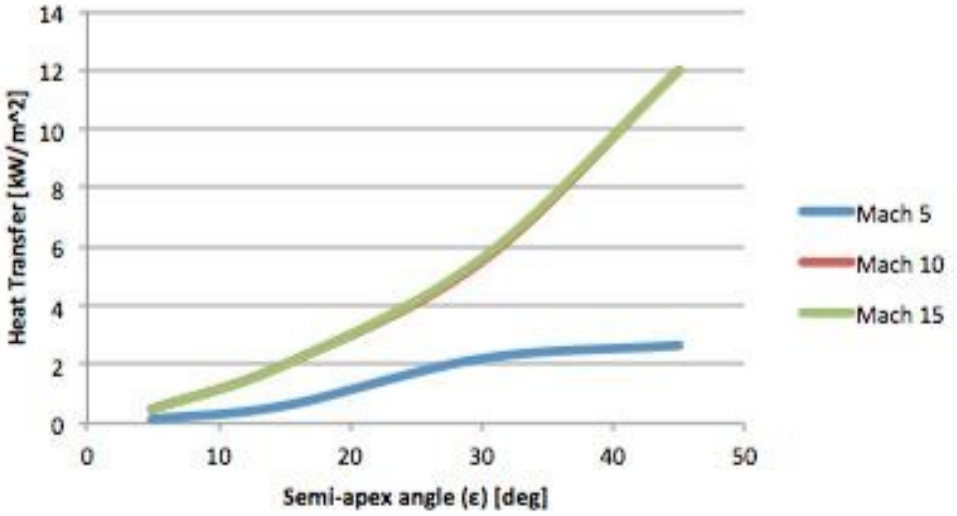

Figure 32: CFD Simulation Heat Transfer as a function of semi-apex angle (ε) for various Mach numbers

SPHERE

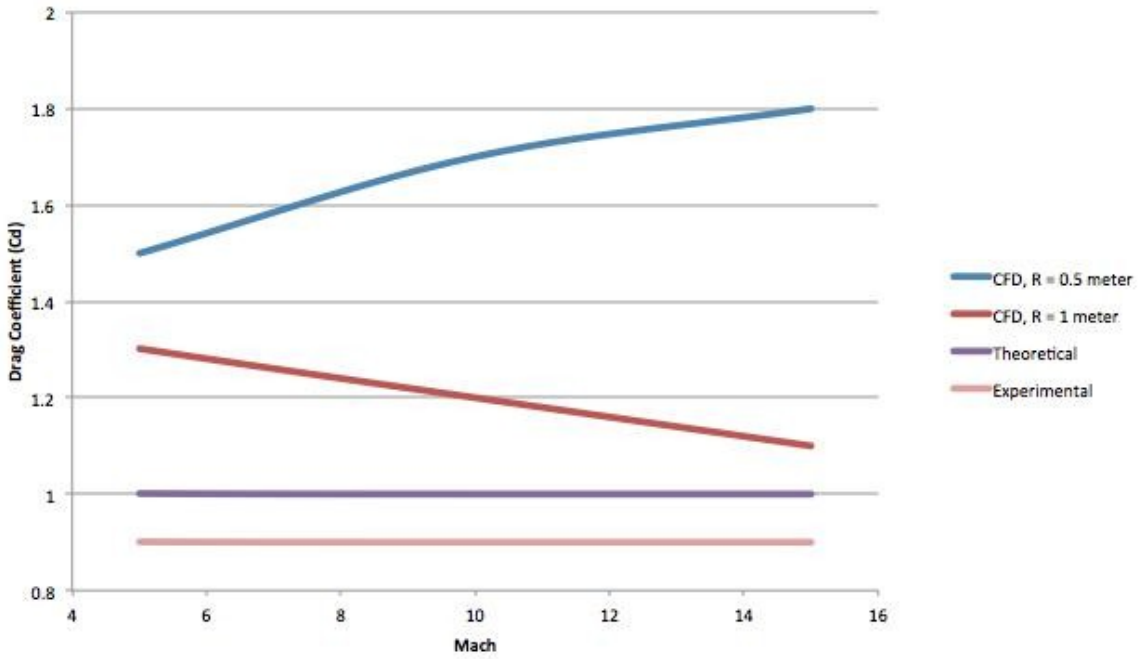

Figure 33: Drag Coefficient as a function of Mach number, theoretical and CFD comparison for 1-meter and 2-meter diameter sphere

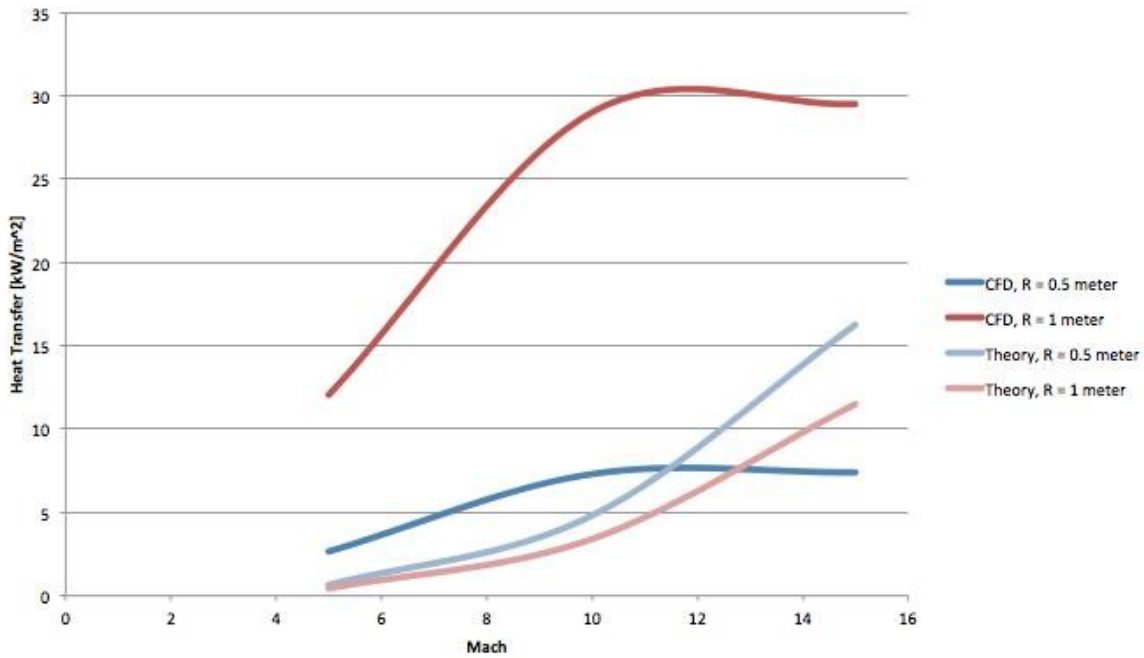

Figure 34: Heat Transfer as a function of Mach number, theoretical and CFD comparison for 1-meter and 2-meter diameter sphere

Table 1: Pressure coefficient distribution for a cone at zero angle of attack at different semi-apex angles (Figure 3)

ε	Theory	Experimental	CFD, M=5	CFD, M=10	CFD, M=15
5	0.0152	0.02	0.01	0.006	0.005
10	0.0603	0.07			
15	0.1339	0.15	0.1	0.065	0.065
20	0.2339	0.25			
25	0.3572	0.33			
30	0.5		1.15	1.05	1.1
35	0.6579				
40	0.8263				
45	1		1.5	5.8	6.25

Table 2: Theoretical lift and drag coefficients for a cone (Figure 18-20, 26-28)

ε	α	C_l	C_d
5	5	0.1384	0.0121
5	10	0.413	0.1106
5	25	0.7772	0.3624
30	5	3.126	0.2734
30	10	3.093	0.8287
30	25	3.0397	1.417
45	5	6.217	0.5439
45	10	5.816	1.558
45	25	5.114	2.385

(Figure 14-16, 22-24)

α	ε	C_l	C_d
5	5	0.1384	0.0121
5	30	3.126	0.273
5	45	6.217	0.543
15	5	0.413	0.110
15	30	3.093	0.828
15	45	5.816	1.558
25	5	0.777	0.3624
25	30	3.039	1.417
25	45	5.11	2.385

Table 3: CFD lift and drag coefficients for a cone at Mach 5 (Figure 18-20, 26-28)

ε	α	C_l	C_d
5	5	0.36	0.35
5	15	0.41	0.42
5	25	0.45	0.45
30	5	1.25	1.27
30	15	1.4	1.3
30	25	1.2	1.54

45	5	6.5	6.6
45	15	7	7
45	25	7.3	7.3

(Figure 14-16, 22-24)

α	**ε**	**C_l**	**C_d**
5	5	0.36	0.35
5	30	1.25	1.27
5	45	6.5	6.6
15	5	0.41	0.41
15	30	1.4	1.3
15	45	7	7
25	5	0.45	0.45
25	30	1.2	1.54
25	45	7.3	7.3

Table 4: CFD lift and drag coefficients for a cone at Mach 10 (Figure 18-20, 26-28)

ε	**α**	**C_l**	**C_d**
5	5	0.26	0.26
5	10	0.3	0.3
5	25	0.33	0.33
30	5	1.14	1.15
30	10	1.3	1.3
30	25	1.4	1.43
45	5	6.25	6.2
45	10	6.7	6.7
45	25	6.9	6.9

(Figure 14-16, 22-24)

α	**ε**	**C_l**	**C_d**
5	5	0.26	0.26
5	30	1.14	1.15
5	45	6.25	6.2
15	5	0.3	0.3
15	30	1.3	1.3
15	45	6.7	6.7
25	5	0.33	0.33
25	30	1.4	1.43
25	45	6.9	6.9

Table 5: Heat transfer data for cone at various semi-apex angles and Mach numbers (Figure 29 & 30)

ε	M	CFD	Theory
5	5	0.14	49.3
5	10	0.47	453.8
5	15	0.46	1661.2
15	5	0.6	144.3
15	10	2	1326.9
15	15	2	4857
30	5	2.2	263.9
30	10	5.5	2426.1
30	15	5.6	8880
45	5	2.65	337.6
45	10	12	3102.6
45	15	12	11339.6

(Figure 31 & 32)

M	ε	CFD	Theory
5	5	0.14	49.3
5	15	0.6	144.3
5	30	2.2	263.9
5	45	2.65	337.6
10	5	0.47	453.8
10	15	2	1326.9
10	30	5.5	2426.1
10	45	12	3102.6
15	5	0.46	1661.2
15	15	2	4857.2
15	30	5.6	8880
15	45	12	11339.6

Table 6: Drag coefficient for a sphere (Figure 33)

M	Theory	Experimental	R = 0.5	R = 1
5	1	~ 0.9	1.5	1.3
10	1	~ 0.9	1.7	1.1
15	1	~ 0.9	1.8	1.1

Table 7: Heat transfer for a sphere (Figure 34)

M	Theory, R = 0.5	Theory, R = 1	CFD, R = 0.5	CFD, R = 1
5	0.601	0.425	2.65	12
10	4.814	3.404	7.3	29
15	16.25	11.49	7.4	29.5

Discussion

Figure 3 shows the pressure coefficient comparison of theoretical and CFD simulation results. The comparison is for a sharp cone at $\alpha = 0$, as ε increases. The theoretical results do not account for Mach number, assuming Newtonian theory for hypersonic flow; hence, the results are valid for hypersonic Mach velocities. The CFD simulation results were calculated at Mach 5, 10 and 15. Where the pressure coefficient obtained at Mach 5 is fairly closed to the theoretical results, with the CFD value being about 30 percent higher and converging towards the theoretical result value as ε increases. The values obtained at Mach 10 and 15 are identical with theoretical results up to $\varepsilon = 25^{o}$, once ε increases beyond 25^{o} the CFD results increase very rapidly being over 6 times higher at $\varepsilon = 45^{o}$. Figure 36 illustrates experimental results, which are also being compared to Newtonian theory. Where experimental results are fairly similar to Newtonian theory and CFD results at high hypersonic Mach values. This comparison shows that Newtonian theory for hypersonic flow is only valid for slender bodies (cones), and it increases in accuracy as Mach increases, since it was not very accurate for Mach 5.

Figures 4-12 illustrate the pressure coefficient variation along the meridian angle, ϕ, in a sharp cone at increasing α. The pressure coefficient is calculated only over the surface where the flow impacts the cone directly, as stated by Newtonian theory for hypersonic flow. The pressure coefficient varies around the cone at every ϕ, as α increases. The change in pressure coefficient also occurs as the cone varies ε. When $\alpha > \varepsilon$, the top part of the cone will not be impacted by the free stream flow, and the bottom section of the cone will be impacted with higher pressure since it becomes the front part of the cone. Therefore, the area not being impacted is not accounted for when

determining pressure coefficient on the cone. As a result, the pressure force on the bottom section increases, as it can be see on the figures for $\phi = 0^o$, and it decreases as ϕ approaches 180^o. The pressure coefficient is not greatly affected at $\phi = 90^o$ since that is the angle on the side of the cone. As ε increases, the flow impacts the whole surface of the cone at $\alpha < \varepsilon$. Hence the plots show how the pressure coefficient is calculated all around the cone. For high α ($\alpha > \varepsilon$), where the pressure coefficient disappears before $\phi = 180^o$, the pressure coefficient is assumed to be zero after that point up to $\phi = 180^o$. Figure 6 illustrates pressure coefficient distribution along ϕ of a $\varepsilon = 15^o$ cone at $\alpha = 6^o$, 12^o, 18^o and 24^o, which can be compared to Figure 37 that displays experimental results of the same ϕ, ε and α values with very close results. The experimental results are also being compared to Newtonian theory, where it can be deduced that as α increases Newtonian theory over predicts the results, in comparison to experimental values.

Figures 13 & 21 show the aerodynamic force coefficients of lift, and drag as a function α, from $\varepsilon = 5^o$ to $\varepsilon = 60^o$. The aerodynamic coefficients were calculated after determining the pressure coefficient over the surface of the cone, Figure 4-12. Once the pressure coefficient is integrated over the surface area that was impacted by the flow, the normal force coefficient can be determined. The normal force coefficient is then used to determine the coefficients of lift and drag. As shown in Figure 13, lift coefficient increases as α increases if $\varepsilon \leq 20^o$. When $20^o < \varepsilon < 30^o$ the lift coefficient begins to decrease after $\alpha = 30^o$. Once $\varepsilon > 30^o$ the lift coefficient decreases as α decreases, due to a major increase in surface area of the cone being impacted causing more drag. Figure 21 illustrates that the drag coefficient increases as α and ε incr eases. As α increases the surface area being impacted by the flow increases as well, hence, causing an increase in

drag. For a cone with $\varepsilon > 45^o$ the drag coefficient peaks at $\alpha = 35 - 40^o$, having a small decrease for $\alpha \cong 60^o$.

Figures 14-16 show the comparison of lift coefficient as a function of ε between the theoretical and CFD simulation results for $\alpha = 5^o$, 15^o and 25^o. The CFD simulations were performed at Mach 5 & 10. As ε increases the theoretical results yield a lower maximum lift coefficient for high ε, such as $\varepsilon > 35^o$, as α increases where the lift coefficient increases slowly for $\varepsilon \leq 25^o$, and increases very rapidly for $\varepsilon > 30^o$. Meanwhile, the CFD results at Mach 5 & 10 are very similar; a small increase in lift coefficient is noticeable as α increases. It is clear that Mach value does not have much of an effect in the lift coefficient as ε and α vary. A small increase in lift coefficient is seen as α increases, but the major increase is seen as ε increases in cones with $\varepsilon > 30^o$.

Figure 17 compiles all the theoretical and CFD results at $\alpha = 5^o$, 15^o and 25^o for lift coefficient as a function of ε, up to $\varepsilon = 45^o$. Where Mach 5 & 10 results are very close together with a lift coefficient much lower than the theoretical for $\varepsilon \leq 40^o$. At $\varepsilon \cong 40^o$ the theoretical and CFD results converge together for all ε values with CFD lift coefficient results exceeding the theoretical for $\varepsilon > 40^o$.

Figures 18-20 illustrate the comparison of lift coefficient as a function of α between the theoretical and CFD simulation for $\varepsilon = 5^o$, 30^o and 45^o. In Figure 18 the theoretical lift coefficient for $\varepsilon = 5^o$ cone is the same as the CFD results for Mach 5 & 10 at $\alpha = 15^o$ & 10^o respectively. In Figure 19, results for a cone with $\varepsilon = 30^o$, the theoretical result is double than the CFD results. In Figure 20, results for a cone with $\varepsilon = 45^o$, the theoretical result are higher than the theoretical and increasing in difference as α increases with similar results only for $\alpha = 5^o$.

Figures 22-24 show the comparison of drag coefficient as a function of ε between the theoretical and CFD simulation for $\alpha = 5^o$, 15^o and 25^o. The CFD results for $\alpha = 5^o$ are higher than the theoretical, where the drag increases very rapidly for $\varepsilon > 30^o$ resulting in higher CFD drag coefficient than the theoretical. For $\alpha = 15^o$ the CFD drag coefficient results are very similar to the theoretical value up to $\varepsilon = 25^o$, with drag value increasing very rapidly for $\varepsilon > 25^o$. The CFD results for $\alpha = 25^o$ drag coefficient is very similar to the theoretical value up to $\varepsilon = 30^o$, with drag value increasing very rapidly for $\varepsilon > 30^o$. The CFD results at Mach 5 & 10 are very similar, with Mach value not displaying much of an effect on the drag coefficient.

Figure 25 compiles all the theoretical and CFD results at $\alpha = 5^o$, 15^o and 25^o for drag coefficient as a function of ε, up to $\varepsilon = 45^o$. Where Mach 5 & 10 results are not very different, where the CFD drag coefficient results are very similar to the theoretical results for $\varepsilon \leq 30^o$, with CFD drag coefficient results exceeding the theoretical results for $\varepsilon > 30^o$.

Figure 26-28 illustrate the comparison of drag coefficient as a function of α between the theoretical and CFD simulation for $\varepsilon = 5^o$, 30^o and 45^o. In Figure 26 the theoretical drag coefficient for a $\varepsilon = 5^o$ cone is much lower than the CFD results for Mach 5 & 10, with equal results only at $\alpha = 23^o$ for Mach 10. In Figure 27, results for a cone with $\varepsilon = 30^o$, the theoretical results are lower than the CFD results, with equal results only at $\alpha = 25^o$ for Mach 10. In Figure 28, results for a cone with $\varepsilon = 45^o$, the CFD results yield a drag coefficient much higher than the theoretical results, with CFD results more than six times higher than theoretical for $\alpha < 12^o$, and about three times higher for $\alpha > 15^o$.

Figures 29 & 30 illustrate the heat flux [kW/m^2] as a function of Mach for theoretical calculations assuming Newtonian flow and CFD simulation for $\varepsilon = 5^o$, 15^o, 30^o and 45^o. The theoretical calculations show that as ε increases the heat flux increases as Mach increases, with approximate values of 1900, 5000, 9000, and 11300 [kW/m^2] for $\varepsilon = 5^o$, 15^o, 30^o and 45^o respectively, at Mach 15. Similarly, the CFD results show that as ε increases the heat flux also increases as Mach increases, with approximate values of 0.5, 2, 6, and 12 [kW/m^2] for $\varepsilon = 5^o$, 15^o, 30^o and 45^o respectively, at Mach 15. The theoretical results yield a much higher heat flux transfer into the body than the CFD results. This shows how using exact methods to calculate the heat flux is not an accurate method for hypersonic flow heat transfer approximation.

Figures 31 & 32 illustrate the heat flux [kW/m^2] as a function of ε for a sharp cone for theoretical calculations assuming Newtonian flow and CFD simulation for Mach 5, 10 &15. The theoretical calculations show that as ε increases the heat flux increases as Mach increases, with approximate values of 300, 3200, and 11300 [kW/m^2] for Mach 5, 10 and 15 respectively, at $\varepsilon = 45^o$. Likewise, the CFD results show that as ε increases the heat flux also increases as Mach increases, with approximate values of 2.5, 12, and 12 [kW/m^2] for Mach 5, 10 and 15 respectively, at $\varepsilon = 45^o$. The theoretical results yield a much higher heat flux transfer into the body than the CFD results.

Figure 33 shows the theoretical and CFD drag coefficient results for a sphere of two different diameters. The theoretical results yield a drag coefficient of about one, as shown in Figure 35, where the CFD results yield a higher drag value, which increases as Mach increases. For a one-meter diameter sphere, the drag coefficient diverges as Mach increases, where as for a two-meter diameter sphere, the drag coefficient converges

towards the value calculated as Mach increases, assuming Newtonian theory. Consequently, showing that Newtonian theory's accuracy increases as Mach increases to very high hypersonic Mach values. A potential discrepancy in the CFD results for a one-meter diameter sphere is the probability of cavitation, the reduction of local pressure in intense turbulence Eddys, in turbulent flow. This phenomenon occurs as Mach increases where the wake area appears to be filled with bubbles and eventually the flow becomes a true cavity flow (turbulent wake). As cavitation develops drag rises and flow is unsteady; particularly where Reynolds numbers is not taking into account when varying the size of the sphere being simulated at higher Mach with the same Reynolds number.

Figure 34 illustrates the theoretical calculations and CFD results of heat flux [kW/m^2] as a function of Mach number for a one-meter and two-meter diameter sphere. The CFD one-meter diameter sphere results are higher than the theoretical results for Mach values up to about 11.5, where the CFD and theoretical results yield the same heat flux into the sphere with about 7 [kW/m^2]. After Mach 12 the theoretical results increase, as the CFD results settle at about 7 [kW/m^2] as Mach keeps increasing. For a two-meter diameter sphere the CFD results are significantly higher than the theoretical with 12 [kW/m^2] for the theoretical and 29 [kW/m^2] for CFD at Mach 15.

Conclusion

As seen in the results section, Newtonian theory for hypersonic flow accurately predicts the pressure coefficient for a slender sharp cone, $\varepsilon \leq 25^{o}$, at any ϕ around the cone, and for $\alpha \leq 25^{o}$. The comparison in between CFD, theoretical and experimental can be seen in Figures 3, 6 and 37. The lift coefficient is over predicted by Newtonian theory in comparison to CFD simulation results for cones up to $\varepsilon \approx 40^{o}$, at $\alpha = 5^{o}, 15^{o}, 25^{o}$. Meanwhile, the drag coefficient was under predicted by Newtonian theory, in comparison to CFD results, at $\alpha = 5^{o}$, with very similar results for $\varepsilon \leq 25^{o}$ at $\alpha \leq 25^{o}$. Lift and drag coefficient results obtained at Mach 10 are comparable to the theoretical values, better than the Mach 5 values. This comparison shows that Newtonian theory for hypersonic flow is only valid for slender bodies (cones), and it increases in accuracy as Mach increases, since it was not very accurate for Mach 5.

The heat flux calculated theoretically is extremely higher than the results yield by CFD simulation for a sharp cone of increasing ε. The CFD and theoretical results conclude that as ε increases the heat flux also increases due to the increase in surface area. The theoretical method used to calculate the heat flux makes use of exact methods to determine certain temperatures in the flow, as an oblique shock wave occurs, having a major over prediction in heat transfers to the cone in comparison to CFD results (Figures 29 & 30). In theoretical approximations the heat transfer increases as Mach increases, while the CFD results show that for Mach 10 & 15, the heat transfer remains very close. This could potentially be a discrepancy in the CFD set up, since a real gas model was used instead of chemically reacting flow.

The drag coefficient results yielded by Newtonian theory and experimental data seem to be similar to a two-meter diameter sphere at high hypersonic Mach numbers. As seen in Figure 33, the CFD results converge towards the theoretical value of $C_d = 1$, as Mach increases past Mach = 15. While for a smaller, one-meter diameter sphere, the CFD results diverge away from the theoretical results. This may be a discrepancy from the CFD set up, where Reynolds number was not taken into account, as the diameter was varied, causing a turbulent flow phenomenon known as cavitation, where drag rises in unsteady flow.

The heat transfer yielded by CFD results increase as diameter increases as well as Mach number. Meanwhile, the theoretical results are higher for a one-meter diameter sphere at Mach < 12, and equaling the CFD results at about Mach 12. As the radius increases, two-meter diameter sphere, theoretical results show that heat transfer decreases and CFD results show an increase in heat transfer.

References

[1] K. P. J. Reddy, et al. "Simultaneous Measurement Of Aerodynamic And Heat Transfer Data For Large Angle Blunt Cones In Hypersonic Shock Tunnel." Sadhana 31.5 (2006): 557-581. Academic Search Premier.

[2] Braun, Robert D., Grant, Michael J. "Analytic Hypersonic Aerodynamics For Conceptual Design of Entry Vehicles." AIAA Aerospace Sciences Meeting; Including the New Horizons Forum and Aerospace Exposition 4 - 7 January 2010, Orlando, Florida.

[3] Anderson, John D., Jr., *Hypersonic and High Temperature Gas Dynamics*, McGraw-Hill, New York 1989; reprinted by the American Institute of Aeronautics and Astronautics, Reston, VA, 2000.

[4] Anderson, John D., Jr., *Fundamentals of Aerodynamics*, 5th ed., McGraw-Hill, New York 2010.

[5] Anderson, John D., Jr., *Modern Compressible Flow with Historical perspective*, 3rd ed., McGraw-Hill Book Company, New York 2003.

[6] Hayes, Wallace D., Probstein, Ronald F., *Hypersonic Flow Theory*, Academic Press Inc, 2nd ed., New York 1966.

[7] Peckham, D. H. "Experiments at Hypersonic Speeds on Circular Cones at Incidence." Ministry of Aviation, Aeronautical research council current papers. London, 1965.

[8] Dorrance, William, H. *Viscous Hypersonic Flow: Theory of Reacting and Hypersonic Boundary Layer.* McGraw-Hill Book Company, Inc. New York 1962.

[9] Tauber, Michael, E. "A Review of High--Speed Convective Heat--Transfer Computation Methods." NASA Technical Paper, 1989.

[10] Crabtree, L. F., Dommett, R. L., Farmborough, R. A. E., Woodley, J.G. "Estimations of Heat Transfer to Flat Plate, Cones and Blunt Bodies." Aeronautical Research Council Reports and Memoranda No. 3637 July 1965.

[11] STAR CCM+ user guide

Appendix 1 – Analytical Calculations

Drag coefficient – Sphere

$$C_{p\ surface} = 2\sin^2\theta$$

Setting this two equation equal to each other gives:

$$P_s - P_\infty = \rho_\infty$$

The drag of the sphere is determined by integrating over the frontal area of the sphere:

$$D = \int$$

Where the first term is the pressure differences, the second term is the area on which the pressure differences act on, and the third term is the x-component of the pressure force.

After substituting for $(\ -\ )$:

$$D = 2$$

$$D = 2 \int$$

$$D = 2$$

$$D = 2$$

$$D = 2 * 1/4$$

D = 1/2

Where C_d is the non dimensional drag coefficient, D is the drag determined by integrating the pressure differences defined using Newtonian theory over the frontal area of the sphere, q_∞ is the dynamic pressure and S is the area of a circle which is seen as the impact surface area of the flow.

Drag coefficient – Cone

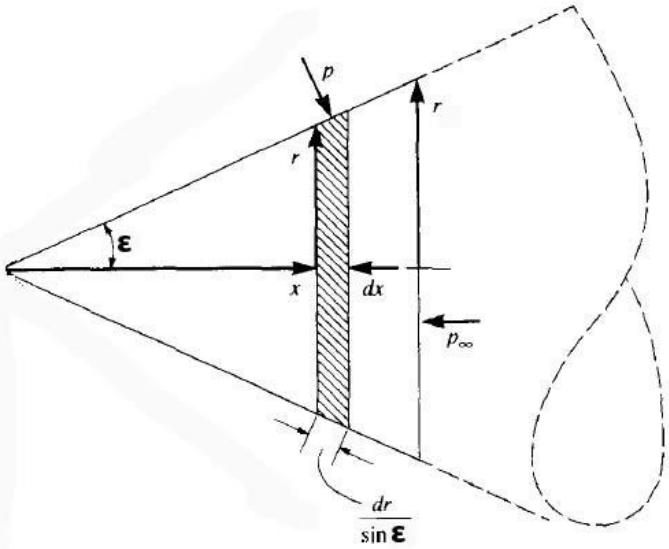

Assuming pressure to be the same as ambient pressure, $p = p_\infty$, and neglecting the effects of friction. The drag force on the shaded strip of surface area can be determined by:

$$(P\sin\varepsilon)(2\pi r)(dr/\sin\varepsilon) = 2\pi r p dr$$

Where ε is the semi apex angle of the cone, r is the radius, P is the pressure on the surface and dr/sinε is the y component of the force.

The total drag due to the pressure acting over the total surface area of cone is determined by:

$$D = \int_{0}^{2\pi} \int_{0}^{r} \quad$$

Where the first integral is the horizontal force on the inclined surface of the cone and the second integral is the force on the base of the cone. Combining both the integrals yields:

$$D = \int_{0}^{2\pi} (\quad) \quad = \pi(p - p_{\infty})r^2$$

Using the base area $S = \pi r^2$ the drag coefficient can be determined by:

$$C_d = \quad = \quad = C_p$$

Therefore the drag coefficient for a cone is equal to its surface pressure coefficient, and in Newtonian Theory that is $C_d = 2\sin^2\varepsilon$

Lift coefficient – Cone at an angle of attack

Starting with the Newtonian Theory pressure coefficient definition, $C_p = 2\sin^2\theta$ and substituting sinθ with Eq. (17) it yields:

$$C_p = 2(\sin\varepsilon * \cos\alpha + \cos\varepsilon * \sin\alpha * \cos\phi)^2$$

Using this equation yields the pressure coefficient at any angle, ϕ, which is the meridional angle along the cone measured windward to leeward as a function of semi apex angle and angle of attack. The normal force coefficient can be determined by integrating the coefficient of pressure.

If $\alpha \leq \varepsilon$

$$C_n = \int \quad = 2\int_{0}^{2\pi}(\sin\varepsilon * \cos\alpha + \cos\varepsilon * \sin\alpha * \cos\phi)^2$$

If $\alpha > \varepsilon$

$$C_n = \int_{!}^{!} {}_{!} = 2\,{}_{!}^{!}(\sin\varepsilon * \cos\alpha + \cos\varepsilon * \sin\alpha * \cos\phi)^{!}$$

Where b is determined by Eq. (18) and that is the angle at which the cones surface is not being impacted by the fluid flow. The lift coefficient is calculated by: $C_l = C_n * \cos\alpha$.

Appendix 2 - Experimental data

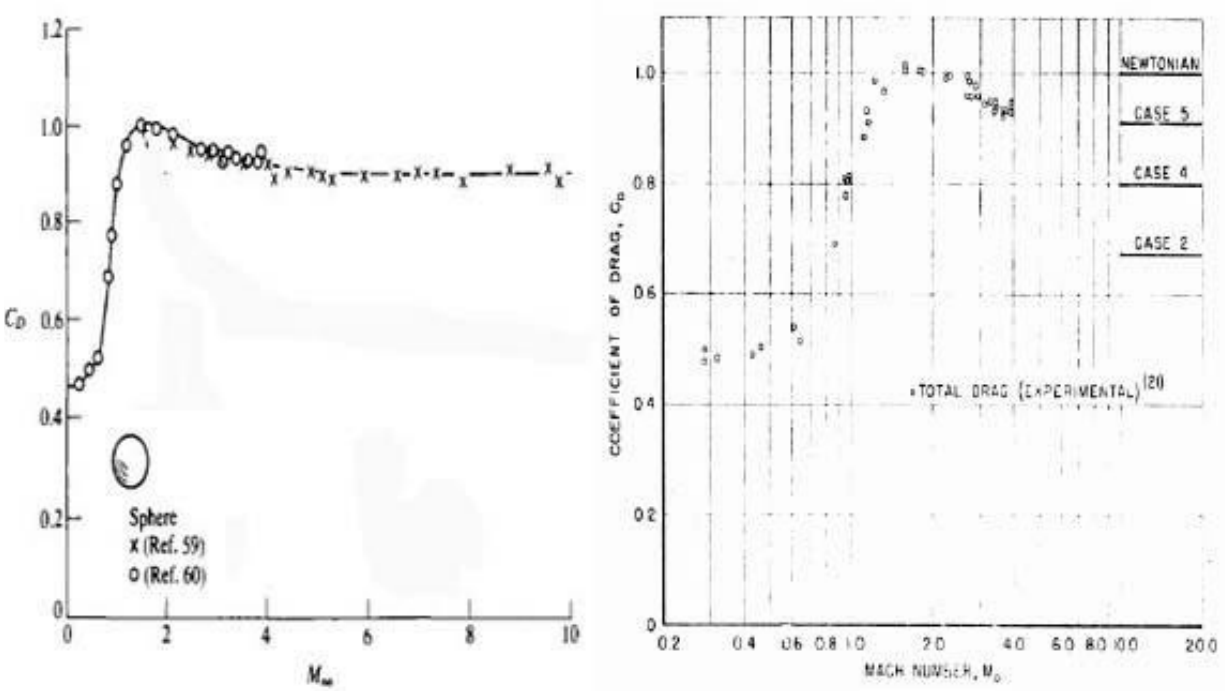

Figure 35: Drag Coefficient as a function of Mach number for a sphere

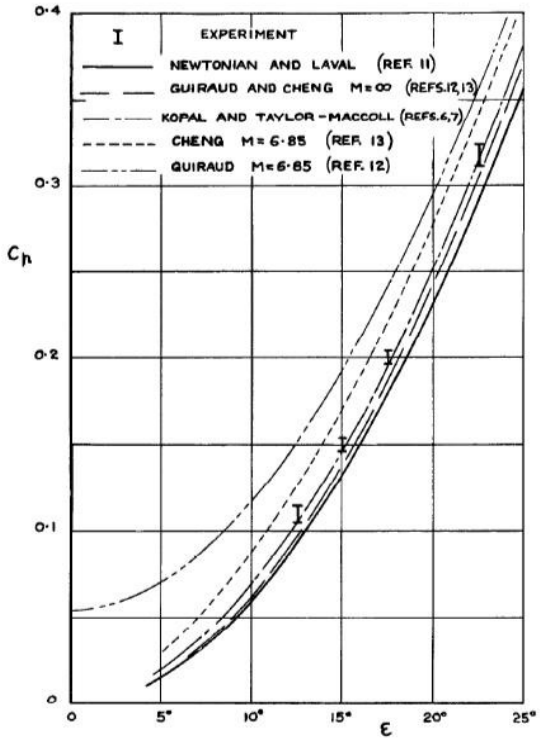

Figure 36: Pressure coefficient as a function of semi-apex angle (ε)

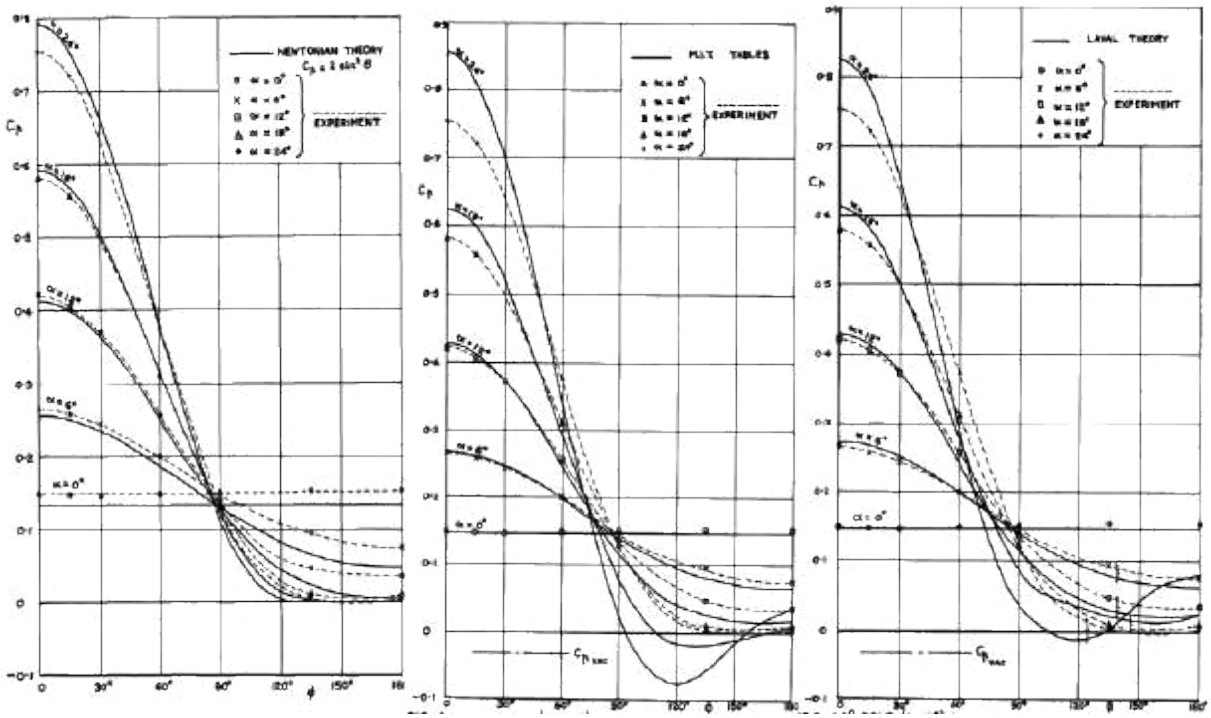

Figure 37: Pressure coefficient as a function of meridian angle (ϕ) and angle of attack (α) for a cone [7]

Appendix 3 – Calculation for pressure coefficient distribution (Fig 4-12)

semi	semi[rad]	AoA	meridian	cp
5	0.0872664	63	0	0	0.0151922 47
5	0.0872664	63	0	45	0.0151922 47
5	0.0872664	63	0	90	0.0151922 47
5	0.0872664	63	0	95	0.0151922 47
5	0.0872664	63	0	100	0.0151922 47
5	0.0872664	63	0	105	0.0151922 47
5	0.0872664	63	0	110	0.0151922 47
5	0.0872664	63	0	115	0.0151922 47
5	0.0872664	63	0	120	0.0151922 47
5	0.0872664	63	0	125	0.0151922 47
5	0.0872664	63	0	130	0.0151922 47
5	0.0872664	63	0	135	0.0151922 47
5	0.0872664	63	0	140	0.0151922 47
5	0.0872664	63	0	145	0.0151922 47
5	0.0872664	63	0	150	0.0151922 47
5	0.0872664	63	0	155	0.0151922 47
5	0.0872664	63	0	160	0.0151922 47
5	0.0872664	63	0	165	0.0151922 47
5	0.0872664	63	0	170	0.0151922 47
5	0.0872664	63	0	175	0.0151922 47
5	0.0872664	63	0	180	0.0151922 47
5	0.0872664	63	5	0	0.0603073 79
5	0.0872664	63	5	45	0.0439371 46

	0.0872664			0.0150768	
5	63	5	90	45	
	0.0872664			0.0125633	
5	63	5	95	03	
	0.0872664			0.0102953	
5	63	5	100	34	
	0.0872664			0.0082824	
5	63	5	105	53	
	0.0872664			0.0065273	
5	63	5	110	31	
	0.0872664			0.0050261	
5	63	5	115	63	
	0.0872664			0.0037692	
5	63	5	120	11	
	0.0872664			0.0027415	
5	63	5	125	29	
	0.0872664			0.0019238	
5	63	5	130	16	
	0.0872664			0.0012933	
5	63	5	135	89	
	0.0872664			0.0008252	
5	63	5	140	34	
	0.0872664			0.0004931	
5	63	5	145	03	
	0.0872664			0.0002706	
5	63	5	150	17	
	0.0872664			0.0001323	
5	63	5	155	48	
	0.0872664			5.48342E--	
5	63	5	160	05	

5	0.08726646	3	5	165	1.7505E-05
5	0.08726646	3	5	170	3.4798E-06
5	0.08726646	3	5	175	2.18318E-07
5	0.08726646	3	5	180	0
5	0.08726646	3	10	0	0.1339745
5	0.08726646	3	10	20	0.1233918
5	0.08726646	3	10	30	0.1110553
5	0.08726646	3	10	35	0.1035440
5	0.08726646	3	10	40	0.0953514
5	0.08726646	3	10	45	0.0866546
5	0.08726646	3	10	50	0.0776383
5	0.08726646	3	10	55	0.0684893
5	0.08726646	3	10	60	0.0593920
5	0.08726646	3	10	65	0.0505233
5	0.08726646	3	10	70	0.0420481
5	0.08726646	3	10	75	0.0341148
5	0.08726646	3	10	80	0.0268519
5	0.08726646	3	10	90	0.0147341
5	0.08726646	3	10	95	0.0100124
5	0.08726646	3	10	100	0.0062256
5	0.08726646	3	10	105	0.0033717
5	0.08726646	3	10	110	0.0014222
5	0.08726646	3	10	115	0.0003238
5	0.08726646	3	10	118	4.26701E-05
5	0.08726646	3	10	119.74	6.9679E--

	3			10
5	0.08726646	3	15	0	0.2339555	57
5	0.08726646	3	15	20	0.2131664	2
5	0.08726646	3	15	30	0.1890841	07
5	0.08726646	3	15	35	0.1745121	14
5	0.08726646	3	15	40	0.1587079	87
5	0.08726646	3	15	45	0.1420469	16
5	0.08726646	3	15	50	0.1249186
5	0.08726646	3	15	55	0.1077162	95
5	0.08726646	3	15	60	0.0908258	31
5	0.08726646	3	15	65	0.0746149	32
5	0.08726646	3	15	70	0.0594231	51
5	0.08726646	3	15	75	0.0455527	11
5	0.08726646	3	15	80	0.0332605	46
5	0.08726646	3	15	85	0.0227517	34

5	0.08726646	3	15	90	0.0141745 59
5	0.08726646	3	15	95	0.0076172 99
5	0.08726646	3	15	100	0.0031068 56
5	0.08726646	3	15	105	0.0006092 56
5	0.08726646	3	15	106	0.0003441 25
5	0.08726646	3	15	107	0.0001549 7
5	0.08726646	3	15	109.05	1.88237E-- 09
5	0.08726646	3	20	0	0.3572123 9
5	0.08726646	3	20	20	0.3233212 34
5	0.08726646	3	20	30	0.2842136 93
5	0.08726646	3	20	45	0.2084307 71
5	0.08726646	3	20	50	0.1810928 58
5	0.08726646	3	20	55	0.1538214 17
5	0.08726646	3	20	60	0.1272691 41
5	0.08726646	3	20	65	0.1020557 77
5	0.08726646	3	20	70	0.0787507 16
5	0.08726646	3	20	75	0.0578571 92
5	0.08726646	3	20	80	0.0397985 45
5	0.08726646	3	20	85	0.0249069 75
5	0.08726646	3	20	90	0.0134150 92
5	0.08726646	3	20	95	0.0054505 2
5	0.08726646	3	20	96	0.0042845 67
5	0.08726646	3	20	97	0.0032605 15
5	0.08726646	3	20	98	0.0023778 42
5	0.08726646	3	20	100	0.0010337

	3			09
	0.08726646			0.0005703
5	3	20	101	7
	0.08726646			0.0002446
5	3	20	102	57
	0.08726646			2.11742E--
5	3	20	103.908	11
	0.08726646			
5	3	25	0	0.5
	0.08726646			0.4505092
5	3	25	20	78
	0.08726646			0.3935536
5	3	25	30	61
	0.08726646			0.3224082
5	3	25	40	81
	0.08726646			0.2837892
5	3	25	45	13
	0.08726646			0.2444542
5	3	25	50	85
	0.08726646			0.2054038
5	3	25	55	17
	0.08726646			0.1676146
5	3	25	60	69
	0.08726646			0.1320121
5	3	25	65	48
	0.08726646			0.0994435
5	3	25	70	98
	0.08726646			0.0706544
5	3	25	75	29

0.08726646				0.0462673
5	3	25	80	36
0.08726646				0.0267652
5	3	25	85	86
0.08726646				0.0124788
5	3	25	90	18
0.08726646				0.0082681
5	3	25	92	8
0.08726646				0.0049246
5	3	25	94	36
0.08726646				0.0024475
5	3	25	96	36
0.08726646				0.0008320
5	3	25	98	47
0.08726646				0.0003447
5	3	25	99	65
0.08726646				0.0001806
5	3	25	99.5	23
0.08726646				0.6579798
5	3	30	0	57
0.08726646				0.5908660
5	3	30	20	07
0.08726646				0.5137817
5	3	30	30	72
0.08726646				0.4675378
5	3	30	35	26
0.08726646				0.4177780
5	3	30	40	59
0.08726646				0.3658325
5	3	30	45	12
0.08726646				0.3130776
5	3	30	50	74
0.08726646				0.2608961
5	3	30	55	91
0.08726646				0.2106365
5	3	30	60	36
0.08726646				0.1635738
5	3	30	65	37
0.08726646				0.1208730
5	3	30	70	52
0.08726646				0.0835555
5	3	30	75	87
0.08726646				0.0524703
5	3	30	80	66
0.08726646				0.0282702
5	3	30	85	02
0.08726646				0.0113941
5	3	30	90	85
0.08726646				0.0067502
5	3	30	92	3

5	0.08726646	3	30	94	0.0033184 48
5	0.08726646	3	30	95	0.0020565 9
5	0.08726646	3	30	96	0.0010964 06
5	0.08726646	3	30	97	0.0004366 78
5	0.08726646	3	30	98.715	1.14766E-- 10
5	0.08726646	3	35	0	0.8263518 22
5	0.08726646	3	35	20	0.7401267 55
5	0.08726646	3	35	25	0.6944369 22
5	0.08726646	3	35	30	0.6412449 55
5	0.08726646	3	35	35	0.5820173 7
5	0.08726646	3	35	40	0.5183795 77
5	0.08726646	3	35	45	0.4520678 24
5	0.08726646	3	35	50	0.3848779 38
5	0.08726646	3	35	55	0.3186124 31
5	0.08726646	3	35	60	0.2550275 46

0.08726646				0.1957818
5	3	35	65	58
0.08726646				0.1423879
5	3	35	70	55
0.08726646				0.0961686
5	3	35	75	68
0.08726646				0.0582191
5	3	35	80	6
0.08726646				0.0293759
5	3	35	85	99
0.08726646				0.0101941
5	3	35	90	51
0.08726646				0.0052947
5	3	35	92	09
0.08726646				0.0019889
5	3	35	94	61
0.08726646				0.0002722
5	3	35	96	33
0.08726646				6.18406E--
5	3	35	97	06
0.08726646				1.1553E--
5	3	35	97.17	08
0.08726646				
5	3	40	0	1
0.08726646				0.9392383
5	3	40	15	81
0.08726646				0.8937563
5	3	40	20	08
0.08726646				0.8375072
5	3	40	25	57
0.08726646				0.7720703
5	3	40	30	07
0.08726646				0.6992768
5	3	40	35	44
0.08726646				0.6211561
5	3	40	40	11
0.08726646				0.5398749
5	3	40	45	34
0.08726646				0.4576734
5	3	40	50	65
0.08726646				0.3767988
5	3	40	55	58
0.08726646				
5	3	40	60	0.2994389
0.08726646				0.2276575
5	3	40	65	87
0.08726646				0.1633345
5	3	40	70	88
5	0.08726646	40	75	0.1081104

	3				32
	0.08726646				0.0633390
5	3	40		80	43
	0.08726646				0.0300490
5	3	40		85	75
	0.08726646				0.0089151
5	3	40		90	76
	0.08726646				0.0039458
5	3	40		92	42
	0.08726646				0.0009765
5	3	40		94	72
	0.08726646				0.0002400
5	3	40		95	56
	0.08726646				7.69068E--
5	3	40	95.9848		14
	0.08726646				1.1736481
5	3	45		0	78
	0.08726646				1.1012528
5	3	45		15	05
	0.08726646				1.0470867
5	3	45		20	1
	0.08726646				0.9801292
5	3	45		25	15
	0.08726646				0.9022827
5	3	45		30	64
	0.08726646				0.8157533
5	3	45		35	8
	0.08726646				0.7229848
5	3	45		40	46

5	0.0872664 63	45	45	0.6265858 66
5	0.0872664 63	45	50	0.5292523 96
5	0.0872664 63	45	55	0.4336875 07
5	0.0872664 63	45	60	0.3425211 81
5	0.0872664 63	45	65	0.2582324 95
5	0.0872664 63	45	70	0.1830764 99
5	0.0872664 63	45	75	0.1190180 33
5	0.0872664 63	45	80	0.0676744 52
5	0.0872664 63	45	85	0.0302689 82
5	0.0872664 63	45	90	0.0075961 23
5	0.0872664 63	45	92	0.0027446 12
5	0.0872664 63	45	94	0.0003120 42
5	0.0872664 63	45	95	1.09994E-- 07
5	0.0872664 63	45	95.0191	6.94031E-- 13

semi	semi[rad]	AoA	meridian	cp
10	0.1745329 25	0	0	0.0603073 79
10	0.1745329 25	0	45	0.0603073 79
10	0.1745329 25	0	90	0.0603073 79
10	0.1745329 25	0	95	0.0603073 79
10	0.1745329 25	0	100	0.0603073 79
10	0.1745329 25	0	105	0.0603073 79
10	0.1745329 25	0	110	0.0603073 79
10	0.1745329 25	0	115	0.0603073 79
10	0.1745329 25	0	120	0.0603073 79
10	0.1745329 25	0	125	0.0603073 79

	0.1745329				0.0603073
10	25		0	130	79
	0.1745329				0.0603073
10	25		0	135	79
	0.1745329				0.0603073
10	25		0	140	79
	0.1745329				0.0603073
10	25		0	145	79
	0.1745329				0.0603073
10	25		0	150	79
	0.1745329				0.0603073
10	25		0	155	79
	0.1745329				0.0603073
10	25		0	160	79
	0.1745329				0.0603073
10	25		0	165	79
	0.1745329				0.0603073
10	25		0	170	79
	0.1745329				0.0603073
10	25		0	175	79
	0.1745329				0.0603073
10	25		0	180	79
	0.1745329				0.1339745
10	25		5	0	96
	0.1745329				0.1092122
10	25		5	45	52
	0.1745329				0.0598492
10	25		5	90	77
	0.1745329				0.0547849
10	25		5	95	17
	0.1745329				0.0499803
10	25		5	100	96

0.17453292 0.0454647
10 5 5 105 1
0.17453292 0.0412598
10 5 5 110 66
0.17453292 0.0373810
10 5 5 115 91
0.17453292 0.0338372
10 5 5 120 26
0.17453292 0.0306312
10 5 5 125 84
0.17453292 0.0277611
10 5 5 130 59
0.17453292 0.0252204
10 5 5 135 47
0.17453292 0.0229993
10 5 5 140 49
0.17453292 0.0210856
10 5 5 145 34
0.17453292 0.0194656
10 5 5 150 19
0.17453292 0.0181251
10 5 5 155 28
0.17453292 0.0170504
10 5 5 160 06
0.17453292 0.0162289
10 5 5 165 52
0.17453292 0.0156502
10 5 5 170 44
0.17453292 0.0153063
10 5 5 175 26
0.17453292 0.0151922
10 5 5 180 47
10
0.17453292 0.2339555
10 5 10 0 57
0.17453292 0.1704491
10 5 10 45 14
0.17453292 0.0584888
10 5 10 90 89
0.17453292 0.0487378
10 5 10 95 93
0.17453292 0.0399395
10 5 10 100 67
0.17453292 0.0321308
10 5 10 105 25
0.17453292 0.0253220
10 5 10 110 33
0.17453292 0.0194984
10 5 10 115 22
10 0.17453292 10 120 0.0146222

	5			22
	0.17453292			0.0106354
10	5	10	125	47
	0.17453292			0.0074632
10	5	10	130	23
	0.17453292			0.0050175
10	5	10	135	53
	0.17453292			0.0032014
10	5	10	140	01
	0.17453292			0.0019129
10	5	10	145	37
	0.17453292			0.0010498
10	5	10	150	28
	0.17453292			0.0005134
10	5	10	155	29
	0.17453292			0.0002127
10	5	10	160	23
	0.17453292			6.79085E--
10	5	10	165	05
	0.17453292			1.34995E--
10	5	10	170	05
	0.17453292			8.46938E--
10	5	10	175	07
	0.17453292			
10	5	10	180	0
10				
10				
	0.17453292			0.3572123
10	5	15	0	9
	0.17453292			0.3316997
10	5	15	20	41
	0.17453292			0.3018176
10	5	15	30	93

0.17453292 0.2635177
10 5 15 40 18
0.17453292 0.2421573
10 5 15 45 16
0.17453292 0.2198766
10 5 15 50 22
0.17453292 0.1742562
10 5 15 60 79
0.17453292 0.1299559
10 5 15 70 21
0.17453292 0.0898811
10 5 15 80 51
0.17453292 0.0562675
10 5 15 90 51
0.17453292 0.0423500
10 5 15 95 42
0.17453292 0.0304899
10 5 15 100 76
0.17453292 0.0207108
10 5 15 105 66
0.17453292 0.0129781
10 5 15 110 42
0.17453292 0.0072027
10 5 15 115 26
0.17453292 0.0032462
10 5 15 120 07
0.17453292 0.0021335
10 5 15 122 77
0.17453292 0.0012701
10 5 15 124 06
0.17453292 0.0006417
10 5 15 126 11
0.17453292 0.0002335
10 5 15 128 89
0.17453292 1.06633E--
10 5 15 131.15 10
10
10
0.17453292
10 5 20 0 0.5
0.17453292 0.4601992
10 5 20 20 78
0.17453292
10 5 20 25 0.4388762
0.17453292 0.4138209
10 5 20 30 46
0.17453292 0.3855931
10 5 20 35 22
0.17453292 0.3221580
10 5 20 45 4

10	0.17453292 5	20	50	0.2883172 4
10	0.17453292 5	20	55	0.2539995 41
10	0.17453292 5	20	60	0.2199011 45
10	0.17453292 5	20	65	0.1866897 34
10	0.17453292 5	20	70	0.1549869 9
10	0.17453292 5	20	75	0.1253526 49
10	0.17453292 5	20	80	0.0982705 67
10	0.17453292 5	20	85	0.0741371 92
10	0.17453292 5	20	90	0.0532527 56
10	0.17453292 5	20	95	0.0358154 55
10	0.17453292 5	20	100	0.0219187 45
10	0.17453292 5	20	105	0.0115518 24
10	0.17453292 5	20	110	0.0046032 57
10	0.17453292 5	20	115	0.0008676 03
10	0.17453292 5	20	118.97	2.39757E-- 09
10				
10				

	0.17453292			0.6579798
10	5	25	0	57
	0.17453292			0.6016532
10	5	25	20	52
	0.17453292			0.5715557
10	5	25	25	2
	0.17453292			0.5362678
10	5	25	30	8
	0.17453292			0.4966215
10	5	25	35	78
	0.17453292			0.4535417
10	5	25	40	61
	0.17453292			0.4080205
10	5	25	45	04
	0.17453292			0.3610892
10	5	25	50	77
	0.17453292			0.3137902
10	5	25	55	81
	0.17453292			0.2671477
10	5	25	60	02
	0.17453292			0.2221397
10	5	25	65	34
	0.17453292			0.1796721
10	5	25	70	97
	0.17453292			0.1405545
10	5	25	75	33
	0.17453292			0.1054788
10	5	25	80	65
	0.17453292			0.0750027
10	5	25	85	51
	0.17453292			0.0495361
10	5	25	90	08
	0.17453292			0.0293326
10	5	25	95	83
	0.17453292			0.0144863
10	5	25	100	06
	0.17453292			0.0049319
10	5	25	105	92
	0.17453292			0.0004518
10	5	25	110	43
	0.17453292			2.69946E--
10	5	25	112.218	12
10				
10				
	0.17453292			0.8263518
10	5	30	0	22
	0.17453292			0.7517636
10	5	30	20	56
	0.17453292			0.7119900
10	5	30	25	84

10	0.17453292 5	30	30	0.6654380 08
10	0.17453292 5	30	35	0.6132501 61
10	0.17453292 5	30	40	0.5566960 57
10	0.17453292 5	30	45	0.4971358 2
10	0.17453292 5	30	50	0.4359815 91
10	0.17453292 5	30	55	0.3746576 38
10	0.17453292 5	30	60	0.3145603 9
10	0.17453292 5	30	65	0.2570195 54
10	0.17453292 5	30	70	0.2032614 96
10	0.17453292 5	30	75	0.1543759 44
10	0.17453292 5	30	80	0.1112870 23
10	0.17453292 5	30	85	0.0747294 39
10	0.17453292 5	30	90	0.0452305 34
10	0.17453292 5	30	95	0.0230987 02
10	0.17453292 5	30	100	0.0084184 91
10	0.17453292 5	30	102	0.0046093 85
10	0.17453292 5	30	105	0.0010525 08

0.17453292 9.54187E--
10 5 30 107.78 10
10
10
0.17453292
10 5 35 0 1
0.17453292 0.9463015
10 5 35 15 42
0.17453292 0.9059694
10 5 35 20 6
0.17453292 0.8559122
10 5 35 25 64
0.17453292 0.7974065
10 5 35 30 61
0.17453292 0.7319351
10 5 35 35 73
0.17453292 0.6611443
10 5 35 40 32
0.17453292 0.5867962
10 5 35 45 66
0.17453292 0.5107186
10 5 35 50 16
0.17453292 0.4347521
10 5 35 55 87
0.17453292 0.3606985
10 5 35 60 95
0.17453292 0.2902693
10 5 35 65 89
0.17453292 0.2250381
10 5 35 70 36
0.17453292 0.1663969
10 5 35 75 26
0.17453292 0.1155185
10 5 35 80 63
0.17453292 0.0733255
10 5 35 85 6
0.17453292 0.0404668
10 5 35 90 59
0.17453292 0.0173029
10 5 35 95 28
0.17453292 0.0038996
10 5 35 100 66
0.17453292 0.0012303
10 5 35 102 52
0.17453292 1.60948E--
10 5 35 104.585 11
10
10
0.17453292 1.1736481
10 5 40 0 78

	0.17453292				1.1084852
10		5	40	15	59
	0.17453292				
10		5	40	20	1.0595852
	0.17453292				0.9989492
10		5	40	25	58
	0.17453292				0.9281637
10		5	40	30	4
	0.17453292				0.8490704
10		5	40	35	28
	0.17453292				0.7637129
10		5	40	40	77
	0.17453292				0.6742775
10		5	40	45	53
	0.17453292				0.5830295
10		5	40	50	07
	0.17453292				0.4922479
10		5	40	55	85
	0.17453292				0.4041604
10		5	40	60	34
	0.17453292				0.3208789
10		5	40	65	59
	0.17453292				0.2443404
10		5	40	70	46
	0.17453292				0.1762522
10		5	40	75	28
	0.17453292				0.1180449
10		5	40	80	12
	0.17453292				0.0708337
10		5	40	85	7
	0.17453292				0.0353898
10		5	40	90	23

	0.1745329				0.0121214
10	25		40	95	63
	0.1745329				0.0010671
10	25		40	100	34
	0.1745329				3.97339E--
10	25		40	102	06
	0.1745329				4.89154E--
10	25		40	102.13	11
10					
10					
	0.1745329				1.3420201
10	25		45	0	43
	0.1745329				1.3333515
10	25		45	5	81
	0.1745329				1.3075796
10	25		45	10	44
	0.1745329				1.2653987
10	25		45	15	06
	0.1745329				1.2079433
10	25		45	20	38
	0.1745329				1.1367549
10	25		45	25	6
	0.1745329				1.0537365
10	25		45	30	55
	0.1745329				0.9610968
10	25		45	35	31
	0.1745329				0.8612854
10	25		45	40	97
	0.1745329				0.7569216
10	25		45	45	07
	0.1745329				0.6507171
10	25		45	50	33
	0.1745329				0.5453980
10	25		45	55	53
	0.1745329				0.4436253
10	25		45	60	39
	0.1745329				0.3479182
10	25		45	65	07
	0.1745329				0.2605819
10	25		45	70	35
	0.1745329				
10	25		45	75	0.1836424
	0.1745329				0.1187893
10	25		45	80	09
	0.1745329				0.0673297
10	25		45	85	82
	0.1745329				0.0301536
10	25		45	90	9
	0.1745329				0.0077117
10	25		45	95	42

10	0.1745329 25	45	100	6.9596E--06

semi	semi[rad]	AoA	meridian	cp
15	0.2617993 88	0	0	0.1339745 96
15	0.2617993 88	0	45	0.1339745 96
15	0.2617993 88	0	90	0.1339745 96
15	0.2617993 88	0	95	0.1339745 96
15	0.2617993 88	0	100	0.1339745 96
15	0.2617993 88	0	105	0.1339745 96
15	0.2617993 88	0	110	0.1339745 96
15	0.2617993 88	0	115	0.1339745 96
15	0.2617993 88	0	120	0.1339745 96
15	0.2617993 88	0	125	0.1339745 96
15	0.2617993 88	0	130	0.1339745 96
15	0.2617993 88	0	135	0.1339745 96
15	0.2617993 88	0	140	0.1339745 96
15	0.2617993 88	0	145	0.1339745 96

	0.26179938			0.1339745	
15	8	0	150	96	
	0.26179938			0.1339745	
15	8	0	155	96	
	0.26179938			0.1339745	
15	8	0	160	96	
	0.26179938			0.1339745	
15	8	0	165	96	
	0.26179938			0.1339745	
15	8	0	170	96	
	0.26179938			0.1339745	
15	8	0	175	96	
	0.26179938			0.1339745	
15	8	0	180	96	
15					
	0.26179938			0.2339555	
15	8	5	0	57	
	0.26179938			0.2014380	
15	8	5	45	9	
	0.26179938			0.1329569	
15	8	5	90	09	
	0.26179938			0.1254973	
15	8	5	95	62	
	0.26179938			0.1183074	
15	8	5	100	79	
	0.26179938			0.1114346	
15	8	5	105	96	
	0.26179938			0.1049194	
15	8	5	110	3	
	0.26179938			0.0987951	
15	8	5	115	27	
	0.26179938			0.0930885	
15	8	5	120	04	
	0.26179938			0.0878199	
15	8	5	125	44	
	0.26179938			0.0830040	
15	8	5	130	47	
	0.26179938			0.0786502	
15	8	5	135	86	
	0.26179938			0.0747637	
15	8	5	140	71	
	0.26179938			0.0713460	
15	8	5	145	51	
	0.26179938			0.0683959	
15	8	5	150	62	
	0.26179938			0.0659104	
15	8	5	155	56	
	0.26179938			0.0638854	
15	8	5	160	04	
15	0.26179938	5	165	0.0623163	

```
           8                                  23
  0.26179938                          0.0611990
15         8        5       170            17
  0.26179938                          0.0605300
15         8        5       175            99
  0.26179938                          0.0603073
15         8        5       180            79
15
  0.26179938                          0.2568551
15         8        6         0            75
  0.26179938                          0.2162129
15         8        6        45            29
  0.26179938                          0.1325107
15         8        6        90            63
  0.26179938                          0.1236052
15         8        6        95            88
  0.26179938                          0.1150738
15         8        6       100             1
  0.26179938                          0.1069707
15         8        6       105            85
  0.26179938                          0.0993407
15         8        6       110            79
  0.26179938                          0.0922186
15         8        6       115            49
  0.26179938                          0.0856299
15         8        6       120            82
  0.26179938                          0.0795917
15         8        6       125            73
  0.26179938                          0.0741132
15         8        6       130            98
  0.26179938                          0.0691971
15         8        6       135            63
  0.26179938                          0.0648404
15         8        6       140            67
```

	0.26179938			0.0610360
15	8	6	145	53
	0.26179938			0.0577737
15	8	6	150	85
	0.26179938			0.0550418
15	8	6	155	13
	0.26179938			0.0528277
15	8	6	160	79
	0.26179938			0.0511199
15	8	6	165	18
	0.26179938			0.0499080
15	8	6	170	16
	0.26179938			0.0489531
15	8	6	179	07
15				
	0.26179938			0.4122147
15	8	12	0	48
	0.26179938			0.3123179
15	8	12	45	52
	0.26179938			0.1281832
15	8	12	90	4
	0.26179938			0.1110712
15	8	12	95	5
	0.26179938			0.0953009
15	8	12	100	94
	0.26179938			0.0809510
15	8	12	105	54
	0.26179938			0.0680629
15	8	12	110	78
	0.26179938			0.0566430
15	8	12	115	18
	0.26179938			0.0466648
15	8	12	120	76
	0.26179938			0.0380733
15	8	12	125	39
	0.26179938			0.0307886
15	8	12	130	88
	0.26179938			0.0247117
15	8	12	135	14
	0.26179938			0.0197291
15	8	12	140	68
	0.26179938			0.0157194
15	8	12	145	74
	0.26179938			0.0125584
15	8	12	150	97
	0.26179938			0.0101251
15	8	12	155	88
	0.26179938			0.0083069
15	8	12	160	15
15	0.26179938	12	165	0.0070043

```
            8                       03
   0.26179938                  0.0061354
15          8       12      170       34
   0.26179938                  0.0056392
15          8       12      175       55
   0.26179938                  0.0054781
15          8       12      180       05
15
15
   0.26179938                  0.5932633
15          8       18        0       57
   0.26179938                  0.5546952
15          8       18       20       43
   0.26179938                  0.5339021
15          8       18       25       45
   0.26179938                  0.5093418
15          8       18       30       18
   0.26179938                  0.4814909
15          8       18       35       02
   0.26179938                  0.4508819
15          8       18       40       06
   0.26179938                  0.4180894
15          8       18       45       15
   0.26179938                  0.3837153
15          8       18       50       37
   0.26179938                  0.3483736
15          8       18       55        2
   0.26179938                  0.3126748
15          8       18       60       66
   0.26179938                  0.2772113
15          8       18       65       13
   0.26179938                  0.2425425
15          8       18       70       79
```

```
  0.26179938                    0.1775881
15          8       18        80        53
  0.26179938                    0.1211811
15          8       18        90        61
  0.26179938                    0.0755203
15          8       18       100        15
  0.26179938                    0.0415081
15          8       18       110        83
  0.26179938                    0.0187822
15          8       18       120         4
  0.26179938                    0.0112338
15          8       18       125        49
  0.26179938                    0.0058942
15          8       18       130         6
  0.26179938                    0.0024624
15          8       18       135        77
  0.26179938                    0.0013976
15          8       18     137.4        99
15
  0.26179938                    0.8263518
15          8       25         0        22
  0.26179938                    0.7642659
15          8       25        20        69
  0.26179938                    0.6917156
15          8       25        30         5
  0.26179938                    0.6474360
15          8       25        35        57
  0.26179938                    0.5990368
15          8       25        40         5
  0.26179938                    0.5475253
15          8       25        45        62
  0.26179938                    0.4939526
15          8       25        50        37
  0.26179938                    0.4393854
15          8       25        55        04
  0.26179938                    0.3848779
15          8       25        60        38
  0.26179938                    0.2800340
15          8       25        70        05
  0.26179938                    0.1866067
15          8       25        80        47
  0.26179938                    0.1459601
15          8       25        85        54
  0.26179938                    0.1100459
15          8       25        90        03
  0.26179938                    0.0791949
15          8       25        95        81
  0.26179938                    0.0535845
15          8       25       100        26
15 0.26179938       25       105 0.0332382
```

		8			32
	0.26179938			0.0180313	
15		8	25	110	75
	0.26179938			0.0077002	
15		8	25	115	51
	0.26179938			0.0018557	
15		8	25	120	17
	0.26179938			0.0006659	
15		8	25	122	2
	0.26179938			5.90897E--	
15		8	25	125.07	10

semi	semi[rad]	AoA	meridian	cp
	0.349065			0.2339555
20	85	0	0	57
	0.349065			0.2339555
20	85	0	45	57
	0.349065			0.2339555
20	85	0	90	57
	0.349065			0.2339555
20	85	0	95	57
	0.349065			0.2339555
20	85	0	100	57
	0.349065			0.2339555
20	85	0	105	57
	0.349065			0.2339555
20	85	0	110	57
	0.349065			0.2339555
20	85	0	115	57
	0.349065			0.2339555
20	85	0	120	57
	0.349065			0.2339555
20	85	0	125	57

	0.3490658			0.2339555
20	5	0	130	57
	0.3490658			0.2339555
20	5	0	135	57
	0.3490658			0.2339555
20	5	0	140	57
	0.3490658			0.2339555
20	5	0	145	57
	0.3490658			0.2339555
20	5	0	150	57
	0.3490658			0.2339555
20	5	0	155	57
	0.3490658			0.2339555
20	5	0	160	57
	0.3490658			0.2339555
20	5	0	165	57
	0.3490658			0.2339555
20	5	0	170	57
	0.3490658			0.2339555
20	5	0	175	57
	0.3490658			0.2339555
20	5	0	180	57
20				
	0.3490658			0.3572123
20	5	5	0	9
	0.3490658			0.3178124
20	5	5	45	26
	0.3490658			0.2321784
20	5	5	90	02
	0.3490658			0.2225520
20	5	5	95	76
	0.3490658			0.2132004
20	5	5	100	98
	0.3490658			0.2041879
20	5	5	105	46
	0.3490658			0.1955717
20	5	5	110	58
	0.3490658			0.1874022
20	5	5	115	36
	0.3490658			0.1797227
20	5	5	120	26
	0.3490658			0.1725698
20	5	5	125	62
	0.3490658			0.1659739
20	5	5	130	5
	0.3490658			0.1599594
20	5	5	135	68
	0.3490658			0.1545456
20	5	5	140	65
20	0.3490658	5	145	0.1497472

```
          5                                  16
  0.3490658                          0.1455749
20        5         5       150             2
  0.3490658                          0.1420363
20        5         5       155            99
  0.3490658                          0.1391367
20        5         5       160            72
  0.3490658                          0.1368792
20        5         5       165            77
  0.3490658                          0.1352658
20        5         5       170            24
  0.3490658                          0.1342974
20        5         5       175            37
  0.3490658                          0.1339745
20        5         5       180            96
20
  0.3490658
20        5        10         0           0.5
  0.3490658                          0.4089821
20        5        10        45            29
  0.3490658                          0.2269009
20        5        10        90            34
  0.3490658                          0.2081445
20        5        10        95             8
  0.3490658                          0.1903307
20        5        10       100             9
  0.3490658                          0.1735677
20        5        10       105             8
  0.3490658                          0.1579384
20        5        10       110            56
  0.3490658                          0.1435011
20        5        10       115             4
  0.3490658                          0.1302909
20        5        10       120            67
```

```
   0.3490658                    0.1183218
20         5        10       125        91
   0.3490658                    0.1075892
20         5        10       130        05
   0.3490658                    0.0980724
20         5        10       135        95
   0.3490658                    0.0897388
20         5        10       140        89
   0.3490658                    0.0825465
20         5        10       145        15
   0.3490658                    0.0764480
20         5        10       150        11
   0.3490658                    0.0713939
20         5        10       155        94
   0.3490658                    0.0673363
20         5        10       160        45
   0.3490658                    0.0642312
20         5        10       165        02
   0.3490658                    0.0620415
20         5        10       170        72
   0.3490658                    0.0607394
20         5        10       175        46
   0.3490658                    0.0603073
20         5        10       180        79
20
   0.3490658                    0.6579798
20         5        15         0        57
   0.3490658                    0.5046945
20         5        15        45        18
   0.3490658                    0.2182835
20         5        15        90        06
   0.3490658                    0.1911708
20         5        15        95        31
   0.3490658                    0.1660413
20         5        15       100        16
   0.3490658                    0.1430254
20         5        15       105        36
   0.3490658                    0.1221991
20         5        15       110         2
   0.3490658                    0.1035861
20         5        15       115        83
   0.3490658                    0.0871622
20         5        15       120         4
   0.3490658                    0.0728599
20         5        15       125        39
   0.3490658                    0.0605753
20         5        15       130        13
   0.3490658                    0.0501750
20         5        15       135         4
20 0.3490658        15       140 0.0415043
```

```
          5                                  52
   0.3490658                          0.0343953
20         5        15       145          14
   0.3490658                          0.0286752
20         5        15       150          16
   0.3490658                          0.0241747
20         5        15       155          76
   0.3490658                          0.0207358
20         5        15       160          96
   0.3490658                          0.0182187
20         5        15       165          07
   0.3490658                          0.0165076
20         5        15       170          83
   0.3490658                          0.0155166
20         5        15       175          07
   0.3490658                          0.0151922
20         5        15       180          47
20
   0.3490658                          0.8263518
20         5        20         0          22
   0.3490658                          0.6020414
20         5        20        45          22
   0.3490658                          0.2065879
20         5        20        90          56
   0.3490658                          0.1721465
20         5        20        95           7
   0.3490658                          0.1410701
20         5        20       100          01
   0.3490658                          0.1134889
20         5        20       105           3
   0.3490658                          0.0894396
20         5        20       110          71
   0.3490658                          0.0688701
20         5        20       115          59
```

	0.3490658			0.0516469
20	5	20	120	89
	0.3490658			0.0375653
20	5	20	125	46
	0.3490658			0.0263607
20	5	20	130	66
	0.3490658			0.0177224
20	5	20	135	45
	0.3490658			0.0113076
20	5	20	140	34
	0.3490658			0.0067566
20	5	20	145	62
	0.3490658			0.0037080
20	5	20	150	87
	0.3490658			0.0018134
20	5	20	155	77
	0.3490658			0.0007513
20	5	20	160	56
	0.3490658			0.0002398
20	5	20	165	59
	0.3490658			4.76814E--
20	5	20	170	05
	0.3490658			2.99146E--
20	5	20	175	06
	0.3490658			
20	5	20	180	0
20				
	0.3490658			
20	5	25	0	1
	0.3490658			0.9334065
20	5	25	20	24
	0.3490658			0.8975284
20	5	25	25	68
	0.3490658			0.8551737
20	5	25	30	7
	0.3490658			0.8071776
20	5	25	35	31
	0.3490658			0.7544727
20	5	25	40	54
	0.3490658			0.6390073
20	5	25	50	78
	0.3490658			0.5172282
20	5	25	60	03
	0.3490658			0.3974795
20	5	25	70	78
	0.3490658			0.3407427
20	5	25	75	14
	0.3490658			0.2871859
20	5	25	80	53
20	0.3490658	25	90	0.1921696

```
          5                                   45
  0.3490658                           0.1161758
20        5       25       100              81
  0.3490658                           0.0858557
20        5       25       105              11
  0.3490658                           0.0404078
20        5       25       115              98
  0.3490658                           0.0248243
20        5       25       120              26
  0.3490658                           0.0135105
20        5       25       125              19
  0.3490658                           0.0059851
20        5       25       130              57
  0.3490658                           0.0017007
20        5       25       135              64
  0.3490658                           0.0004410
20        5       25       138              14
  0.3490658                           2.05709E--
20        5       25   141.309              11
20
  0.3490658                           1.1736481
20        5       30         0              78
  0.3490658                           1.0884298
20        5       30        20              56
  0.3490658                           1.0426358
20        5       30        25              76
  0.3490658                           0.9886907
20        5       30        30              08
  0.3490658                           0.9277227
20        5       30        35              65
  0.3490658                           0.8609902
20        5       30        40              89
  0.3490658                           0.7898476
20        5       30        45              37
```

	0.3490658			0.7157092
20	5	30	50	58
	0.3490658			
20	5	30	55	0.6400124
	0.3490658			0.5641796
20	5	30	60	45
	0.3490658			0.4895823
20	5	30	65	64
	0.3490658			0.4175061
20	5	30	70	46
	0.3490658			0.3491192
20	5	30	75	05
	0.3490658			0.2854446
20	5	30	80	57
	0.3490658			0.2273374
20	5	30	85	63
	0.3490658			0.1754666
20	5	30	90	68
	0.3490658			0.0921150
20	5	30	100	56
	0.3490658			0.0367211
20	5	30	110	67
	0.3490658			0.0075092
20	5	30	120	46
	0.3490658			0.0014263
20	5	30	125	53
	0.3490658			4.46868E--
20	5	30	129.08	11
20				
	0.3490658			1.3420201
20	5	35	0	43
	0.3490658			1.2376277
20	5	35	20	56
	0.3490658			1.1816557
20	5	35	25	78
	0.3490658			1.1158437
20	5	35	30	27
	0.3490658			1.0416371
20	5	35	35	47
	0.3490658			0.9606459
20	5	35	40	78
	0.3490658			0.8746005
20	5	35	45	52
	0.3490658			0.7853045
20	5	35	50	71
	0.3490658			0.6945864
20	5	35	55	78
	0.3490658			0.6042506
20	5	35	60	3
20	0.3490658	35	65	0.5160297

	5			24
	0.3490658			0.4315398
20	5	35	70	47
	0.3490658			0.3522394
20	5	35	75	78
	0.3490658			0.2793936
20	5	35	80	09
	0.3490658			0.2140440
20	5	35	85	19
	0.3490658			0.1569865
20	5	35	90	35
	0.3490658			0.0696187
20	5	35	100	01
	0.3490658			0.0183639
20	5	35	110	36
	0.3490658			0.0054876
20	5	35	115	15
	0.3490658			0.0002278
20	5	35	120	57
	0.3490658			5.04672E--
20	5	35	121.319	13
20				
	0.3490658			
20	5	40	0	1.5
	0.3490658			1.3764669
20	5	40	20	22
	0.3490658			1.3103641
20	5	40	25	25
	0.3490658			1.2327693
20	5	40	30	48
	0.3490658			1.1454595
20	5	40	35	44
	0.3490658			1.0504118
20	5	40	40	33

20	0.3490658	5	40	45	0.9497485	73
20	0.3490658	5	40	50	0.8456786	97
20	0.3490658	5	40	55	0.7404370	68
20	0.3490658	5	40	60	0.6362236	23
20	0.3490658	5	40	65	0.5351441	3
20	0.3490658	5	40	70	0.4391542	74
20	0.3490658	5	40	75	0.3500087	25
20	0.3490658	5	40	80	0.2692166	68
20	0.3490658	5	40	85	0.1980050	71
20	0.3490658	5	40	90	0.1372907	56
20	0.3490658	5	40	95	0.0876620	27
20	0.3490658	5	40	110	0.0061415	72
20	0.3490658	5	40	105	0.0223323	12
20	0.3490658	5	40	110	0.0061415	72
20	0.3490658	5	40	115.7	7.85435E--09	
20						
20	0.3490658	5	45	0	1.6427876	1
20	0.3490658	5	45	20	1.5007287	96
20	0.3490658	5	45	25	1.4248501	77
20	0.3490658	5	45	30	1.3359148	44
20	0.3490658	5	45	35	1.2360353	67
20	0.3490658	5	45	40	1.1275603	66
20	0.3490658	5	45	45	1.0130083	67
20	0.3490658	5	45	50	0.8949972	01
20	0.3490658	5	45	55	0.7761710	22
20	0.3490658	5	45	60	0.6591271	

		5			39
	0.3490658				
20		5	45	65	0.5463448
	0.3490658				0.4401180
20		5	45	70	67
	0.3490658				0.3424947
20		5	45	75	27
	0.3490658				0.2552230
20		5	45	80	53
	0.3490658				0.1797079
20		5	45	85	56
	0.3490658				0.1169777
20		5	45	90	78
	0.3490658				0.0676626
20		5	45	95	93
	0.3490658				0.0319852
20		5	45	100	59
	0.3490658				0.0097633
20		5	45	105	76
	0.3490658				0.0004254
20		5	45	110	46
	0.3490658				4.16143E--
20		5	45	111.34	09

semi	semi[rad]	AoA	meridian	cp
	0.4363323			0.3572123
25	13	0	0	9
	0.4363323			0.4348577
25	13	4	45	01
	0.4363323			0.3554742
25	13	4	90	07
	0.4363323			0.3462430
25	13	4	95	13

	0.43633231			0.3372021
25	3	4	100	33
	0.43633231			0.3284162
25	3	4	105	69
	0.43633231			0.3199455
25	3	4	110	79
	0.43633231			0.3118454
25	3	4	115	32
	0.43633231			0.3041662
25	3	4	120	54
	0.43633231			0.2969534
25	3	4	125	91
	0.43633231			0.2902476
25	3	4	130	57
	0.43633231			0.2840844
25	3	4	135	61
	0.43633231			0.2784950
25	3	4	140	03
	0.43633231			0.2735060
25	3	4	145	15
	0.43633231			0.2691401
25	3	4	150	42
	0.43633231			0.2654162
25	3	4	155	29
	0.43633231			0.2623496
25	3	4	160	21
	0.43633231			0.2599524
25	3	4	165	37
	0.43633231			0.2582338
25	3	4	170	21
	0.43633231			0.2572001
25	3	4	175	47
	0.43633231			0.2568551
25	3	4	180	75
25				
	0.43633231			
25	3	5	0	0.5
	0.43633231			0.4547992
25	3	5	45	85
	0.43633231			0.3544989
25	3	5	90	61
	0.43633231			0.3430001
25	3	5	95	01
	0.43633231			0.3317761
25	3	5	100	77
	0.43633231			0.3209061
25	3	5	105	99
	0.43633231			0.3104624
25	3	5	110	26
25	0.43633231	5	115	0.3005101

	3			35
25	0.436332313	5	120	0.291107554
25	0.436332313	5	125	0.282305954
25	0.436332313	5	130	0.274149872
25	0.436332313	5	135	0.266677455
25	0.436332313	5	140	0.259920898
25	0.436332313	5	145	0.253906948
25	0.436332313	5	150	0.248657451
25	0.436332313	5	155	0.244189909
25	0.436332313	5	160	0.240518034
25	0.436332313	5	165	0.237652257
25	0.436332313	5	170	0.235600181
25	0.436332313	5	175	0.234366956
25	0.436332313	5	180	0.233955557
25				
25	0.436332313	10	0	0.657979857
25	0.436332313	10	45	0.556473009
25	0.436332313	10	90	0.346441119

```
   0.43633231                    0.3239823
25          3       10        95        67
   0.43633231                    0.3024385
25          3       10       100        36
   0.43633231                    0.2819481
25          3       10       105        38
   0.43633231                    0.2626255
25          3       10       110        65
   0.43633231                    0.2445614
25          3       10       115        78
   0.43633231                    0.2278238
25          3       10       120        31
   0.43633231                    0.2124594
25          3       10       125        64
   0.43633231                    0.1984962
25          3       10       130        01
   0.43633231                    0.1859453
25          3       10       135        36
   0.43633231                    0.1748044
25          3       10       140        41
   0.43633231                    0.1650603
25          3       10       145        56
   0.43633231                    0.1566922
25          3       10       150        66
   0.43633231                    0.1496747
25          3       10       155        47
   0.43633231                    0.1439806
25          3       10       160        64
   0.43633231                    0.1395838
25          3       10       165        29
   0.43633231                    0.1364613
25          3       10       170        08
   0.43633231                    0.1345953
25          3       10       175        13
   0.43633231                    0.1339745
25          3       10       180        96
25
   0.43633231                    0.8263518
25          3       15         0        22
   0.43633231                    0.6591442
25          3       15        45        59
   0.43633231                    0.3332836
25          3       15        90        97
   0.43633231                    0.3007370
25          3       15        95        33
   0.43633231                    0.2700908
25          3       15       100        77
   0.43633231                    0.2415219
25          3       15       105         3
25 0.43633231       15       110 0.2151553
```

```
           3                    08
  0.43633231                0.1910663
25         3       15       115        92
  0.43633231                0.1692840
25         3       15       120        62
  0.43633231                0.1497951
25         3       15       125         7
  0.43633231                0.1325500
25         3       15       130        76
  0.43633231                0.1174690
25         3       15       135        39
  0.43633231                0.1044492
25         3       15       140         4
  0.43633231                0.0933721
25         3       15       145        71
  0.43633231                0.0841111
25         3       15       150        51
  0.43633231                0.0765386
25         3       15       155        99
  0.43633231                0.0705335
25         3       15       160         2
  0.43633231                0.0659868
25         3       15       165        67
  0.43633231                0.0628080
25         3       15       170        57
  0.43633231                0.0609289
25         3       15       175        72
  0.43633231                0.0603073
25         3       15       180        79
25
  0.43633231
25         3       20         0         1
  0.43633231                0.7596934
25         3       20        45        21
```

	0.43633231			0.3154264
25	3	20	90	78
	0.43633231			0.2739703
25	3	20	95	97
	0.43633231			0.2357160
25	3	20	100	66
	0.43633231			0.2008559
25	3	20	105	03
	0.43633231			0.1694940
25	3	20	110	12
	0.43633231			0.1416502
25	3	20	115	97
	0.43633231			0.1172669
25	3	20	120	51
	0.43633231			0.0962170
25	3	20	125	95
	0.43633231			0.0783152
25	3	20	130	36
	0.43633231			0.0633291
25	3	20	135	81
	0.43633231			0.0509930
25	3	20	140	02
	0.43633231			0.0410206
25	3	20	145	04
	0.43633231			0.0331194
25	3	20	150	46
	0.43633231			0.0270039
25	3	20	155	67
	0.43633231			0.0224082
25	3	20	160	56
	0.43633231			0.0190975
25	3	20	165	77
	0.43633231			0.0168783
25	3	20	170	44
	0.43633231			0.0156062
25	3	20	175	48
	0.43633231			0.0151922
25	3	20	180	47
25				
	0.43633231			1.1736481
25	3	25	0	78
	0.43633231			0.8550653
25	3	25	45	59
	0.43633231			0.2934120
25	3	25	90	44
	0.43633231			0.2444957
25	3	25	95	49
	0.43633231			0.2003585
25	3	25	100	66
25	0.43633231	25	105	0.1611856

	3			74
25	0.436332313	25	110	0.127029075
25	0.436332313	25	115	0.097814677
25	0.436332313	25	120	0.073353011
25	0.436332313	25	125	0.053353182
25	0.436332313	25	130	0.03743958
25	0.436332313	25	135	0.025170774
25	0.436332313	25	140	0.016059968
25	0.436332313	25	145	0.009596329
25	0.436332313	25	150	0.005266509
25	0.436332313	25	155	0.002575639
25	0.436332313	25	160	0.001067134
25	0.436332313	25	165	0.000340666
25	0.436332313	25	170	6.77208E--05
25	0.436332313	25	175	4.2487E--06
25	0.436332313	25	180	0
25				
25	0.436332313	30	0	1.342020143

	0.43633231				1.2539689
25		3	30	20	76
	0.43633231				1.2065104
25		3	30	25	11
	0.43633231				1.1504653
25		3	30	30	02
	0.43633231				1.0869279
25		3	30	35	43
	0.43633231				1.0171206
25		3	30	40	97
	0.43633231				0.8640336
25		3	30	50	26
	0.43633231				0.7022904
25		3	30	60	92
	0.43633231				0.5428526
25		3	30	70	38
	0.43633231				0.4671249
25		3	30	75	33
	0.43633231				0.3954939
25		3	30	80	43
	0.43633231				0.2679092
25		3	30	90	93
	0.43633231				0.1650926
25		3	30	100	97
	0.43633231				0.1237166
25		3	30	105	04
	0.43633231				0.0608914
25		3	30	115	54
	0.43633231				0.0388765
25		3	30	120	44
	0.43633231				0.0225058
25		3	30	125	29
	0.43633231				0.0111650
25		3	30	130	94
	0.43633231				0.0041532
25		3	30	135	42
	0.43633231				0.0017098
25		3	30	138	59
	0.43633231				2.54199E--
25		3	30	143.868	11
25					
	0.43633231				
25		3	35	0	1.5
	0.43633231				1.3933660
25		3	35	20	78
	0.43633231				1.3360263
25		3	35	25	99
	0.43633231				1.2684437
25		3	35	30	37
25	0.43633231		35	35	1.1920111

		3			8
	0.43633231			1.1082826	
25		3	35	40	64
	0.43633231			1.0189316	
25		3	35	45	08
	0.43633231			0.9257066	
25		3	35	50	93
	0.43633231			0.8303860	
25		3	35	55	8
	0.43633231			0.7347314	
25		3	35	60	11
	0.43633231			0.6404429	
25		3	35	65	16
	0.43633231			0.5491169	
25		3	35	70	28
	0.43633231			0.4622070	
25		3	35	75	4
	0.43633231			0.3809899	
25		3	35	80	92
	0.43633231			0.3065372	
25		3	35	85	57
	0.43633231			0.2396931	
25		3	35	90	12
	0.43633231			0.1309899	
25		3	35	100	92
	0.43633231			0.0567130	
25		3	35	110	51
	0.43633231			0.0148851	
25		3	35	120	01
	0.43633231			0.0046123	
25		3	35	125	17
	0.43633231			4.96354E--	
25		3	35	131.755	11
25					

	0.43633231				1.6427876
25		3	40	0	1
	0.43633231				1.5178914
25		3	40	20	62
	0.43633231				1.4508748
25		3	40	25	06
	0.43633231				1.3720262
25		3	40	30	36
	0.43633231				1.2830494
25		3	40	35	43
	0.43633231				1.1858426
25		3	40	40	23
	0.43633231				1.0824469
25		3	40	45	26
	0.43633231				0.9749913
25		3	40	50	83
	0.43633231				0.8656359
25		3	40	55	23
	0.43633231				0.7565141
25		3	40	60	56
	0.43633231				0.6496775
25		3	40	65	91
	0.43633231				0.5470429
25		3	40	70	25
	0.43633231				0.4503439
25		3	40	75	24
	0.43633231				0.3610892
25		3	40	80	77
	0.43633231				0.2805276
25		3	40	85	42
	0.43633231				0.2096208
25		3	40	90	35
	0.43633231				0.0990866
25		3	40	100	47
	0.43633231				0.0309984
25		3	40	110	82
	0.43633231				0.0120256
25		3	40	115	58
	0.43633231				0.0021076
25		3	40	120	49
	0.43633231				
25		3	40	123.76	4.885E--11
25					
	0.43633231				1.7660444
25		3	45	0	43
	0.43633231				1.6237614
25		3	45	20	88
	0.43633231				1.5475660
25		3	45	25	22
25	0.43633231		45	30	1.4580654

	3				97
	0.43633231				1.3572765
25	3	45	35		83
	0.43633231				1.2474439
25	3	45	40		55
	0.43633231				1.1309783
25	3	45	45		18
	0.43633231				1.0103902
25	3	45	50		05
	0.43633231				0.8882215
25	3	45	55		26
	0.43633231				0.7669768
25	3	45	60		68
	0.43633231				0.6490565
25	3	45	65		88
	0.43633231				0.5366936
25	3	45	70		48
	0.43633231				0.4318960
25	3	45	75		38
	0.43633231				0.3363964
25	3	45	80		71
	0.43633231				0.2516107
25	3	45	85		76
	0.43633231				0.1786061
25	3	45	90		95
	0.43633231				0.1180804
25	3	45	95		32
	0.43633231				0.0126883
25	3	45	110		87
	0.43633231				0.0353622
25	3	45	105		56
	0.43633231				0.0126883
25	3	45	110		87
	0.43633231				1.53122E--
25	3	45	117.794		10

semi	semi[rad]	AoA	meridian	cp
30	0.5235987 76	0	0	0.5
30	0.5235987 76	3	45	0.5646951 13
30	0.5235987 76	3	90	0.4986304 74
30	0.5235987 76	3	95	0.4907719 7
30	0.5235987 76	3	100	0.4830349 82
30	0.5235987 76	3	105	0.4754762 82
30	0.5235987 76	3	110	0.4681499 51
30	0.5235987 76	3	115	0.4611070 67
30	0.5235987 76	3	120	0.4543954 66
30	0.5235987 76	3	125	0.4480595 47
30	0.5235987 76	3	130	0.4421401 38
30	0.5235987 76	3	135	0.4366744 13
30	0.5235987 76	3	140	0.4316958 46
30	0.5235987 76	3	145	0.4272342 02
30	0.5235987 76	3	150	0.4233155 6
30	0.5235987 76	3	155	0.4199623 53
30	0.5235987 76	3	160	0.4171934 19
30	0.5235987 76	3	165	0.4150240 66
30	0.5235987 76	3	170	0.4134661 27
30	0.5235987 76	3	175	0.4125280 11
30	0.5235987 76	3	180	0.4122147 48
30	0.5235987 76	5	0	0.6579798 57
30	0.5235987 76	5	45	0.6082363 88

	0.5235987			0.4962019
30	76	5	90	38
	0.5235987			0.4831816
30	76	5	95	84
	0.5235987			0.4704316
30	76	5	100	54
	0.5235987			0.4580430
30	76	5	105	3
	0.5235987			0.4461005
30	76	5	110	39
	0.5235987			0.4346820
30	76	5	115	98
	0.5235987			0.4238586
30	76	5	120	18
	0.5235987			0.4136939
30	76	5	125	45
	0.5235987			0.4042449
30	76	5	130	41
	0.5235987			0.3955616
30	76	5	135	73
	0.5235987			0.3876876
30	76	5	140	97
	0.5235987			0.3806604
30	76	5	145	09
	0.5235987			0.3745114
30	76	5	150	44
	0.5235987			0.3692671
30	76	5	155	03
	0.5235987			0.3649487
30	76	5	160	73
	0.5235987			0.3615733
30	76	5	165	26

```
  0.52359877                    0.3591534
30          6         5      170         8
  0.52359877                    0.3576980
30          6         5      175        94
  0.52359877                    0.3572123
30          6         5      180         9
30
  0.52359877                    0.8263518
30          6        10        0        22
  0.52359877                    0.7169821
30          6        10       45        31
  0.52359877                    0.4849231
30          6        10       90        55
  0.52359877                    0.4594513
30          6        10       95        64
  0.52359877                    0.4348527
30          6        10      100        57
  0.52359877                    0.4112913
30          6        10      105        09
  0.52359877                    0.3889083
30          6        10      110        95
  0.52359877                    0.3678228
30          6        10      115        69
  0.52359877                    0.3481317
30          6        10      120        22
  0.52359877                    0.3299112
30          6        10      125        76
  0.52359877                    0.3132188
30          6        10      130        33
  0.52359877                    0.2980947
30          6        10      135        14
  0.52359877                    0.2845645
30          6        10      140        89
  0.52359877                    0.2726419
30          6        10      145        93
  0.52359877                    0.2623309
30          6        10      150        49
  0.52359877                    0.2536285
30          6        10      155        62
  0.52359877                    0.2465275
30          6        10      160        23
  0.52359877                    0.2410183
30          6        10      165        92
  0.52359877                    0.2370916
30          6        10      170        05
  0.52359877                    0.2347391
30          6        10      175        03
  0.52359877                    0.2339555
30          6        10      180        57
30
```

```
  0.52359877
30          6        15         0          1
  0.52359877                              0.8229330
30          6        15        45         42
  0.52359877                              0.4665063
30          6        15        90         51
  0.52359877                              0.4295300
30          6        15        95         73
  0.52359877                              0.3943443
30          6        15       100         56
  0.52359877                              0.3611653
30          6        15       105         64
  0.52359877                              0.3301613
30          6        15       110         23
  0.52359877                              0.3014537
30          6        15       115         95
  0.52359877                              0.2751202
30          6        15       120         37
  0.52359877                              0.2511976
30          6        15       125         88
  0.52359877                              0.2296874
30          6        15       130         58
  0.52359877                              0.2105606
30          6        15       135         07
  0.52359877                              0.1937640
30          6        15       140         17
  0.52359877                              0.1792268
30          6        15       145         39
  0.52359877                              0.1668670
30          6        15       150         61
  0.52359877                              0.1565979
30          6        15       155         95
  0.52359877                              0.1483344
30          6        15       160         19
```

	0.52359877				0.1419981
30		6	15	165	99
	0.52359877				0.1375231
30		6	15	170	61
	0.52359877				0.1348590
30		6	15	175	75
	0.52359877				0.1339745
30		6	15	180	96
30					
	0.52359877				1.1736481
30		6	20	0	78
	0.52359877				0.9228698
30		6	20	45	59
	0.52359877				0.4415111
30		6	20	90	11
	0.52359877				0.3943269
30		6	20	95	55
	0.52359877				0.3501372
30		6	20	100	78
	0.52359877				0.3091882
30		6	20	105	48
	0.52359877				0.2716443
30		6	20	110	22
	0.52359877				0.2375914
30		6	20	115	68
	0.52359877				0.2070425
30		6	20	120	78
	0.52359877				0.1799448
30		6	20	125	53
	0.52359877				0.1561888
30		6	20	130	76
	0.52359877				0.1356190
30		6	20	135	3
	0.52359877				0.1180449
30		6	20	140	12
	0.52359877				0.1032533
30		6	20	145	16
	0.52359877				0.0910204
30		6	20	150	04
	0.52359877				0.0811236
30		6	20	155	27
	0.52359877				0.0733530
30		6	20	160	11
	0.52359877				0.0675214
30		6	20	165	25
	0.52359877				0.0634734
30		6	20	170	86
	0.52359877				0.0610928
30		6	20	175	12
30	0.52359877		20	180	0.0603073

```
            6                       79
30
   0.52359877                  1.3420201
30          6        25          0         43
   0.52359877                  1.0137560
30          6        25         45          5
   0.52359877                  0.4106969
30          6        25         90         02
   0.52359877                  0.3549116
30          6        25         95         39
   0.52359877                  0.3035747
30          6        25        100         33
   0.52359877                  0.2569392
30          6        25        105         58
   0.52359877                  0.2151354
30          6        25        110         03
   0.52359877                  0.1781763
30          6        25        115         12
   0.52359877                  0.1459672
30          6        25        120         52
   0.52359877                  0.1183177
30          6        25        125         53
   0.52359877                  0.0949563
30          6        25        130         03
   0.52359877                  0.0755470
30          6        25        135         47
   0.52359877                  0.0597079
30          6        25        140         61
   0.52359877                  0.0470298
30          6        25        145         44
   0.52359877                  0.0370955
30          6        25        150          4
   0.52359877                  0.0294987
30          6        25        155         08
```

	0.52359877			0.0238615
30	6	25	160	7
	0.52359877			0.0198510
30	6	25	165	09
	0.52359877			0.0171925
30	6	25	170	42
	0.52359877			0.0156816
30	6	25	175	65
	0.52359877			0.0151922
30	6	25	180	47
30				
	0.52359877			
30	6	30	0	1.5
	0.52359877			1.0928300
30	6	30	45	86
	0.52359877			
30	6	30	90	0.375
	0.52359877			0.3124817
30	6	30	95	39
	0.52359877			
30	6	30	100	0.2560715
	0.52359877			0.2060059
30	6	30	105	53
	0.52359877			0.1623515
30	6	30	110	59
	0.52359877			0.1250136
30	6	30	115	27
	0.52359877			
30	6	30	120	0.09375
	0.52359877			0.0681888
30	6	30	125	96
	0.52359877			0.0478502
30	6	30	130	59
	0.52359877			0.0321699
30	6	30	135	14
	0.52359877			0.0205257
30	6	30	140	01
	0.52359877			0.0122647
30	6	30	145	44
	0.52359877			0.0067309
30	6	30	150	47
	0.52359877			0.0032918
30	6	30	155	37
	0.52359877			0.0013638
30	6	30	160	67
	0.52359877			0.0004353
30	6	30	165	93
	0.52359877			8.65516E--
30	6	30	170	05
30	0.52359877	30	175	5.43012E--

```
           6                        06
  0.52359877
30         6       30      180        0
30
  0.52359877                   1.6427876
30         6       35        0        1
  0.52359877                   1.5359828
30         6       35       20       38
  0.52359877                   1.4784016
30         6       35       25       45
  0.52359877                   1.4103881
30         6       35       30       71
  0.52359877                   1.3332624
30         6       35       35       03
  0.52359877                   1.2484990
30         6       35       40        5
  0.52359877                   1.0625001
30         6       35       50       72
  0.52359877
30         6       35       60 0.8657751
  0.52359877                   0.6715670
30         6       35       70       02
  0.52359877                   0.5791885
30         6       35       75       94
  0.52359877                   0.4916999
30         6       35       80        1
  0.52359877                   0.3355050
30         6       35       90       36
  0.52359877                   0.2090709
30         6       35      100       42
  0.52359877                   0.1579359
30         6       35      105       17
  0.52359877                   0.0797187
30         6       35      115       33
```

	0.52359877			0.0519774	
30	6	35	120	18	
	0.52359877			0.0310814	
30	6	35	125	21	
	0.52359877			0.0163020	
30	6	35	130	4	
	0.52359877			0.0068056	
30	6	35	135	23	
	0.52359877			0.0016886	
30	6	35	140	67	
	0.52359877			1.09714E--	
30	6	35	145.542	13	
30					
	0.52359877			1.7660444	
30	6	40	0	43	
	0.52359877			1.6421115	
30	6	40	20	77	
	0.52359877			1.5754436	
30	6	40	25	37	
	0.52359877			1.4968407	
30	6	40	30	59	
	0.52359877			1.4079088	
30	6	40	35	43	
	0.52359877			1.3104396	
30	6	40	40	1	
	0.52359877				
30	6	40	45	1.2063631	
	0.52359877			1.0976968	
30	6	40	50	7	
	0.52359877			0.9864934	
30	6	40	55	08	
	0.52359877			0.8747872	
30	6	40	60	77	
	0.52359877			0.7645435	
30	6	40	65	27	
	0.52359877			0.6576088	
30	6	40	70	62	
	0.52359877			0.5556669	
30	6	40	75	7	
	0.52359877			0.4601992	
30	6	40	80	78	
	0.52359877			0.3724522	
30	6	40	85	38	
	0.52359877			0.2934120	
30	6	40	90	44	
	0.52359877			0.1640011	
30	6	40	100	45	
	0.52359877			0.0742124	
30	6	40	110	27	
30	0.52359877	40	120	0.0219187	

```
           6                                45
  0.52359877                          0.0081228
30         6       40       125             21
  0.52359877                          4.56916E--
30         6       40   133.476             11
30
  0.52359877                          1.8660254
30         6       45         0             04
  0.52359877                          1.7260643
30         6       45        20             48
  0.52359877                          1.6509309
30         6       45        25             21
  0.52359877
30         6       45        30         1.5625
  0.52359877                          1.4626640
30         6       45        35             34
  0.52359877                          1.3535320
30         6       45        40             15
  0.52359877                          1.2373724
30         6       45        45             36
  0.52359877                          1.1165523
30         6       45        50             33
  0.52359877                          0.9934742
30         6       45        55             11
  0.52359877                          0.8705127
30         6       45        60             02
  0.52359877                          0.7499527
30         6       45        65             97
  0.52359877                          0.6339314
30         6       45        70             67
  0.52359877                          0.5243843
30         6       45        75             42
  0.52359877
30         6       45        80       0.422999
```

30	0.5235987 76	45	85	0.3311761 8
30	0.5235987 76	45	90	0.25
30	0.5235987 76	45	100	0.1222315 34
30	0.5235987 76	45	110	0.0415352 01
30	0.5235987 76	45	115	0.0179564 96
30	0.5235987 76	45	120	0.0044872 98
30	0.5235987 76	45	125.264	2.31286E-- 11

semi	semi[rad]	AoA	meridian	cp
35	0.6108652 38	0	0	0.6579798 57
35	0.6108652 38	4	45	0.7505186 41
35	0.6108652 38	4	90	0.6547781 49
35	0.6108652 38	4	95	0.6434295 31
35	0.6108652 38	4	100	0.6322653 62
35	0.6108652 38	4	105	0.6213672 53
35	0.6108652 38	4	110	0.6108126 68
35	0.6108652 38	4	115	0.6006744 99
35	0.6108652 38	4	120	0.5910207 37
35	0.6108652 38	4	125	0.5819142 38
35	0.6108652 38	4	130	0.5734125 58
35	0.6108652 38	4	135	0.5655678 82
35	0.6108652 38	4	140	0.5584269 99
35	0.6108652 38	4	145	0.5520313 43
35	0.6108652 38	4	150	0.5464170 7
35	0.6108652 38	4	155	0.5416151 6
35	0.6108652	4	160	0.5376515

```
   38                                          41
   0.6108652                                0.5345472
35 38                 4       165           13
   0.6108652                                0.5323183
35 38                 4       170           68
   0.6108652                                0.5309764
35 38                 4       175            9
   0.6108652                                0.5305284
35 38                 4       180           37
35
   0.6108652                                0.8263518
35 38                 5         0           22
   0.6108652                                0.7734616
35 38                 5        45           29
   0.6108652                                0.6529817
35 38                 5        90            6
   0.6108652                                0.6388374
35 38                 5        95           79
   0.6108652                                0.6249539
35 38                 5       100           52
   0.6108652                                0.6114316
35 38                 5       105           06
   0.6108652                                0.5983648
35 38                 5       110           01
   0.6108652                                0.5858413
35 38                 5       115           79
   0.6108652                                0.5739423
35 38                 5       120           43
   0.6108652                                0.5627416
35 38                 5       125           76
   0.6108652                                0.5523062
35 38                 5       130           84
```

	0.61086523			0.5426960
35	8	5	135	42
	0.61086523			0.5339639
35	8	5	140	34
	0.61086523			0.5261562
35	8	5	145	57
	0.61086523			0.5193128
35	8	5	150	89
	0.61086523			0.5134675
35	8	5	155	74
	0.61086523			0.5086482
35	8	5	160	22
	0.61086523			0.5048772
35	8	5	165	06
	0.61086523			0.5021716
35	8	5	170	17
	0.61086523			0.5005434
35	8	5	175	98
	0.61086523			
35	8	5	180	0.5
35				
	0.61086523			
35	8	10	0	1
	0.61086523			0.8856325
35	8	10	45	05
	0.61086523			0.6381393
35	8	10	90	36
	0.61086523			0.6104354
35	8	10	95	12
	0.61086523			0.5835501
35	8	10	100	13
	0.61086523			0.5576672
35	8	10	105	64
	0.61086523			0.5329499
35	8	10	110	04
	0.61086523			0.5095400
35	8	10	115	77
	0.61086523			0.4875591
35	8	10	120	49
	0.61086523			0.4671086
35	8	10	125	12
	0.61086523			0.4482713
35	8	10	130	12
	0.61086523			0.4311130
35	8	10	135	27
	0.61086523			0.4156843
35	8	10	140	26
	0.61086523			0.4020226
35	8	10	145	14
35	0.61086523	10	150	0.3901542

```
           8                        81
  0.61086523                 0.3800968
35         8       10       155      55
  0.61086523                 0.3718610
35         8       10       160      85
  0.61086523                 0.3654528
35         8       10       165      53
  0.61086523                 0.3608748
35         8       10       170      59
  0.61086523
35         8       10       175  0.358128
  0.61086523                 0.3572123
35         8       10       180       9
35
  0.61086523                 1.1736481
35         8       15         0      78
  0.61086523                 0.9910842
35         8       15        45      28
  0.61086523                 0.6139035
35         8       15        90      64
  0.61086523                 0.5736366
35         8       15        95      38
  0.61086523                 0.5350263
35         8       15       100      74
  0.61086523                 0.4983204
35         8       15       105      35
  0.61086523                 0.4637227
35         8       15       110      65
  0.61086523                 0.4313943
35         8       15       115      27
  0.61086523                 0.4014549
35         8       15       120      85
  0.61086523                 0.3739864
35         8       15       125      28
```

	0.61086523			0.3490359
35	8	15	130	91
	0.61086523			0.3266212
35	8	15	135	03
	0.61086523			0.3067348
35	8	15	140	99
	0.61086523			0.2893506
35	8	15	145	65
	0.61086523			0.2744284
35	8	15	150	51
	0.61086523			0.2619201
35	8	15	155	04
	0.61086523			0.2517746
35	8	15	160	53
	0.61086523			0.2439431
35	8	15	165	37
	0.61086523			0.2383828
35	8	15	170	13
	0.61086523			0.2350605
35	8	15	175	85
	0.61086523			0.2339555
35	8	15	180	57
35				
	0.61086523			1.3420201
35	8	20	0	43
	0.61086523			1.0866127
35	8	20	45	01
	0.61086523			0.5810108
35	8	20	90	35
	0.61086523			0.5295592
35	8	20	95	7
	0.61086523			0.4808571
35	8	20	100	04
	0.61086523			0.4351943
35	8	20	105	41
	0.61086523			0.3927868
35	8	20	110	15
	0.61086523			0.3537785
35	8	20	115	48
	0.61086523			0.3182460
35	8	20	120	82
	0.61086523			0.2862045
35	8	20	125	94
	0.61086523			0.2576155
35	8	20	130	35
	0.61086523			0.2323955
35	8	20	135	03
	0.61086523			0.2104260
35	8	20	140	26
35	0.61086523	20	145	0.1915638

```
           8                    91
  0.61086523                0.1756516
35         8       20      150        7
  0.61086523                0.1625280
35         8       20      155       59
  0.61086523                0.1520376
35         8       20      160       91
  0.61086523                0.1440400
35         8       20      165       69
  0.61086523                0.1384173
35         8       20      170       36
  0.61086523                0.1350805
35         8       20      175       96
  0.61086523                0.1339745
35         8       20      180       96
35
  0.61086523
35         8       25        0      1.5
  0.61086523                1.1693153
35         8       25       45       41
  0.61086523                0.5404605
35         8       25       90       78
  0.61086523                0.4795425
35         8       25       95       77
  0.61086523                0.4226882
35         8       25      100        1
  0.61086523                0.3702070
35         8       25      105       37
  0.61086523                0.3222974
35         8       25      110       07
  0.61086523                0.2790510
35         8       25      115       56
  0.61086523                0.2404607
35         8       25      120       01
```

	0.61086523			0.2064303	
35	8	25	125	16	
	0.61086523			0.1767877	
35	8	25	130	09	
	0.61086523			0.1512989	
35	8	25	135	26	
	0.61086523			0.1296840	
35	8	25	140	04	
	0.61086523			0.1116334	
35	8	25	145	93	
	0.61086523			0.0968252	
35	8	25	150	2	
	0.61086523			0.0849406	
35	8	25	155	98	
	0.61086523			0.0756806	
35	8	25	160	56	
	0.61086523			0.0687791	
35	8	25	165	54	
	0.61086523			0.0640158	
35	8	25	170	3	
	0.61086523			0.0612258	
35	8	25	175	73	
	0.61086523			0.0603073	
35	8	25	180	79	
35					
	0.61086523			1.6427876	
35	8	30	0	1	
	0.61086523			1.2366792	
35	8	30	45	69	
	0.61086523			0.4934848	
35	8	30	90	93	
	0.61086523			0.4251062	
35	8	30	95	89	
	0.61086523			0.3622871	
35	8	30	100	23	
	0.61086523			0.3053331	
35	8	30	105	3	
	0.61086523			0.2543963	
35	8	30	110	27	
	0.61086523			0.2094824	
35	8	30	115	09	
	0.61086523			0.1704623	
35	8	30	120	11	
	0.61086523			0.1370874	
35	8	30	125	96	
	0.61086523			0.1090084	
35	8	30	130	25	
	0.61086523			0.0857955	
35	8	30	135	51	
35	0.61086523	30	140	0.0669621	

	8			38
	0.61086523			0.0519881
35	8	30	145	16
	0.61086523			0.0403442
35	8	30	150	04
	0.61086523			0.0315154
35	8	30	155	75
	0.61086523			0.0250236
35	8	30	160	19
	0.61086523			0.0204471
35	8	30	165	55
	0.61086523			0.0174389
35	8	30	170	48
	0.61086523			0.0157404
35	8	30	175	55
	0.61086523			0.0151922
35	8	30	180	47
35				
	0.61086523			1.7660444
35	8	35	0	43
	0.61086523			1.2866576
35	8	35	45	67
	0.61086523			0.4415111
35	8	35	90	11
	0.61086523			0.3679044
35	8	35	95	26
	0.61086523			
35	8	35	100	0.3014891
	0.61086523			0.2425437
35	8	35	105	79
	0.61086523			0.1911467
35	8	35	110	13
	0.61086523			0.1471864
35	8	35	115	14

	0.61086523			0.1103777	
35	8	35	120	78	
	0.61086523			0.0802830	
35	8	35	125	8	
	0.61086523			0.0563371	
35	8	35	130	23	
	0.61086523			0.0378756	
35	8	35	135	65	
	0.61086523				
35	8	35	140	0.0241662	
	0.61086523			0.0144400	
35	8	35	145	55	
	0.61086523			0.0079247	
35	8	35	150	68	
	0.61086523			0.0038756	
35	8	35	155	86	
	0.61086523			0.0016057	
35	8	35	160	67	
	0.61086523			0.0005126	
35	8	35	165	16	
	0.61086523			0.0001019	
35	8	35	170	03	
	0.61086523			6.39322E--	
35	8	35	175	06	
	0.61086523				
35	8	35	180	0	
35					
	0.61086523			1.8660254	
35	8	40	0	04	
	0.61086523			1.7453529	
35	8	40	20	01	
	0.61086523			1.6802856	
35	8	40	25	57	
	0.61086523			1.6034204	
35	8	40	30	92	
	0.61086523			1.5162439	
35	8	40	35	52	
	0.61086523			1.4204169	
35	8	40	40	78	
	0.61086523			1.2100668	
35	8	40	50	15	
	0.61086523			0.9874493	
35	8	40	60	18	
	0.61086523			0.7674925	
35	8	40	70	95	
	0.61086523			0.6627776	
35	8	40	75	78	
	0.61086523			0.5635352	
35	8	40	80	64	
35	0.61086523	40	90	0.3861184	

```
           8                        3
  0.61086523                0.3096750
35         8       40       95       38
  0.61086523                0.2421414
35         8       40      100       59
  0.61086523                0.1837468
35         8       40      105       08
  0.61086523                0.1344703
35         8       40      110       74
  0.61086523                0.0940559
35         8       40      115       04
  0.61086523                0.0620327
35         8       40      120        4
  0.61086523                0.0377430
35         8       40      125       42
  0.61086523                0.0025965
35         8       40      140       24
  0.61086523                7.32986E--
35         8       40   146.56       11
35
  0.61086523                1.9396926
35         8       45        0       21
  0.61086523                1.8045289
35         8       45       20       54
  0.61086523                1.7318041
35         8       45       25       84
  0.61086523                1.6460451
35         8       45       30       63
  0.61086523                1.5489955
35         8       45       35       76
  0.61086523                1.4426011
35         8       45       40       13
  0.61086523                1.3289579
35         8       45       45       89
```

35	0.6108652 38	45	50	1.2102579
35	0.6108652 38	45	55	1.0887310 28
35	0.6108652 38	45	60	0.9665887 57
35	0.6108652 38	45	65	0.8459677 46
35	0.6108652 38	45	70	0.7288770 01
35	0.6108652 38	45	75	0.6171494 27
35	0.6108652 38	45	80	0.5123992 69
35	0.6108652 38	45	85	0.4159866 12
35	0.6108652 38	45	90	0.3289899 28
35	0.6108652 38	45	100	0.1860474 47
35	0.6108652 38	45	110	0.0860893 91
35	0.6108652 38	45	120	0.0268961 36
35	0.6108652 38	45	125	0.0107599 39
35	0.6108652 38	45	134.44	1.39357E-- 09

semi	semi[rad]	AoA	meridian	cp
40	0.6981317 01	0	0	0.8263518 22
40	0.6981317 01	4	45	0.9221014 59
40	0.6981317 01	4	90	0.8223308 23
40	0.6981317 01	4	95	0.8104287 47
40	0.6981317 01	4	100	0.7987030 26
40	0.6981317 01	4	105	0.7872399 68
40	0.6981317 01	4	110	0.7761220 22
40	0.6981317 01	4	115	0.7654273
40	0.6981317 01	4	120	0.7552291 81
40	0.6981317	4	125	0.7455959

```
   01                                    93
   0.6981317                        0.7365907
40 01                4       130         77
   0.6981317                        0.7282711
40 01                4       135         18
   0.6981317                        0.7206890
40 01                4       140         42
   0.6981317                        0.7138909
40 01                4       145         61
   0.6981317                        0.7079176
40 01                4       150         63
   0.6981317                        0.7028043
40 01                4       155         35
   0.6981317                        0.6985806
40 01                4       160         07
   0.6981317                        0.6952706
40 01                4       165         09
   0.6981317                        0.6928930
40 01                4       170          3
   0.6981317                        0.6914611
40 01                4       175         75
   0.6981317                        0.6909830
40 01                4       180         06
40
   0.6981317
40 01                5         0          1
   0.6981317                        0.9454547
40 01                5        45         21
   0.6981317                        0.8200747
40 01                5        90         52
   0.6981317                        0.8052379
40 01                5        95         63
```

0.69813170				0.7906479
40	1	5	100	9
0.69813170				0.7764112
40	1	5	105	92
0.69813170				0.7626287
40	1	5	110	4
0.69813170				0.7493950
40	1	5	115	78
0.69813170				0.7367985
40	1	5	120	1
0.69813170				0.7249204
40	1	5	125	08
0.69813170				0.7138351
40	1	5	130	33
0.69813170				0.7036099
40	1	5	135	59
0.69813170				0.6943050
40	1	5	140	77
0.69813170				0.6859736
40	1	5	145	75
0.69813170				0.6786620
40	1	5	150	68
0.69813170				0.6724098
40	1	5	155	63
0.69813170				0.6672501
40	1	5	160	48
0.69813170				0.6632096
40	1	5	165	8
0.69813170				0.6603090
40	1	5	170	58
0.69813170				0.6585628
40	1	5	175	81
0.69813170				0.6579798
40	1	5	180	57
40				
0.69813170				1.1736481
40	1	10	0	78
0.69813170				1.0572997
40	1	10	45	75
0.69813170				0.8014342
40	1	10	90	66
0.69813170				0.7723469
40	1	10	95	38
0.69813170				0.7440125
40	1	10	100	1
0.69813170				0.7166284
40	1	10	105	46
0.69813170				0.6903734
40	1	10	110	66
40	0.69813170	10	115	0.6654070

```
           1                    97
  0.69813170              0.6418696
40         1       10       120        77
  0.69813170              0.6198828
40         1       10       125        01
  0.69813170              0.5995501
40         1       10       130        37
  0.69813170              0.5809585
40         1       10       135         8
  0.69813170              0.5641796
40         1       10       140        45
  0.69813170              0.5492710
40         1       10       145        53
  0.69813170              0.5362784
40         1       10       150        16
  0.69813170              0.5252369
40         1       10       155        53
  0.69813170              0.5161731
40         1       10       160        55
  0.69813170              0.5091063
40         1       10       165        34
  0.69813170              0.5040499
40         1       10       170        81
  0.69813170              0.5010128
40         1       10       175        92
  0.69813170
40         1       10       180       0.5
40
  0.69813170              1.3420201
40         1       15         0        43
  0.69813170              1.1584886
40         1       15        45        27
  0.69813170              0.7709967
40         1       15        90        46
```

```
   0.69813170                    0.7286781
40          1       15        95        24
   0.69813170                    0.6878623
40          1       15       100        79
   0.69813170                    0.6488197
40          1       15       105        55
   0.69813170                    0.6117814
40          1       15       110        39
   0.69813170                    0.5769398
40          1       15       115         1
   0.69813170                    0.5444496
40          1       15       120        88
   0.69813170                    0.5144305
40          1       15       125        16
   0.69813170                    0.4869693
40          1       15       130        28
   0.69813170                    0.4621243
40          1       15       135        86
   0.69813170                    0.4399293
40          1       15       140        21
   0.69813170                    0.4203975
40          1       15       145        94
   0.69813170                    0.4035271
40          1       15       150        21
   0.69813170                    0.3893048
40          1       15       155        66
   0.69813170                    0.3777112
40          1       15       160        41
   0.69813170                    0.3687241
40          1       15       165        36
   0.69813170                    0.3623224
40          1       15       170        43
   0.69813170                    0.3584889
40          1       15       175        32
   0.69813170                    0.3572123
40          1       15       180         9
40
   0.69813170
40          1       20         0       1.5
   0.69813170                    1.2459467
40          1       20        45        06
   0.69813170                    0.7296870
40          1       20        90        22
   0.69813170                    0.6755583
40          1       20        95        78
   0.69813170                    0.6239036
40          1       20       100         9
   0.69813170                    0.5750455
40          1       20       105        52
40 0.69813170       20       110 0.5292406
```

	1			39
40	0.698131701	20	115	0.486681251
40	0.698131701	20	120	0.4474986
40	0.698131701	20	125	0.411767668
40	0.698131701	20	130	0.379513415
40	0.698131701	20	135	0.350718095
40	0.698131701	20	140	0.32532939
40	0.698131701	20	145	0.303269055
40	0.698131701	20	150	0.284441764
40	0.698131701	20	155	0.26874383
40	0.698131701	20	160	0.2560715
40	0.698131701	20	165	0.246328529
40	0.698131701	20	170	0.239432764
40	0.698131701	20	175	0.23532152
40	0.698131701	20	180	0.233955557
40				
40	0.698131701	25	0	1.64278761
40	0.698131701	25	45	1.317016642

	0.69813170				0.6787602
40		1	25	90	67
	0.69813170				0.6146017
40		1	25	95	14
	0.69813170				0.5540797
40		1	25	100	94
	0.69813170				0.4975474
40		1	25	105	29
	0.69813170				0.4452590
40		1	25	110	26
	0.69813170				0.3973738
40		1	25	115	81
	0.69813170				0.3539622
40		1	25	120	23
	0.69813170				0.3150136
40		1	25	125	15
	0.69813170				0.2804473
40		1	25	130	92
	0.69813170				0.2501247
40		1	25	135	29
	0.69813170				0.2238619
40		1	25	140	11
	0.69813170				0.2014443
40		1	25	145	27
	0.69813170				0.1826406
40		1	25	150	94
	0.69813170				0.1672170
40		1	25	155	31
	0.69813170				0.1549498
40		1	25	160	96
	0.69813170				0.1456384
40		1	25	165	41
	0.69813170				0.1391148
40		1	25	170	85
	0.69813170				0.1352530
40		1	25	175	35
	0.69813170				0.1339745
40		1	25	180	96
40					
	0.69813170				1.7660444
40		1	30	0	43
	0.69813170				1.3695390
40		1	30	45	11
	0.69813170				0.6197638
40		1	30	90	67
	0.69813170				0.5476602
40		1	30	95	71
	0.69813170				0.4805122
40		1	30	100	56
40	0.69813170		30	105	0.4186801

	1			28
	0.69813170			0.3623883
40	1	30	110	38
	0.69813170			0.3117312
40	1	30	115	59
	0.69813170			0.2666826
40	1	30	120	12
	0.69813170			0.2271081
40	1	30	125	81
	0.69813170			0.1927813
40	1	30	130	31
	0.69813170			0.1634007
40	1	30	135	67
	0.69813170			0.1386099
40	1	30	140	23
	0.69813170			0.1180173
40	1	30	145	02
	0.69813170			0.1012170
40	1	30	150	85
	0.69813170			0.0878093
40	1	30	155	1
	0.69813170			0.0774189
40	1	30	160	56
	0.69813170			0.0697132
40	1	30	165	9
	0.69813170			0.0644169
40	1	30	170	13
	0.69813170			0.0613240
40	1	30	175	07
	0.69813170			0.0603073
40	1	30	180	79
40				
	0.69813170			1.8660254
40	1	35	0	04

```
   0.69813170                    1.4019179
40          1       35        45        48
   0.69813170                    0.5544903
40          1       35        90        96
   0.69813170                    0.4767680
40          1       35        95         3
   0.69813170                    0.4054363
40          1       35       100        88
   0.69813170                    0.3408399
40          1       35       105        91
   0.69813170                    0.2831465
40          1       35       110        61
   0.69813170                    0.2323555
40          1       35       115        93
   0.69813170                    0.1883117
40          1       35       120        14
   0.69813170                    0.1507223
40          1       35       125        27
   0.69813170                    0.1191789
40          1       35       130        19
   0.69813170                    0.0931812
40          1       35       135        72
   0.69813170                    0.0721637
40          1       35       140        64
   0.69813170                    0.0555228
40          1       35       145        69
   0.69813170                    0.0426449
40          1       35       150        52
   0.69813170                    0.0329334
40          1       35       155         3
   0.69813170                    0.0258344
40          1       35       160        19
   0.69813170                    0.0208600
40          1       35       165        22
   0.69813170                    0.0176085
40          1       35       170        09
   0.69813170                    0.0157807
40          1       35       175        33
   0.69813170                    0.0151922
40          1       35       180        47
40
   0.69813170                    1.9396926
40          1       40         0        21
   0.69813170                    1.4131696
40          1       40        45        36
   0.69813170                    0.4849231
40          1       40        90        55
   0.69813170                    0.4040790
40          1       40        95        16
40 0.69813170       40       100 0.3311333
```

	1			33	
0.69813170				0.2663921	
40	1	40	105	51	
0.69813170				0.2099414	
40	1	40	110	15	
0.69813170				0.1616586	
40	1	40	115	73	
0.69813170				0.1212307	
40	1	40	120	89	
0.69813170				0.0881769	
40	1	40	125	99	
0.69813170				0.0618765	
40	1	40	130	3	
0.69813170				0.0415998	
40	1	40	135	3	
0.69813170				0.0265423	
40	1	40	140	67	
0.69813170				0.0158598	
40	1	40	145	89	
0.69813170				0.0087039	
40	1	40	150	79	
0.69813170				0.0042567	
40	1	40	155	67	
0.69813170				0.0017636	
40	1	40	160	56	
0.69813170				0.0005630	
40	1	40	165	2	
0.69813170				0.0001119	
40	1	40	170	22	
0.69813170				7.02184E--	
40	1	40	175	06	
0.69813170					
40	1	40	180	0	
40					

	0.6981317			1.9848077
40	01	45	0	53
	0.6981317			
40	01	45	20	1.8567712
	0.6981317			1.7877285
40	01	45	25	18
	0.6981317			1.7061625
40	01	45	30	1
	0.6981317			1.6136480
40	01	45	35	69
	0.6981317			1.5119449
40	01	45	40	29
	0.6981317			1.2886597
40	01	45	50	1
	0.6981317			1.0522858
40	01	45	60	1
	0.6981317			0.8186453
40	01	45	70	78
	0.6981317			0.7073726
40	01	45	75	74
	0.6981317			0.6018808
40	01	45	80	94
	0.6981317			0.4131759
40	01	45	90	11
	0.6981317			0.3318018
40	01	45	95	48
	0.6981317			0.2598607
40	01	45	100	51
	0.6981317			0.1975986
40	01	45	105	69
	0.6981317			0.1449972
40	01	45	110	01
	0.6981317			0.1017885
40	01	45	115	88
	0.6981317			0.0674780
40	01	45	120	57
	0.6981317			0.0413726
40	01	45	125	05
	0.6981317			0.0031319
40	01	45	140	16
	0.6981317			1.41114E--
40	01	45	147.04	09

semi	semi[rad]	AoA	meridian	cp
	0.7853981			
45	63	0	0	1
	0.7853981			1.0959772
45	63	4	45	61
45	0.7853981	4	90	0.9951340

	63				34
	0.7853981				0.9830412
45	63		4	95	62
	0.7853981				0.9711136
45	63		4	100	06
	0.7853981				0.9594393
45	63		4	105	43
	0.7853981				0.9481032
45	63		4	110	4
	0.7853981				0.9371860
45	63		4	115	32
	0.7853981				0.9267639
45	63		4	120	75
	0.7853981				0.9169084
45	63		4	125	77
	0.7853981				0.9076857
45	63		4	130	89
	0.7853981				0.8991567
45	63		4	135	74
	0.7853981				0.8913767
45	63		4	140	2
	0.7853981				0.8843952
45	63		4	145	16
	0.7853981				0.8782560
45	63		4	150	68
	0.7853981				0.8729972
45	63		4	155	43
	0.7853981				0.8686508
45	63		4	160	54
	0.7853981				0.8652431
45	63		4	165	5
	0.7853981				0.8627945
45	63		4	170	24

0.78539816 0.8613195
45 3 4 175 32
0.78539816 0.8608268
45 3 4 180 99
45
0.78539816 1.1736481
45 3 5 0 78
0.78539816 1.1189897
45 3 5 45 42
0.78539816 0.9924038
45 3 5 90 77
0.78539816 0.9773271
45 3 5 95 42
0.78539816 0.9624792
45 3 5 100 38
0.78539816 0.9479692
45 3 5 105 65
0.78539816 0.9339012
45 3 5 110 8
0.78539816
45 3 5 115 0.9203737
0.78539816 0.9074788
45 3 5 120 19
0.78539816 0.8953024
45 3 5 125 22
0.78539816 0.8839235
45 3 5 130 15
0.78539816 0.8734141
45 3 5 135 34
0.78539816 0.8638392
45 3 5 140 43
0.78539816 0.8552566
45 3 5 145 92
0.78539816 0.8477172
45 3 5 150 36
0.78539816 0.8412645
45 3 5 155 9
0.78539816 0.8359355
45 3 5 160 11
0.78539816 0.8317598
45 3 5 165 97
0.78539816 0.8287608
45 3 5 170 77
0.78539816 0.8269549
45 3 5 175 05
0.78539816 0.8263518
45 3 5 180 22
45
0.78539816 1.3420201
45 3 10 0 43

0.78539816				1.2267679
45	3	10	45	18
0.78539816				0.9698463
45	3	10	90	1
0.78539816				0.9402663
45	3	10	95	42
0.78539816				0.9113643
45	3	10	100	81
0.78539816				0.8833448
45	3	10	105	98
0.78539816				0.8563958
45	3	10	110	44
0.78539816				0.8306879
45	3	10	115	88
0.78539816				0.8063746
45	3	10	120	61
0.78539816				0.7835918
45	3	10	125	76
0.78539816				0.7624587
45	3	10	130	78
0.78539816				0.7430783
45	3	10	135	93
0.78539816				0.7255385
45	3	10	140	92
0.78539816				0.7099132
45	3	10	145	4
0.78539816				0.6962634
45	3	10	150	45
0.78539816				0.6846388
45	3	10	155	45
0.78539816				0.6750788
45	3	10	160	84
0.78539816				0.6676139
45	3	10	165	96

```
  0.78539816                    0.6622666
45          3       10      170        66
  0.78539816                    0.6590522
45          3       10      175        95
  0.78539816                    0.6579798
45          3       10      180        57
45
45
  0.78539816
45          3       15        0       1.5
  0.78539816                    1.3200597
45          3       15       45        42
  0.78539816                    0.9330127
45          3       15       90        02
  0.78539816                    0.8899436
45          3       15       95        74
  0.78539816                    0.8482085
45          3       15      100        27
  0.78539816                    0.8080904
45          3       15      105        77
  0.78539816                    0.7698386
45          3       15      110        56
  0.78539816                    0.7336679
45          3       15      115        17
  0.78539816                    0.6997595
45          3       15      120        26
  0.78539816                    0.6682626
45          3       15      125         3
  0.78539816                    0.6392964
45          3       15      130        35
  0.78539816                    0.6129529
45          3       15      135         6
  0.78539816                    0.5893002
45          3       15      140        41
  0.78539816                    0.5683858
45          3       15      145        31
  0.78539816                    0.5502404
45          3       15      150        74
  0.78539816                    0.5348817
45          3       15      155         6
  0.78539816                    0.5223176
45          3       15      160        64
  0.78539816                    0.5125497
45          3       15      165        89
  0.78539816                    0.5055762
45          3       15      170        09
  0.78539816                    0.5013938
45          3       15      175        07
  0.78539816
45          3       15      180       0.5
```

```
45
  0.78539816                    1.6427876
45          3       20         0         1
  0.78539816                    1.3960305
45          3       20        45        88
  0.78539816                    0.8830222
45          3       20        90        22
  0.78539816                    0.8278881
45          3       20        95        68
  0.78539816                    0.7749306
45          3       20       100        36
  0.78539816                    0.7244925
45          3       20       105        72
  0.78539816                    0.6768597
45          3       20       110        12
  0.78539816                    0.6322613
45          3       20       115        95
  0.78539816                    0.5908728
45          3       20       120        61
  0.78539816                    0.5528189
45          3       20       125        06
  0.78539816                    0.5181787
45          3       20       130        11
  0.78539816                    0.4869916
45          3       20       135        33
  0.78539816                    0.4592637
45          3       20       140        23
  0.78539816                    0.4349747
45          3       20       145        05
  0.78539816                    0.4140851
45          3       20       150        56
  0.78539816                    0.3965436
45          3       20       155        28
```

	0.78539816			0.3822934
45	3	20	160	26
	0.78539816			0.3712788
45	3	20	165	22
	0.78539816			0.3634504
45	3	20	170	67
	0.78539816			0.3587698
45	3	20	175	14
	0.78539816			0.3572123
45	3	20	180	9
45				
	0.78539816			1.7660444
45	3	25	0	43
	0.78539816			1.4523721
45	3	25	45	23
	0.78539816			0.8213938
45	3	25	90	05
	0.78539816			0.7559853
45	3	25	95	47
	0.78539816			0.6937572
45	3	25	100	19
	0.78539816			0.6350912
45	3	25	105	6
	0.78539816			0.5802841
45	3	25	110	31
	0.78539816			0.5295496
45	3	25	115	07
	0.78539816			0.4830231
45	3	25	120	32
	0.78539816			0.4407684
45	3	25	125	02
	0.78539816			0.4027857
45	3	25	130	06
	0.78539816			0.3690216
45	3	25	135	82
	0.78539816			0.3393801
45	3	25	140	34
	0.78539816			0.3137334
45	3	25	145	89
	0.78539816			0.2919345
45	3	25	150	03
	0.78539816			0.2738277
45	3	25	155	83
	0.78539816			0.2592607
45	3	25	160	34
	0.78539816			0.2480935
45	3	25	165	42
	0.78539816			0.2402078
45	3	25	170	57
45	0.78539816	25	175	0.2355138

	3			73
45	0.785398163	25	180	0.233955557
45				
45				
45	0.785398163	30	0	1.866025404
45	0.785398163	30	45	1.487372436
45	0.785398163	30	90	0.75
45	0.785398163	30	95	0.676419944
45	0.785398163	30	100	0.607154689
45	0.785398163	30	105	0.542602956
45	0.785398163	30	110	0.483046312
45	0.785398163	30	115	0.428653398
45	0.785398163	30	120	0.379487298
45	0.785398163	30	125	0.335515717
45	0.785398163	30	130	0.296623579
45	0.785398163	30	135	0.262627564
45	0.785398163	30	140	0.233292074
45	0.785398163	30	145	0.208346038

0.78539816
45 3 30 150 0.1875
0.78539816 0.1704628
45 3 30 155 84
0.78539816 0.1569578
45 3 30 160 74
0.78539816 0.1467368
45 3 30 165 72
0.78539816 0.1395930
45 3 30 170 46
0.78539816 0.1353710
45 3 30 175 53
0.78539816 0.1339745
45 3 30 180 96
45
45
0.78539816 1.9396926
45 3 35 0 21
0.78539816 1.4999680
45 3 35 45 6
0.78539816 0.6710100
45 3 35 90 72
0.78539816 0.5916095
45 3 35 95 11
0.78539816 0.5177544
45 3 35 100 21
0.78539816 0.4498378
45 3 35 105 71
0.78539816 0.3881007
45 3 35 110 78
0.78539816 0.3326384
45 3 35 115 49
0.78539816 0.2834112
45 3 35 120 43
0.78539816
45 3 35 125 0.2402589
0.78539816 0.2029180
45 3 35 130 12
0.78539816 0.1710420
45 3 35 135 11
0.78539816 0.1442229
45 3 35 140 76
0.78539816 0.1220144
45 3 35 145 96
0.78539816 0.1039548
45 3 35 150 37
0.78539816 0.0895896
45 3 35 155 21
0.78539816 0.0784932
45 3 35 160 67

```
   0.78539816                    0.0702884
45          3       35      165        82
   0.78539816                    0.0646631
45          3       35      170        61
   0.78539816                    0.0613841
45          3       35      175        45
   0.78539816                    0.0603073
45          3       35      180        79
45
45
   0.78539816                    1.9848077
45          3       40        0        53
   0.78539816                    1.4897762
45          3       40       45        85
   0.78539816                    0.5868240
45          3       40       90        89
   0.78539816                    0.5041309
45          3       40       95        73
   0.78539816                    0.4282727
45          3       40      100        95
   0.78539816                    0.3596146
45          3       40      105        25
   0.78539816
45          3       40      110 0.2983324
   0.78539816                    0.2444221
45          3       40      115        26
   0.78539816                    0.1977141
45          3       40      120         9
   0.78539816                    0.1578922
45          3       40      125        81
   0.78539816                    0.1245162
45          3       40      130        01
```

0.78539816 0.0970478
45 3 40 135 04
0.78539816 0.0748791
45 3 40 140 6
0.78539816 0.0573620
45 3 40 145 02
0.78539816 0.0438374
45 3 40 150 9
0.78539816 0.0336652
45 3 40 155 87
0.78539816 0.0262510
45 3 40 160 21
0.78539816 0.0210712
45 3 40 165 2
0.78539816 0.0176949
45 3 40 170 11
0.78539816 0.0158012
45 3 40 175 03
0.78539816 0.0151922
45 3 40 180 47
45
45
0.78539816
45 3 45 0 2
0.78539816 1.4571067
45 3 45 45 81
0.78539816
45 3 45 90 0.5
0.78539816 0.4166423
45 3 45 95 19
0.78539816 0.3414286
45 3 45 100 67
0.78539816 0.2746746
45 3 45 105 04
0.78539816 0.2164687
45 3 45 110 46
0.78539816 0.1666848
45 3 45 115 36
0.78539816
45 3 45 120 0.125
0.78539816 0.0909185
45 3 45 125 28
0.78539816 0.0638003
45 3 45 130 46
0.78539816 0.0428932
45 3 45 135 19
0.78539816 0.0273676
45 3 45 140 01
0.78539816 0.0163529
45 3 45 145 92

0.78539816			0.0089745	
45	3	45	150	96
0.78539816			0.0043891	
45	3	45	155	15
0.78539816			0.0018184	
45	3	45	160	9
0.78539816			0.0005805	
45	3	45	165	25
0.78539816			0.0001154	
45	3	45	170	02
0.78539816			7.24016E--	
45	3	45	175	06
0.78539816				
45	3	45	180	0

Appendix 4 – Calculations for aerodynamic coefficients (Fig 13 & 21)

semi	AoA	AoA[rad]	Cn	Cl	Cd
5	1	0.017453293	0.0483	0.096585287	0.001685902
5	2	0.034906585	0.0508	0.101538108	0.003545789
5	3	0.052359878	0.0552	0.110248701	0.00577789
5	4	0.06981317	0.0614	0.122500865	0.008566095
5	5	0.087266463	0.0695	0.138471063	0.012114648
5	10	0.174532925	0.1314	0.258807477	0.045634741
5	15	0.261799388	0.2138	0.413029883	0.110671024
5	20	0.34906585	0.3138	0.589751089	0.214651842
5	25	0.436332313	0.4288	0.777249558	0.362437421
5	30	0.523598776	0.5546	0.960595378	0.5546
5	35	0.610865238	0.6878	1.126825552	0.789011746
5	40	0.698131701	0.8269	1.2668843	1.063042149
5	45	0.785398163	0.9623	1.360897711	1.360897711
5	50	0.872664626	1.0948	1.40744775	1.677330913

semi	AoA	AoA[rad]	Cn	Cl	Cd
10	1	0.017453293	0.1897	0.379342216	0.006621443
10	2	0.034906585	0.1917	0.383166443	0.013380467
10	3	0.052359878	0.1954	0.390264422	0.020452892
10	4	0.06981317	0.2009	0.400821235	0.028028151
10	5	0.087266463	0.2081	0.414616233	0.03627422
10	10	0.174532925	0.2696	0.53100834	0.093631097
10	15	0.261799388	0.3726	0.719807926	0.192871952
10	20	0.34906585	0.4882	0.917515875	0.333948468
10	25	0.436332313	0.6151	1.11493984	0.519904986
10	30	0.523598776	0.7487	1.29678644	0.7487
10	35	0.610865238	0.8874	1.453831048	1.017983459
10	40	0.698131701	1.0218	1.565488424	1.313600759
10	45	0.785398163	1.1528	1.630305395	1.630305395
10	50	0.872664626	1.2711	1.634094661	1.947438183

semi	AoA	AoA[rad]	Cn	Cl	Cd
15	1	0.017453293	0.4207	0.841271851	0.014684455
15	2	0.034906585	0.4221	0.843685736	0.029462155
15	3	0.052359878	0.425	0.848835105	0.044485563
15	4	0.06981317	0.4295	0.856907519	0.059920811
15	5	0.087266463	0.4355	0.867685582	0.075912652

15	10	0.174532925	0.488	0.961172367	0.169480621
15	15	0.261799388	0.5762	1.113132922	0.298263068
15	20	0.34906585	0.7068	1.328349489	0.483479675
15	25	0.436332313	0.8357	1.514802835	0.706364163
15	30	0.523598776	0.9727	1.684765821	0.9727
15	35	0.610865238	1.1046	1.809670696	1.267145063
15	40	0.698131701	1.2292	1.883243659	1.58022906
15	45	0.785398163	1.3428	1.899005972	1.899005972
15	50	0.872664626	1.4428	1.854827927	2.210497845

semi	AoA	AoA[rad]	Cn	Cl	Cd
20	1	0.017453293	0.7344	1.468576295	0.025634095
20	2	0.034906585	0.7351	1.469304394	0.05130924
20	3	0.052359878	0.7371	1.47217966	0.077153667
20	4	0.06981317	0.7403	1.476993333	0.103281435
20	5	0.087266463	0.7447	1.483732383	0.129809763
20	10	0.174532925	0.7852	1.546542095	0.272697098
20	15	0.261799388	0.855	1.651733163	0.442580567
20	20	0.34906585	0.9523	1.789738566	0.651411565
20	25	0.436332313	1.0907	1.977019807	0.921899476
20	30	0.523598776	1.213	2.10097763	1.213
20	35	0.610865238	1.3297	2.178452947	1.525369175
20	40	0.698131701	1.4372	2.201918147	1.847628705
20	45	0.785398163	1.5267	2.159079846	2.159079846
20	50	0.872664626	1.6001	2.057048909	2.451495427

semi	AoA	AoA[rad]	Cn	Cl	Cd
25	1	0.017453293	1.1212	2.242058472	0.039135276
25	2	0.034906585	1.1212	2.241033991	0.078258631
25	3	0.052359878	1.1221	2.241124402	0.117452353
25	4	0.06981317	1.1238	2.242124959	0.15678465
25	5	0.087266463	1.1264	2.244227416	0.196344457
25	10	0.174532925	1.1527	2.270375794	0.400328509
25	15	0.261799388	1.2002	2.318608353	0.621269236
25	20	0.34906585	1.2675	2.382120794	0.867021063
25	25	0.436332313	1.3525	2.451562564	1.143182398
25	30	0.523598776	1.4777	2.559451478	1.4777
25	35	0.610865238	1.5707	2.573284232	1.801833017
25	40	0.698131701	1.6505	2.528712707	2.1218419

	25	45	0.785398163	1.7145	2.424669153	2.424669153
	25	50	0.872664626	1.7543	2.255284607	2.687743533

semi	AoA	AoA[rad]	Cn	Cl	Cd
30	1	0.017453293	1.5694	3.138321946	0.054779613
30	2	0.034906585	1.5686	3.135288903	0.109486701
30	3	0.052359878	1.5683	3.132301399	0.16415696
30	4	0.06981317	1.5684	3.129158913	0.218812107
30	5	0.087266463	1.569	3.126058963	0.273494721
30	10	0.174532925	1.5792	3.110416807	0.548450404
30	15	0.261799388	1.6011	3.093087681	0.828790346
30	20	0.34906585	1.6341	3.071103423	1.117790232
30	25	0.436332313	1.677	3.039756318	1.41746165
30	30	0.523598776	1.7286	2.994023026	1.7286
30	35	0.610865238	1.8195	2.980894289	2.087244652
30	40	0.698131701	1.8643	2.856273311	2.396697881
30	45	0.785398163	1.8903	2.673287897	2.673287897
30	50	0.872664626	1.8969	2.438607634	2.906219408

semi	AoA	AoA[rad]	Cn	Cl	Cd
35	1	0.017453293	2.0654	4.130170859	0.072092401
35	2	0.034906585	2.0637	4.124885699	0.144044183
35	3	0.052359878	2.0621	4.118547927	0.215843951
35	4	0.06981317	2.0605	4.110961451	0.287466428
35	5	0.087266463	2.059	4.102329767	0.358907349
35	10	0.174532925	2.0518	4.041257095	0.712582662
35	15	0.261799388	2.0457	3.951988926	1.058932241
35	20	0.34906585	2.0409	3.83563734	1.396057821
35	25	0.436332313	2.0374	3.693022971	1.722084893
35	30	0.523598776	2.0355	3.525589419	2.0355
35	35	0.610865238	2.03526	3.334374779	2.334754356
35	40	0.698131701	2.074	3.17755235	2.666283005
35	45	0.785398163	2.0567	2.908613034	2.908613034
35	50	0.872664626	2.0184	2.594805023	3.092368208

semi	AoA	AoA[rad]	Cn	Cl	Cd
40	1	0.017453293	2.594	5.187209842	0.090543085

40	2	0.034906585	2.5916	5.180042535	0.180891071
40	3	0.052359878	2.5887	5.170304553	0.27096418
40	4	0.06981317	2.5853	5.158004678	0.360682823
40	5	0.087266463	2.5815	5.143353226	0.4499851
40	10	0.174532925	2.556	5.034337233	0.887689484
40	15	0.261799388	2.5203	4.86884572	1.304603279
40	20	0.34906585	2.4755	4.652418166	1.69334173
40	25	0.436332313	2.4229	4.391786274	2.047923573
40	30	0.523598776	2.3641	4.094741314	2.3641
40	35	0.610865238	2.301	3.769737708	2.63959876
40	40	0.698131701	2.2353	3.424678287	2.873646288
40	45	0.785398163	2.2095	3.124704866	3.124704866
40	50	0.872664626	2.1236	2.730047536	3.253543959

semi	AoA	AoA[rad]	Cn	Cl	Cd
45	1	0.017453293	3.1393	6.277643739	0.109576679
45	2	0.034906585	3.1361	6.268379145	0.218896623
45	3	0.052359878	3.1319	6.25521568	0.327821963
45	4	0.06981317	3.1268	6.238366545	0.436229084
45	5	0.087266463	3.1207	6.217649589	0.543973853
45	10	0.174532925	3.0766	6.059719066	1.068491967
45	15	0.261799388	3.0107	5.81622577	1.558452998
45	20	0.34906585	2.9248	5.496825955	2.00068103
45	25	0.436332313	2.8217	5.114657365	2.385003898
45	30	0.523598776	2.7044	4.684158204	2.7044
45	35	0.610865238	2.5766	4.221254315	2.955754092
45	40	0.698131701	2.442	3.74136106	3.139374686
45	45	0.785398163	2.3048	3.259479419	3.259479419
45	50	0.872664626	2.2095	2.840478447	3.385150394

semi	AoA	AoA[rad]	Cn	Cl	Cd
50	1	0.017453293	3.6846	7.368077635	0.128610274
50	2	0.034906585	3.6806	7.356715756	0.256902175
50	3	0.052359878	3.6752	7.340326532	0.384690213
50	4	0.06981317	3.6684	7.318927924	0.511789297
50	5	0.087266463	3.6602	7.292543668	0.638014899
50	10	0.174532925	3.5978	7.086282668	1.249502827
50	15	0.261799388	3.5018	6.764958117	1.812665064
50	20	0.34906585	3.3751	6.343113129	2.308704371

50	25	0.436332313	3.2217	5.839703595	2.723098508
50	30	0.523598776	3.046	5.27582676	3.046
50	35	0.610865238	2.8536	4.675064547	3.273515438
50	40	0.698131701	2.6502	4.060341966	3.407031446
50	45	0.785398163	2.442	3.453509519	3.453509519
50	50	0.872664626	2.2353	2.873646288	3.424678287

semi	AoA	AoA[rad]	Cn	Cl	Cd
55	1	0.017453293	4.2134	8.425516558	0.147067939
55	2	0.034906585	4.2088	8.412472226	0.293770003
55	3	0.052359878	4.2023	8.393081788	0.439862778
55	4	0.06981317	4.1938	8.367168228	0.585089399
55	5	0.087266463	4.1835	8.335161039	0.7292321
55	10	0.174532925	4.1036	8.082514191	1.425165324
55	15	0.261799388	3.9787	7.68625817	2.059526669
55	20	0.34906585	3.8128	7.165720049	2.608108805
55	25	0.436332313	3.6107	6.544811053	3.051895515
55	30	0.523598776	3.3786	5.851906858	3.3786
55	35	0.610865238	3.1237	5.117570481	3.583361428
55	40	0.698131701	2.8536	4.371968846	3.668517446
55	45	0.785398163	2.5766	3.643862665	3.643862665
55	50	0.872664626	2.301	2.95810858	3.525336527

semi	AoA	AoA[rad]	Cn	Cl	Cd
60	1	0.017453293	4.7096	9.41776541	0.164387707
60	2	0.034906585	4.7045	9.403268291	0.328369364
60	3	0.052359878	4.6969	9.380926124	0.491633506
60	4	0.06981317	4.687	9.351165407	0.653897185
60	5	0.087266463	4.6748	9.314021949	0.814871332
60	10	0.174532925	4.5787	9.018278517	1.590165822
60	15	0.261799388	4.4271	8.552500451	2.291635589
60	20	0.34906585	4.2244	7.939275014	2.889659787
60	25	0.436332313	3.9769	7.208590877	3.36142113
60	30	0.523598776	3.6921	6.394904787	3.6921
60	35	0.610865238	3.3786	5.535174194	3.875770696
60	40	0.698131701	3.046	4.666742747	3.915862118
60	45	0.785398163	2.7044	3.824599158	3.824599158
60	50	0.872664626	2.3641	3.039228376	3.622011336